https://doi.org/10.1070/RCR4920

Layered rare-earth hydroxides: a new family of anion-exchangeable layered inorganic materials

Alexey D. Yapryntsev,[a] Alexander E. Baranchikov,[a, b] Vladimir K. Ivanov [a, b]

[a] *Kurnakov Institute of General and Inorganic Chemistry of the Russian Academy of Sciences, Leninsky prosp. 31, 119991 Moscow, Russian Federation*
[b] *M.V.Lomonosov Moscow State University, Leninskie Gory 1, 119899 Moscow, Russian Federation*

The review summarizes the data on the chemical composition, crystal structure and functional properties of layered rare-earth hydroxides (LRHs), a new family of anion-exchangeable inorganic compounds. Comprehensive information is given on methods for the synthesis of LRHs including hydrothermal and hydrothermal-microwave treatment. Particular attention is paid to the methods of chemical design of hybrid functional materials based on LRHs. Prospects for fabrication of phosphors, heterogeneous catalysts and biomedical materials based on LRHs are analyzed.
The bibliography includes 295 references.

Contents

1. Introduction 629
2. Classification of layered inorganic compounds 630
3. Layered double hydroxides: general 631
4. The structure of layered rare-earth hydroxides 633
   4.1. The LREH-I category 633
   4.2. The LREH-II category 636
   4.3. The LREH-III category 638
5. Formation conditions and methods for the synthesis of layered rare-earth hydroxides 639
   5.1. Precipitation using strong bases 639
      5.1.1. Treatment under pre-hydrothermal conditions 641
      5.1.2. Hydro- and solvothermal treatment 641
   5.2. Homogeneous hydrolysis 642
      5.2.1. Homogeneous hydrolysis in the presence of hexamethylenetetramine 643
      5.2.2. Homogeneous hydrolysis in the presence of urea 644
      5.2.3. Homogeneous hydrolysis in the presence of melamine 644
6. Modification of layered rare-earth hydroxides 645
   6.1. Anion-exchange reactions 645
   6.2. Exfoliation 648
   6.3. Reactions involving host layers of layered rare-earth hydroxides 649
7. Luminescent and magnetic properties of layered rare-earth hydroxides 653
   7.1. Luminescent properties 653
   7.2. Magnetic properties of layered rare-earth hydroxides 656
8. Functional materials based on layered rare-earth hydroxides 657
   8.1. Luminescent materials 657
      8.1.1. Phosphors 657
      8.1.2. Sensor materials 657
   8.2. Biomaterials 658
   8.3. Catalysts 660
9. Conclusion 662

1. Introduction

Layered inorganic compounds exhibit specific physicochemical and mechanical properties that underlie a wide range of their practical applications.[1] Natural layered compounds include numerous aluminosilicate minerals, in particular, clays and mica. Among the best studied layered synthetic materials, there are layered silicates,[2–4] graphite-based materials,[5–7] copper-containing high-temperature superconducting oxides (*e.g.*, $YBa_2Cu_3O_{7-\delta}$, $HgBa_2Ca_{n-1}Cu_nO_{2n+2+\delta}$, $YBa_2Cu_3O_6F_2$ and $HgBa_2Ca_2Cu_3O_8F_\delta$),[8–10] the MAX and MXene phases

Received 22 August 2019

© 2020 Uspekhi Khimii, ZIOC RAS, Russian Academy of Sciences and IOP Publishing Limited

(*e.g.*, Ti_2GaC and Ti_2C),[11,12] layered transition metal dichalcogenides MX_2 (M = Nb, Mo, W; X = S, Se)[13,14] and ion-exchangeable materials based on metal hydroxides.[15–18]

Until recently, layered double hydroxides (LDHs) have been the sole class of layered inorganic compounds exhibiting anion-exchange properties. These compounds are derived from the mineral hydrotalcite $Mg_6Al_2CO_3(OH)_{16}\cdot 4H_2O$. They can be additionally functionalized through intercalation with various rare-earth cations †.[19–21] Interest in such systems has increased in line with interest in metal-organic polymers based on rare-earth elements.[22,23] Eventually, this led to the discovery of a new family of layered inorganic compounds, *viz.*, layered rare-earth hydroxides (LRHs).

The term 'LRHs' was introduced in 2006.[24] Although layered basic salts of rare-earth elements were not unknown at that time, they were not highlighted as a particular family of inorganic materials. Data on the formation of crystalline phases in systems $Ln^{3+}-OH^{-}-X^{-}-H_2O$ (Ln is a rare-earth element; $X^- = NO_3^-$, Cl^-, SO_4^{2-} or acetate anion) at temperatures below 100 °C under normal pressure were reported in the studies carried out in the 1960—70s.[25–35] Basic salts of rare-earth elements were also synthesized under supercritical conditions (at temperatures above 400 °C) to obtain large single crystals and to determine the crystal structure.[36–44] More recent publications included the results of studies on the formation of basic salts of rare-earth elements in systems $Ln^{3+}-OH^{-}-X^{-}-H_2O$ (Ln = Y, Eu; $X^- = NO_3^-$, Cl^- and terephthalate anion) under hydrothermal treatment conditions at much lower temperatures (about 200 °C).[45–47] The literature reported since 2006 includes the description of the crystal structures of various layered basic salts formed by all rare-earth elements as well as their anion-exchange, luminescent, magnetic and catalytic properties.

Specific features of the structure of LRHs underlie the possibility of anion exchange in the interlayer space without significant changes in the structure of the metal hydroxide host. Such a variability of the anionic composition and a great potential for changing the cationic composition allows one to efficiently control the optical and magnetic properties of LRHs through charge transfer and magnetic ordering to design multifunctional materials. Exfoliation of LRHs to quasi-2D monolayers offers prospects for engineering new systems by successive modification and assembly of the monolayers. This review presents a thorough consideration of the structures of LRHs, methods for the synthesis of these compounds, as well as their properties and possible fields of application of materials based on LRHs.

The list of notations and abbreviations used in the review is as follows:

A^{m-} — anion,
AP — activity product,
FM — formamide,
HMT — hexamethylenetetramine,
HTPS — 8-hydroxypyrene-1,3,6-trisulfonate anion,
LDHs — layered double hydroxides,
LRHs — layered rare-earth hydroxides,
Ln — rare-earth elements,
LREH-I — category of LRHs with the general formula $Ln(OH)_{2.5}A_{0.5}\cdot nH_2O$,
LREH-II — category of LRHs with the general formula $Ln(OH)_2A\cdot nH_2O$,
LREH-III — category of LRHs with the general formula $Ln(OH)_{3-x}A_x\cdot nH_2O$ ($x = 0.5–0.7$),
NPX — naproxen,
OS — octanesulfonate anion,
SCD — surface charge density.

2. Classification of layered inorganic compounds

A layered structure is characterized by strong interactions in two orthogonal directions and much weaker interaction in the third orthogonal direction. A well-known example of a layered compound is graphite where layers formed by covalently bonded $C(sp^2)$ atoms (bond energy ~ 524 kJ mol^{-1}) are held together by van der Waals forces (bond energy ~ 7 kJ mol^{-1}).[48]

Layered materials can be classified by comparing forces that hold layers together.[49–65] First of all, these are electrostatic, hydrogen and van der Waals interactions. Table 1 presents classification of layered materials with respect to the charge of individual layers. In turn, electrically neutral layered compounds can be divided into conductors (metals and semiconductors) and dielectrics. Among compounds with charged layers, there are cationic and anionic ones. Their layers bear a positive and a negative charge, respectively.[16] The space between charged layers is usually filled with counterions and water molecules that interact with the layers electrostatically and through hydrogen bonds. Often, the mobility of cations and anions is high enough to provide the possibility of substitution within the layered structure; in other words, such materials exhibit ion-exchange properties. Classification of layered materials with respect to charge is conditional since many anions form covalent bonds with layers, and the layers thus become electrically neutral as in the case of, *e.g.*, copper hydroxide acetate $Cu_2(OH)_3(OAc)\cdot H_2O$. This compound belongs to simple layered hydroxides, which exhibit ion-exchange properties.[51,52]

Layered inorganic compounds with negatively charged metal-organic host include numerous natural and synthetic compounds, such as β-alumina,[53] clays,[1] layered perovskites[8,9,54] and complex transition and alkali metal oxides[55] (see Table 1).[11,12,56–65] The number of layered inorganic compounds with positively charged metal-organic host is much smaller. Almost all of them represent metal

† In this review all rare-earth elements, including, lanthanides and two non-lanthanide elements, yttrium and scandium, are denoted as Ln.

A.D.Yapryntsev. Junior Researcher at IGIC RAS.
Telephone: +7(495)633–8534, e-mail: yaprynsev@mail.ru
Current research interests: layered rare-earth hydroxides, sonochemistry, zirconia, anion exchange, chemistry of rare-earth elements, ion-exchangeable materials, microwave-assisted hydrothermal synthesis.
A.E.Baranchikov. Candidate of Sciences (Chemistry), Head of Laboratory at IGIC RAS and Senior Researcher at the Department of Chemistry, MSU.
Telephone: +7 (495) 633–8534, e-mail: a.baranchikov@yandex.ru
Current research interests: size effects, transition and rare-earth element oxides, photocatalysis, 2D nanostructures.
V.K.Ivanov. Corresponding Member of the Russian Academy of Sciences, Doctor of Sciences (Chemistry), Director of the IGIC RAS and Professor of Faculty of Materials Science, MSU.
Telephone: +7 (495) 952–0224, e-mail: van@igic.ras.ru
Current research interests: solid state chemistry, functional materials, nanomaterials, rare-earth elements.

Translation: A.M.Raevskiy

Table 1. Classification of layered inorganic materials with respect to layer type.

Material	Chemical composition	Ref.
	Electrically neutral layers	
	Dielectric layers	
Clays		58
kaolinite	$Al_2Si_2O_5(OH)_4$	
serpentine	$Mg_3Si_2O_5(OH)_4$	
Nickel cyanide	$Ni(CN)_2$	59
Hexagonal boron nitride	h-BN	60
	Conductive layers	
Graphite	C	61
Transition metal dichalcogenides	MX_2 (M = Ti, Zr, Hf, V, Nb, Ta, Bi, Mo, W; X = S, Se, Te)	62
Metal carbides and nitrides, MAX- and MXene phases	$M_{n+1}(A)_mX_n$ (n = 1 – 3; m = 0, 1; M = Ti, Zr, Hf, V, Nb, Ta, Bi, Mo, W; A = Si, Ge, Al, S, Sn; X = C, N)	11, 12
Metal oxyphosphates	$MOPO_4$ (M = V, Nb, Ta)	63
	Charged layers	
	Negatively charged layers	
Clays		58
montmorillonite	$Na_x(Al_{2-x}Mg_x)(Si_4O_{10})(OH)_2$	
saponite	$Ca_{x/2}Mg_3(Al_xSi_{4-x}O_{10})(OH)_2$	
vermiculite	$(Na,Ca)_x(Mg_{3-x}Li_xSi_4O_{10})(OH)_2$	
muscovite	$KAl_2(AlSi_3O_{10})(OH)_2$	
β-Alumina	$NaAl_{11}O_{17}$	53
Complex transition metal and alkali metal oxides	$M'XO_2$ (M' is alkali metal; X = Ti, V, Cr, Mn, Co, Ni)	55
Layered perovskites		8, 9, 54
Ruddlesden – Popper phases	$M_{n+1}X_nO_{3n+1}$ (M are Group 1 – Group 3 elements; X are transition elements)	
Dion – Jacobson phases	$M'Ln_{n-1}X_nO_{3n+1}$ (M' is alkali metal; Ln = rare-earth element;	
Aurivillius phases	X = Nb, Ta) $(Bi_2O_2)M_{n-11}X_nO_{3n+1}$ (M are Group 1 – Group 3 elements; X are transition elements)	
	Positively charged layers	
Layered double hydroxides	$[M^{2+}_{1-x}M^{3+}_x(OH)_2]A_{n-x/n}\cdot m\,H_2O$	64
Layered transition-metal hydroxides	$M''_2(OH)_3X$ (M'' = Co, Cu, Ni, Mn, Zn; X^- = NO_3^-, AcO^-, Cl^-)	65
Layered rare-earth hydroxides		56
LREH-I category	$Ln_2(OH)_5(A^{m-})_{1/m}\cdot n\,H_2O$ (Ln = rare-earth element, A^{m-} = anion, n = 1 – 2)	
LREH-II category	$Ln(OH)_2(A^{m-})_{1/m}\cdot n\,H_2O$ (n = 0 – 2)	
LREH-III category	$Ln_2(OH)_{5-x}(A^{m-})_{(1+x)/m}\cdot n\,H_2O$ (n = 0 – 2; 0 < x < 1)	
Boehmite	AlOOH	16
Antimony oxyhydroxide	$[Sb_4O_4(OH)_2](O_3SCH_2CH_2SO_3)\cdot H_2O$	57

hydroxides. Besides, there are only two naturally occurring minerals, *viz*., boehmite and hydrotalcite, and a synthetic compound antimony oxyhydroxide $[Sb_4O_4(OH)_2](O_3SCH_2CH_2SO_3)\cdot H_2O$.[57] Layered inorganic compounds with positively charged host include three groups of layered hydroxides, namely, LDHs,[64] layered simple hydroxides[65] and LRHs.[56]

3. Layered double hydroxides: general

Among anion-exchangeable layered materials, LDHs have been best studied as yet.[64, 66 – 68] Structural features of LDHs have been thoroughly investigated, various methods for the synthesis of LDHs have been developed, a large body of information on their anion-exchange properties has been accumulated and numerous field of application were demonstrated. The results obtained are intensively used in the studies of LRHs owing to similarity between the structures and certain chemical properties of LDHs and LRHs (see below).

Layered double hydroxides are built of positively charged 2D layers whose charge is compensated by ions filling the interlayer space. The chemical composition of LDHs is described by the general formula $[M^{2+}_{1-x}M^{3+}_x(OH)_2]A_{n-x/n}\cdot m\,H_2O$, where A is an anion with the valence n. These compounds have a brucite-like crystal structure [brucite is $Mg(OH)_2$] in which M^{2+} ions are partially replaced by M^{3+} ones. As a result of heterovalent substitution, layers acquire a positive charge and intercalate various anions (Fig. 1). Water molecules usually form hydrogen bonds with the metal hydroxide layers or with anions in the interlayer space.[64]

Layered double hydroxides can contain cations whose ionic radii fall in a specific range of values.[64] In particular, Mg^{2+}, Mn^{2+}, Fe^{2+}, Co^{2+}, Ni^{2+}, Cu^{2+}, Zn^{2+}, Cd^{2+} cations (61 – 95 pm) can act as M^{2+} ions, while the role of

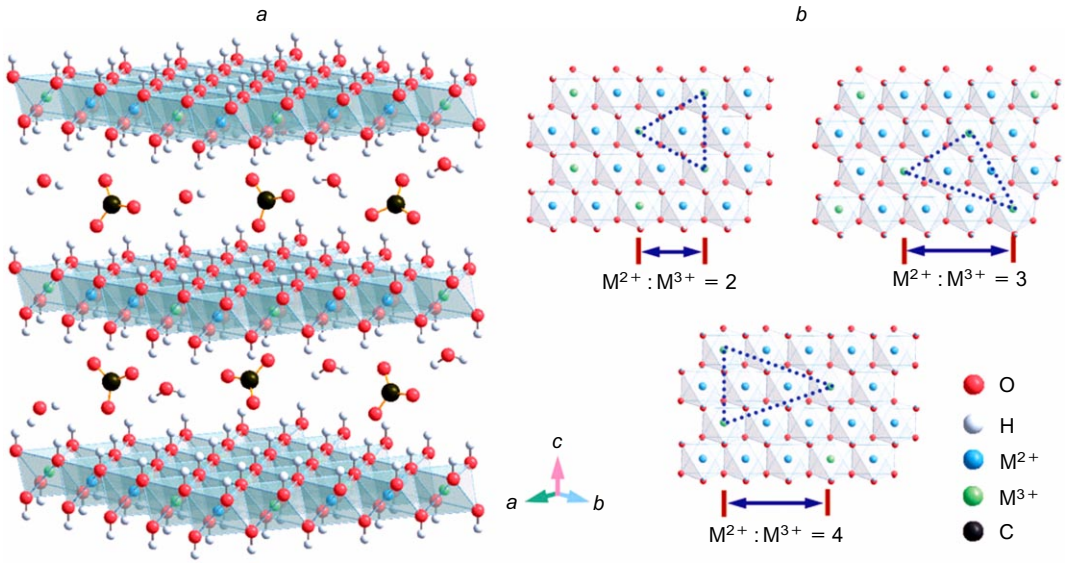


Figure 1. Three-dimensional structure of carbonate-intercalated LDHs $[M^{2+}_{1-x}M^{3+}_{x}(OH)_2](CO_3)_{x/n}\cdot m\,H_2O$ with different M^{2+}/M^{3+} cation ratios (*a*) and its projection along the *c* direction (*b*).[69] Dotted lines denote the shortest distances between M^{3+} cations.

M^{3+} can be played by Al^{3+}, V^{3+}, Cr^{3+}, Ga^{3+} and Fe^{3+} cations (54–64 pm). However, LDHs containing larger cations including rare-earth ions were also reported.[19–21]

Traditionally, LDHs are synthesized using 'soft chemistry' methods;[70] however, they can also be obtained by, *e.g.*, mechanochemical[71] or electrochemical synthesis.[72] The most widely used technique is co-precipitation[73] including homogeneous precipitation.[70] These approaches allow one to obtain LDHs with different composition and microstructure that can be varied over a wide range. Often, these methods are modified by exposing reaction mixtures to various physical factors including microwave radiation[74] and sonication.[75] A number of synthetic procedures are aimed at obtaining LDHs in the form of quasi-2D particles.[67,76–78] The syntheses of LDH composites with graphene,[79–81] metal and metal oxide nanoparticles (TiO_2, ZnO, CeO_2, Au, Ag, *etc.*)[82] and polymers[83] were reported. A widely used synthetic approach involves *in situ* precipitation of LDHs onto substrates (*e.g.*, carbon nanotubes) whose surfaces are modifies with OH, CO or COO groups.[84]

Specific features of the crystal structure allow one to vary the anionic composition of LDHs with ease by carrying out anion-exchange reactions. The kinetics and thermodynamics of such processes have been thoroughly studied for simple inorganic and organic anions. In particular, anion-exchange isotherms were constructed for reactions with halide, hydroxide, nitrate, carbonate and sulfate ions. A comparison of the equilibrium constants of the corresponding reactions showed that the completeness of anion-exchange processes for LDHs decreases as follows:[85,86]

$$CO_3^{2-} > SO_4^{2-} > OH^- > F^- > Cl^- > Br^- > NO_3^- > I^-$$

The kinetics of anion-exchange reactions is described using methods of solid-phase kinetics, namely, the Avrami–Erofeev model for the kinetic-controlled mode and the Sharp–Hancock model for the diffusion-controlled reaction.[87] The results obtained in the studies on the kinetics and thermodynamics of anion-exchange reactions of LDHs were used to make some assumptions of the reaction mechanisms. If the sizes of the exchanging anions are comparable (*e.g.*, halide ions), the reaction often involves the formation of intermediates (solid solutions) containing both types of anions and proceeds by the topotactic mechanism.[17,86] If the sizes and nature of the anions involved differ significantly, the ion-exchange reaction can be treated as dissolution of the original LDHs and followed by its reprecipitation with the new anion in the structure.[17,86]

Layered double hydroxides have a wide range of industrial applications.[88,89] The anion-exchange properties of LDHs enable efficient sorption of toxic organic and inorganic anions (including those containing radioactive isotopes) from the environment.[88,90,91] Besides, an efficient and reversible sorption of gases, *e.g.*, CO_2 and NO_x, is possible.[88] Novel luminescent[92,93] and magnetic materials[94,95] can be fabricated by intercalating various anions into the interlayer space and by doping the LDH hosts with rare-earth elements. Layered double hydroxides with basic sites are widely used in heterogeneous catalysis; their selectivity and catalytic activity can be controlled with ease by varying the chemical composition and structure.[69,96–98] In addition, LDHs are used as substrates for catalysts and as precursors of metal oxide catalysts.[69,97,99] Composites prepared from intercalated LDHs and nanoparticles or biomolecules (in particular, enzymes) proved their efficiency for electro-, photo- and electrophotocatalysis.[82,98] Low toxicity of LDHs allows them to be used as platforms for pharmaceuticals for normalizing the pH level in the gastrointestinal tract, for drug delivery systems (including targeted delivery ones), biosensors and contrast agents for luminescence microscopy and magnetic resonance imaging (MRI).[18,66,100–105] Also, LDHs are utilized as components of materials for electrochemical devices (*e.g.*, supercapacitors),[106,107] as 2D nanoreactors for fabrication of nanoparticles[108,109] and in some other fields.[70,83,110]

The available synthetic routes to LDHs and methods of investigation of their properties are to a great extent applicable to their chemical analogues, namely, LRHs

representing a new family of layered anion-exchangeable compounds.

4. The structure of layered rare-earth hydroxides

The term 'LRHs' was proposed by Monge and co-workers,[24] who pioneered in determining the crystal structures of layered compounds of the general formula $[Ln_4(OH)_{10}(H_2O)_4]_nA_n$ (Ln = Y, Dy, Ho, Yb; A = naphthalene-2,6-disulfonate or anthraquinone-2,6-disulfonate anion). Their publication [24] was followed by a number of studies on solving the structures of LRHs containing certain simple inorganic anions, such as chloride, nitrate or sulfate.

Layered rare-earth hydroxides are described by the general formula $Ln_2(OH)_{6-x}(A^{m-})_{x/m}\cdot n\,H_2O$, where A^{m-} is an anion, $x = 1$ or 2, $n = 0-2$, Ln is a rare-earth element except radioactive promethium (the most stable isotope, ^{145}Pm, has a half-life of 17.7 years). An increase in the number of synthesized LRHs made it possible to classify them. In particular, Sasaki and co-workers [92] specified two main categories of LRHs, *viz.*, LREH-I of the general formula $Ln_2(OH)_5(A^{m-})_{1/m}\cdot n\,H_2O$ (Ln is a rare-earth element; $A^{m-} = NO_3^-$, Cl^-) and LREH-II of the general formula $Ln_2(OH)_4(A^{m-})_{2/m}\cdot n\,H_2O$ [$A^{m-} = NO_3^-$, Cl^-, SO_4^{2-}, $O_3S(CH_2)'_nSO_3$ ($n' = 3, 4$)]. The authors of Ref. 111 considered three categories of LRHs, namely, the '251 phase' of the general formula $Ln_2(OH)_5A\cdot n\,H_2O$ (Ln is a rare-earth element; $A^- = NO_3^-$, Cl^-, Br^-; $n \approx 1.5$), the '241 phase' of the general formula $Ln_2(OH)_4SO_4\cdot n\,H_2O$ ($n \approx 2.0$) and the '121 phase' of the general formula $Ln(OH)_2A\cdot n\,H_2O$ ($A^- = NO_3^-$, Cl^-; $n = 0, 1$). All categories of rare-earth hydroxides have layered structures; however, the intralayer local structures differ significantly. In the '241' and '121' compounds, anions present in the interlayer space are constituents of the coordination sphere of the rare-earth cation, whereas in the '251' compounds they are mainly electrostatically bound to the host layers. In the text below we will use the classification proposed by Sasaki and co-workers [92] because the '241' and '121' phases [111] are structurally and stoichiometrically similar, being different only in the charge of the anion.

4.1. The LREH-I category

The crystal structures of the following layered rare-earth compounds belonging to the LREH-I category were determined: hydroxychlorides,[112] hydroxynitrates [113] and hydroxides intercalated with naphthalene-2,6-disulfonate and anthraquinone-2,6-disulfonate anions.[24]

The structures of the LRHs were for the first time determined taking layered ytterbium hydroxide intercalated with anthraquinone-2,6-disulfonate anions and layered yttrium hydroxide intercalated with naphthalene-2,6-disulfonate anions as examples.[24] These are the first representatives of a new family of hybrid organic-inorganic compounds with infinitely long metal hydroxide host layers. In both compounds the positive charge of metal hydroxide layers is compensated by interlayer anions. The host layers are built of alternating chains formed by the coordination polyhedra of the eight- and nine-coordinated Ln atoms connected through shared μ_3-OH groups (Fig. 2 *a*). Anions form hydrogen bonds with the layers (Fig. 2 *b*). These compounds crystallize in the orthorhombic system (space group *Ibam*) with the formation of pseudohexagonal sublattice (Fig. 2 *c*). Thus, from the standpoint of crystallography, LRHs are structurally similar to LDHs that crystallize in the hexagonal system.

Layered rare-earth hydroxychlorides crystallize in the orthorhombic system (space group $P2_12_12$). Their host layers are essentially structurally similar to those of layered ytterbium and yttrium hydroxides (see above). Consider the structure of LRHs in more detail taking layered europium hydroxychloride $Eu_2(OH)_5Cl\cdot 1.6\,H_2O$ as an example.[114] The lattice constants of this compound are as follows: $a = 12.9152(3)$, $b = 7.3761(1)$ and $c = 8.7016(3)$ Å. The $a:b$ ratio equal to 3.06 is indicative of nearly hexagonal arrangement of europium cations, which manifests itself in the formation of pseudohexagonal sublattice, as in the case of the structure discussed above (see Fig. 2 *c*). Deviation from hexagonal arrangement of europium cations in the structure is due to the presence of three types of coordination environment (Fig. 3). Type-1 europium ion (Eu1) is surrounded by seven OH groups and one H_2O molecule. Type-2 and type-3 europium ions (Eu2 and Eu3, respectively) are coordinated by eight OH groups and one H_2O

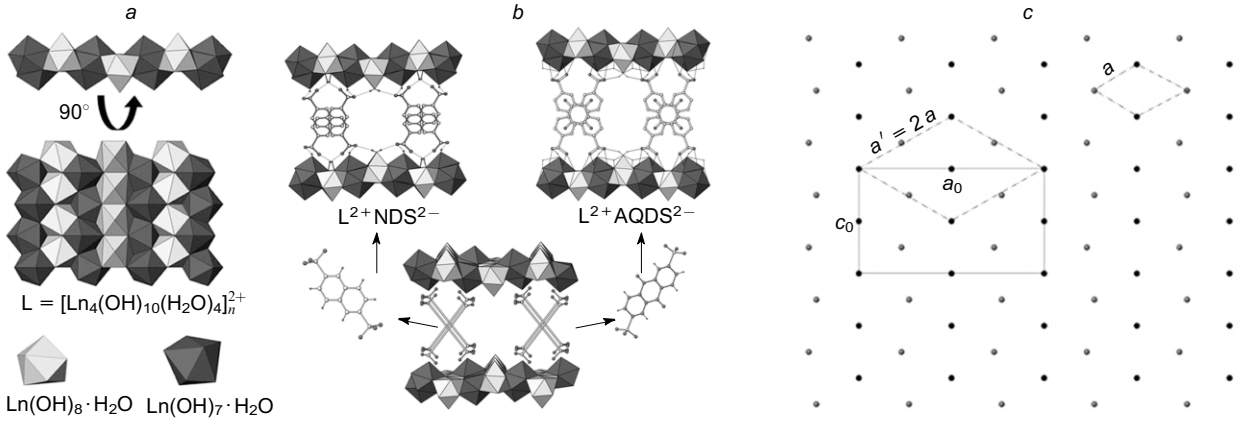


Figure 2. Host layer pattern (*a*), arrangement of anions in the interlayer space of layered ytterbium hydroxide (Ln = Yb) intercalated with anthraquinone-2,6-disulfonate anions ($AQDS^{2-}$), and layered yttrium hydroxide (Ln = Y) intercalated with naphthalene-2,6-disulfonate anions (NDS^{2-}) (*b*), and relationship between orthorhombic lattice (lattice constants a_0 and c_0) and pseudohexagonal sublattice (lattice constant a') in the structure of these LRHs (*c*).[24]

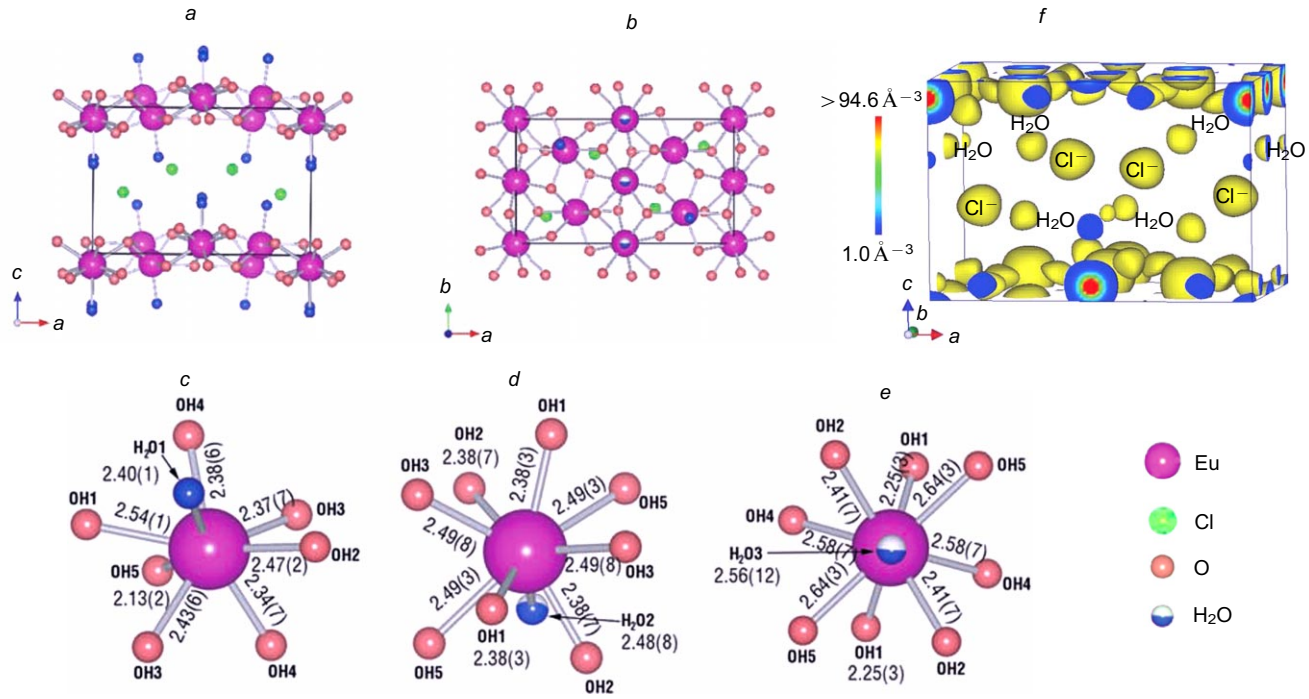


Figure 3. Crystal structure of layered europium hydroxychloride projected along the *b* (*a*) and *c* (*b*) directions (refinement using synchrotron X-ray diffraction pattern); coordination environment for three nonequivalent europium positions: Eu1 (*c*), Eu2 (*d*), Eu3 (*e*); and the electron density distribution in the structure of layered europium hydroxide (*f*).[114]

molecule. Each hydroxyl group is bonded to three europium atoms. Alternating chains of different-type europium ions form layers described by the formula $\{[Eu_2(OH)_5(H_2O)_2]^+\}_\infty$. Chloride anions occupy well-defined positions in the interlayer space (see Fig. 3); this is different from LDHs where interlayer anions are disordered.[64, 115] A rather short distance between Cl atom and O atom of one water molecule (~3.0 Å) suggests the formation of hydrogen bonds between water and chloride anions.

The lattice constants *a* and *b* of rare-earth hydroxychlorides regularly decrease with decreasing ionic radius of Ln owing to lanthanide contraction.[112] The interlayer distance along the [001] direction (d_{001}) in the rare-earth hydroxychlorides correlates with the lattice constant *c* and demonstrates a stepwise change at the mid-point of the Ln series, namely, on going from Gd (~0.870 nm) to Eu (0.845 nm).

The d_{001} distance in rare-earth hydroxychlorides also correlates with the degree of hydration, that is, the number of water molecules per unit cell. The degree of hydration depends on the number of water molecules in the coordination sphere of the Ln atom. Ideally, when each rare-earth ion is coordinated by a water molecule, the number of water molecules in the LRH unit cell is 8. Rietveld refinement gives the following values of the degree of hydration: 7.4, 6.3 and 7.2 for hydroxychlorides of the elements of the cerium subgroup (Nd, Sm and Eu) and 5.8, 5.6, 5.4 and 4.9 for hydroxychlorides of the elements of the yttrium subgroup (Tb, Dy, Ho and Er), respectively.

Thus, water plays a significant role in the formation of the $\{[Ln_2(OH)_5(H_2O)_2]^+\}_\infty$ layers, especially for the light lanthanides characterized by high degrees of hydration. As a consequence, rare-earth hydroxychlorides demonstrate different humidity dependence behaviour (Fig. 4).[112] For $Nd_2(OH)_5Cl \cdot n\,H_2O$ the interlayer distance remains almost unchanged upon exposure to atmosphere with different relative humidity at room temperature. Layered samarium, europium and gadolinium hydroxychlorides are characterized by two sets of interplanar distances (d_{001} = 8.5–8.6 and 8.3–8.4 Å) indicating the formation of two phases containing different amount of water, *viz.*, a high-hydration phase corresponding to the longer d_{001} distance and a low-hydration phase corresponding to the shorter d_{001} distance. Changes in the relative humidity of atmospheric air can cause reversible transitions between these phases. The interlayer distance in the layered terbium, thulium and yttrium hydroxychlorides is 8.3 Å throughout the entire relative humidity range. It follows that these compounds exist only as the low-hydration phase.

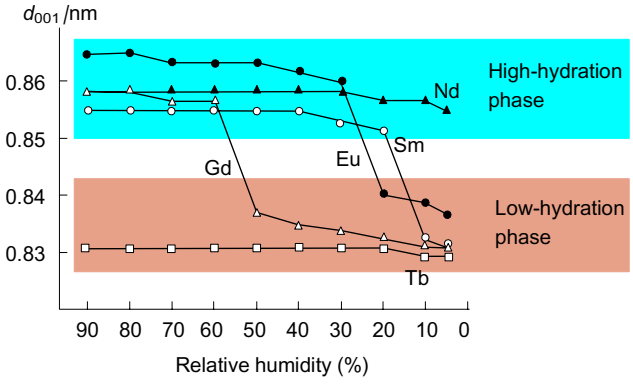


Figure 4. Interplanar distance d_{001} in layered rare-earth hydroxychlorides of the general formula $Ln_2(OH)_5Cl \cdot n\,H_2O$ plotted *vs.* relative humidity.[112]

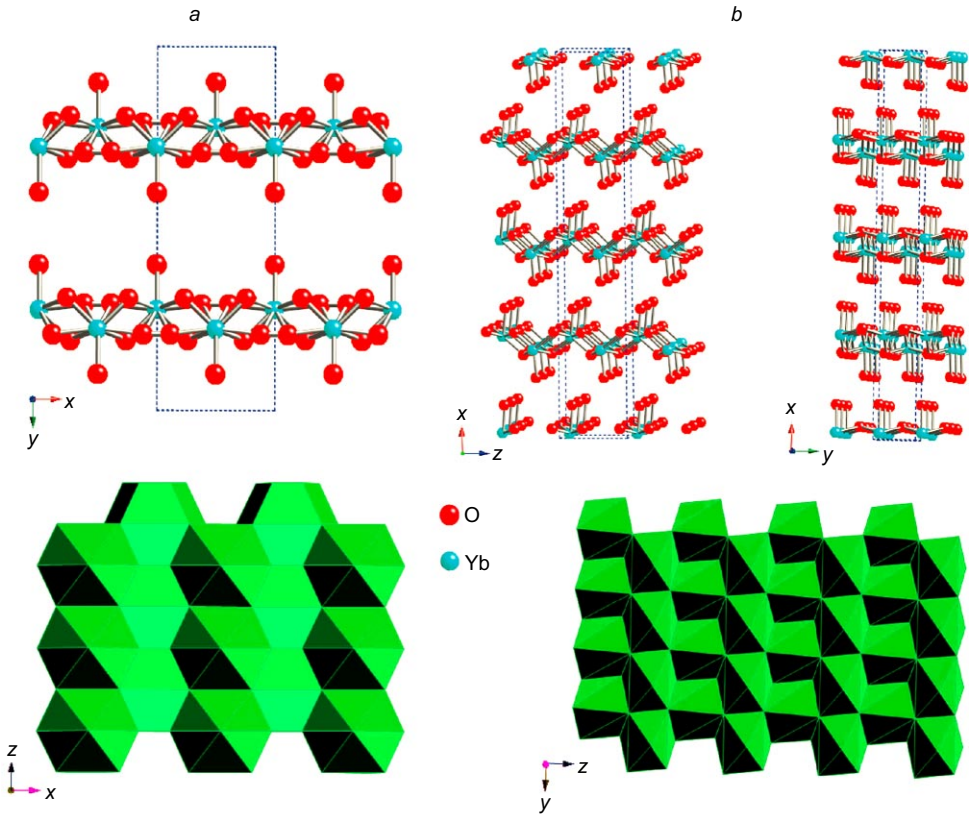


Figure 5. Crystal structures of $Yb_2(OH)_5NO_3 \cdot 2\,H_2O$ (*a*) and $Yb_2(OH)_5NO_3 \cdot H_2O$ (*b*).[113] Dashed lines confine the unit cells; positions of nitrogen atoms were not refined.

The composition of layered rare-earth hydroxynitrates is described by the general formula $Ln_2(OH)_5NO_3 \cdot n\,H_2O$ (Ln = Y, La, Sm – Tm; $1 < n < 2$). It is analogous to the general formula for rare-earth hydroxychlorides, except that the chloride anion is replaced by the nitrate ion. The composition $Y_2(OH)_{5.14}(NO_3)_{0.86} \cdot H_2O$ was also determined for yttrium hydroxynitrate.[116, 117] The authors of the early studies reported that layered hydroxynitrates crystallize in the orthorhombic system similarly to layered hydroxychlorides;[36] however, this was not confirmed in the recent publications.[118] It was found[119] that layered hydroxynitrates most likely crystallize in the monoclinic system. In this case, the lattice constants *a* and *b* of rare-earth hydroxynitrates are very similar to those of rare-earth hydroxychlorides, which allows one to assume a similar structure of the host layers. In particular, layered rare-earth hydroxynitrates are also characterized by the formation of pseudohexagonal sublattice (according to electron diffraction data).[120] Noteworthy, the lattice constant *c* of layered hydroxynitrates is twice as large as that of layered hydroxychlorides (interplanar distance d_{002} in the former is nearly equal to the d_{001} distance in the latter). This is indicative of more complex structure of layered hydroxynitrates and misorientation of layers relative to one another. An analysis of certain indexed powder X-ray diffraction patterns revealed systematic extinction conditions ($l = 2n + 1$ for $h0l$). It was assumed that layered rare-earth hydroxynitrates can crystallize in the space groups *Pc*, $P2/c$ or $P2_1/c$ (monoclinic system).[119]

Layered hydroxynitrates of the general formula $Ln_2(OH)_5NO_3 \cdot n\,H_2O$ (Ln = Y, Sm – Lu; $1 < n < 2$) were studied by Fogg and co-workers,[113, 121 – 125] who established the existence of three phases of layered ytterbium hydroxynitrate with different degrees of hydration and refined the structures of two of them (Fig. 5). The phase $Yb_2(OH)_5NO_3 \cdot 2\,H_2O$ crystallizes in the space group *Cmcm* ($a = 6.000$, $b = 18.85$ and $c = 3.7556$ Å, Fig. 5 *a*), while the phase $Yb_2(OH)_5NO_3 \cdot H_2O$ crystallizes in the space group $Pna2_1$ ($a = 33.866$, $b = 3.7305$ and $c = 5.9417$ Å, Fig. 5 *b*).[113] The coordination number (CN) of ytterbium is 8 – 9 in the former and 7 in the latter structure. Hydroxide groups and nitrate ions seem to be disordered, the nitrate ion being a constituent of the coordination sphere of ytterbium (Yb – O bond is directed along the normal to the metal hydroxide layer, see Fig. 5 *a*).

Dehydration/rehydration of layered rare-earth hydroxynitrates proceed similarly to those of rare-earth hydroxychlorides (see above). In Fig. 6 the interplanar distances d_{002} are plotted *vs.* relative humidity of atmospheric air in the course of a dehydration/rehydration cycle. As the relative humidity decreases, the high-hydration phase of layered samarium hydroxynitrate ($d_{002} = 0.88$ nm) undergoes an irreversible transition to the low-hydration phase ($d_{002} = 0.83$ nm). Certain rare-earth hydroxynitrates (Ln = Eu – Ho) demonstrate a reversible transition between the high- and low-hydration phases under similar conditions. The changes in the d_{002} distance in these compounds are as large as 0.05 – 0.07 nm, being several times larger than those in the corresponding hydroxychlorides (0.02 nm). As to the layered hydroxynitrates of heavier lanthanides (Er, Tm), the d_{002} value remains almost unchanged in the relative humidity range from 5% to 90% and corresponds to the high-hydration phase.

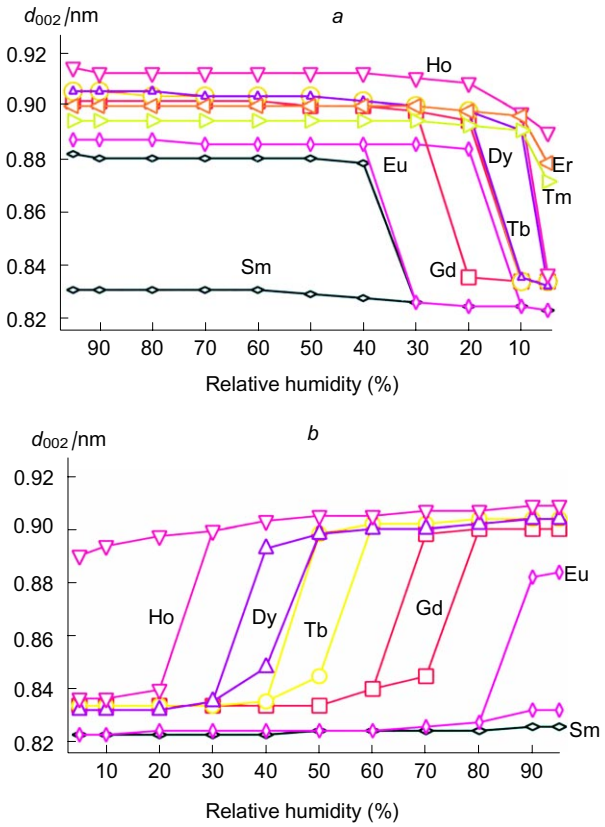


Figure 6. Interplanar distances d_{002} in layered rare-earth hydroxynitrates plotted *vs.* relative humidity: dehydration (*a*) and rehydration (*b*).[119]

Similar ionic radii of Ln allow one to carry out isomorphous substitution in various compounds, and surely in LRHs. To date, binary and ternary solid solutons of LRHs have been synthesized.[126–128] Europium- and terbium-containing hydroxynitrates with the cationic compositions $Gd_{0.5}Tb_{0.5-x}Eu_x$, $Tb_{1-x}Eu_x$ and $Y_{1-x-y}Eu_xTb_y$, $Y_{0.95-x}Gd_xEu_{0.05}$ have been best studied.[129–134] However, the existence ranges of solid solutions in these systems are not known with certainty due to the low symmetry of the crystal structure, to related problems in structure refinement and to the presence of differently hydrated phases. Isomorphous substitution involving other cations, *e.g.*, Bi^{3+} (Ref. 135) is also possible. Of particular interest is the possibility to carry out isomorphous replacement of rare-earth cations by di- or tetravalent cations and thus, potentially, change the charge density of the host layers of LRHs. Note that the structure[136] and anion-exchange properties[89] of LDHs can be modified in targeted manner by changing the charge density ($M^{2+}:M^{3+}$ ratio).

Isomorphous substitution of not only cations, but also anions in the structure of LRHs is possible.[137] Layered rare-earth hydroxides can be doubly intercalated with functional anions (including inorganic ones, *e.g.*, MoS_4^{2-}) and aliphatic sulfonic acid anions, which facilitate exfoliation of the layered structure of LRHs.[138] When layered rare-earth hydroxynitrates and chlorides as well as products of anion-exchange reactions involving these compounds are brought in contact with atmospheric air, chloride and nitrate ions are often isomorphously replaced by carbonate ions whose content varies in the range of 0.5 mass % – 5 mass %.[119,121] Layered rare-earth hydroxysulfates synthesized from rare-earth nitrates can contain nitrate ions as impurity.[139,140] The aforesaid suggests that the commonly used general formula $Ln_2(OH)_{6-x}(A^{m-})_{x/m}\cdot n\,H_2O$ describing the chemical composition of LRHs is to some extent incorrect.

4.2. The LREH-II category

The crystal structures of compounds of the general formula $Ln(OH)_2(A^{m-})_{1/m}\cdot n\,H_2O$ (Ln is a rare-earth element; $m = 1, 2$; $n = 0-2$) were determined for corresponding hydroxychlorides,[40,43,141] hydroxynitrates,[121,142–144] hydroxysulfates,[140,145] hydroxyalkylsulfates[146,147] and hydroxyalkanedisulfonates.[148] Pioneering structural studies of the LREH-II compounds of the composition $Ln(OH)_2Cl$ (Ln = Y, Pr, Sm, Gd) carried out by Klevtsova *et al.*[40,42,43] in the 1960s revealed the existence of two polymorphs of these hydroxychlorides, *viz.*, monoclinic (space group $P2_1/m$) and orthorhombic ones (space group *Pbnm* or $Pbn2_1$). For the monoclinic polymorph, the coordination polyhedron of the rare-earth cation is a bicapped trigonal prism comprised of two chlorine atoms and six oxygen atoms from μ_3-OH groups (Fig. 7). These polyhedra form chains connected through shared bases of the prisms while the chains form 2D layers that are held together through hydrogen bonds OH – Cl.

To date, the crystal structures of almost all lanthanide hydroxychlorides except those of La, Ce and Pm have been determined.[40,43,141] All these compounds crystallize in the monoclinic system (space group $P2_1/m$). Hydroxychlorides of heavier lanthanides (Tm, Yb, Lu) can also crystallize in the orthorhombic system (space group *Pnma*). Both polymorphs have $PuBr_3$-type structures. The coordination polyhedron of the Ln atom is composed of eight atoms including six oxygen atoms from μ_3-OH groups and two μ_2-Cl atoms.[141] A decrease in the size of the lanthanide atom is followed by contraction of its coordination polyhedron, shortening of hydrogen bonds and a decrease in the lattice constants *b* and *c*.

Basic rare-earth nitrates of the composition $Ln(OH)_2NO_3\cdot n\,H_2O$ ($n = 0$, 1; Ln = La, Y, Pr, Nd, Sm and Gd)[121,142–144] crystallize in the monoclinic system (space group $P2_1$ for $n = 0$ and $C2/m$ for $n = 1$). The host

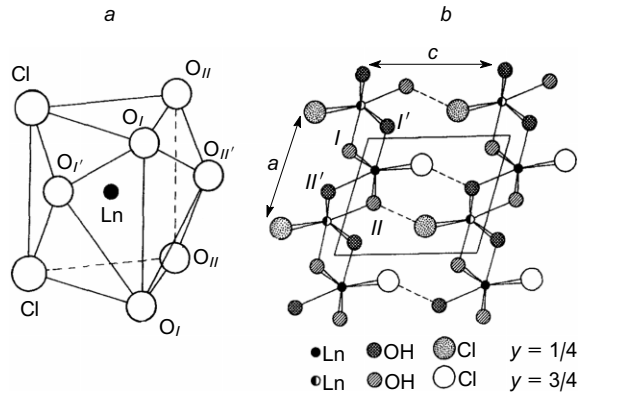


Figure 7. Coordination polyhedron of the rare-earth cation (*a*) and projection of the structure of $Ln(OH)_2Cl$ on the (010) plane (*b*).[40] Pairs of oxygen atoms with the subscripts *I*, *II* and *II′* specify the shared edges connecting polyhedra in the structure of $Ln(OH)_2Cl$.

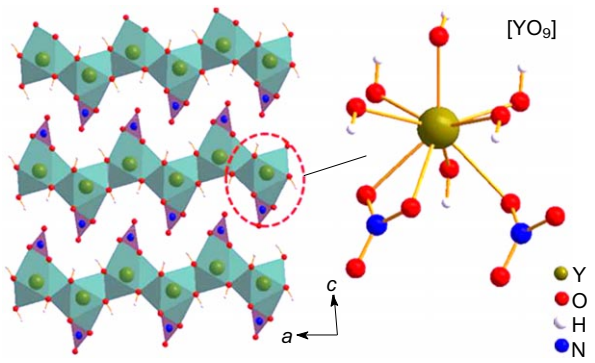


Figure 8. Crystal structure of $Y(OH)_2NO_3$.[144]

layers in compounds $Ln(OH)_2NO_3$ are formed by $[LnO_9]$ polyhedra composed of six oxygen atoms from bridging hydroxyl groups and three O atoms from bidentate nitrate anions (Fig. 8). In the case of $Ln(OH)_2NO_3 \cdot H_2O$ the coordination polyhedron $[LnO_9]$ also contains water molecule, while nitrate ions are coordinated to the rare-earth cation in monodentate fashion.

The crystal structures of hydrated $[Ln_2(OH)_4SO_4 \cdot 2H_2O$, Ln = Ce, Pr, Nd, Sm, Eu, Gd, Tb$]$[145,149] and anhydrous $[Ln_2(OH)_4SO_4$, Ln = Eu – Lu, Y$]$[140] rare-earth hydroxysulfates were determined. These compounds crystallize in the monoclinic system (space group $A2/m$ for hydrated and $C2/m$ for anhydrous phases). The interlayer distance (~6.85 Å) and the unit cell volume (~314.97 Å^3) of the anhydrous phase are smaller than those of the hydrated phase (~8.32 Å and ~388.14 Å^3, respectively). The metal hydroxide layers in both phases are formed by chains of $[LnO_9]$ polyhedra. The rare-earth cation in structure of hydrated hydroxysulfate is surrounded by six oxygen atoms from μ_3-OH groups, two O atoms from μ_2-H_2O and one O atom from the sulfate anion (Fig. 9 *a*). In the structure of anhydrous hydroxysulfate the rare-earth cation is also surrounded by six oxygen atoms from the bridging groups μ_3-OH and three O atoms from sulfate anion (Fig. 9 *b*). Interestingly, in the latter case CN(Ln) is 10 since one oxygen atom of the sulfate anion can equiprobably occupy two positions with similar energy values. As the atomic number of the lanthanide increases, the unit cell parameters of both phases decrease. For the anhydrous phase the lattice constant *a* decreases more slowly than *b* and *c* owing to the rigidity of the host specified by the tridentate sulfate anions.

Layered europium hydroxyterephthalates $Eu_2(OH)_4(C_8H_4O_4) \cdot 2H_2O$ and $Eu_2(OH)_4(C_8H_4O_4)$ were for the first time synthesized in 2002.[45] They are compositionally and structurally similar to hydrated and anhydrous phases of layered rare-earth hydroxysulfates, respectively. The metal hydroxide layers are formed by $[EuO_9]$ polyhedra. In hydrated europium hydroxyterephthalate the cation is surrounded by seven oxygen atoms from μ_3-OH groups, one O atom from μ_2-H_2O and one O atom from carboxyl group of the terephthalate anion (Fig. 9 *c*). In anhydrous europium hydroxyterephthalate the cation is also surrounded by seven oxygen atoms from bridging μ_3-OH groups and two O atoms from carboxyl groups of the terephthalate anion (Fig. 9 *d*).

Layered hydroxides of the elements of the cerium subgroup $Ln_2(OH)_4[O_3S(CH_2)_nSO_3] \cdot 2H_2O$ (Ln = La, Ce, Pr, Nd, Sm; n = 3, 4) crystallize in the monoclinic system (space group $P2_1/n$).[148] They are structurally similar to hydrated

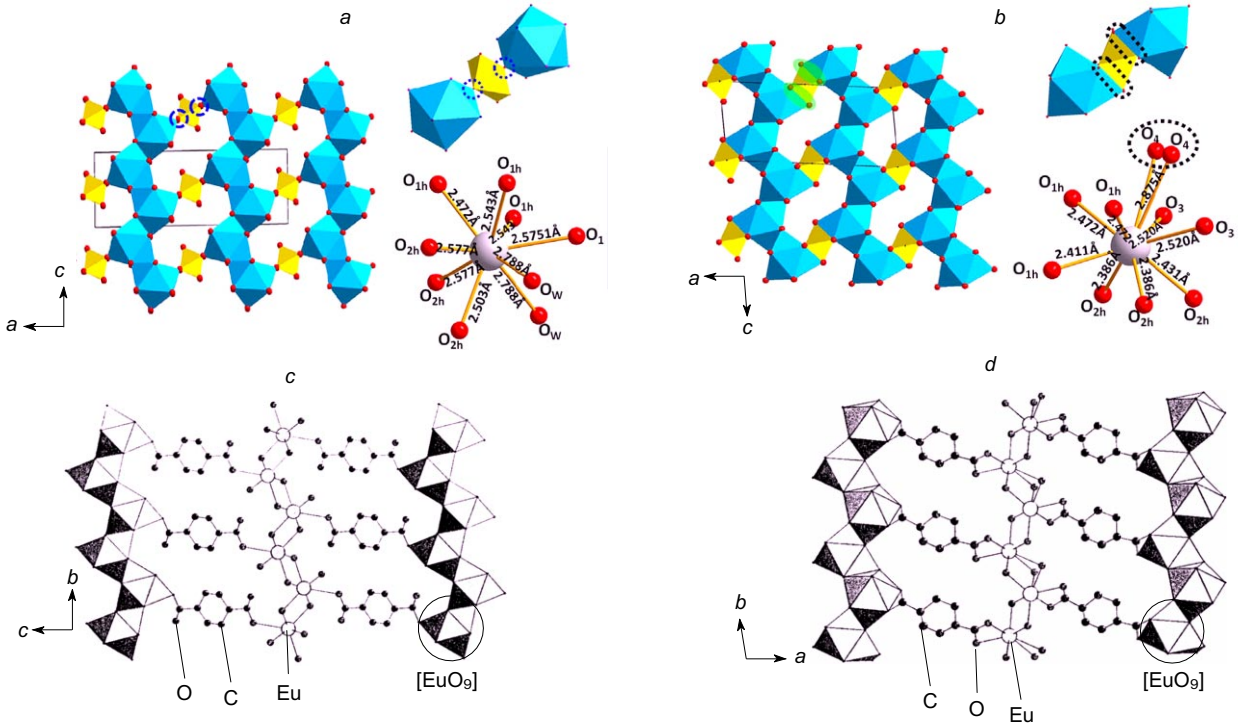


Figure 9. Crystal structures of $Gd_2(OH)_4SO_4 \cdot 2H_2O$ (*a*), $Gd_2(OH)_4SO_4$ (*b*),[140] $Eu_2(OH)_4(C_8H_4O_4) \cdot 2H_2O$ (*c*) and $Eu_2(OH)_4(C_8H_4O_4)$ (*d*).[45] Nonequivalent positions of bridging hydroxyl oxygen atoms with an occupancy of 1 are denoted as O_{1h} and O_{2h}; positions of sulfate oxygen atoms with an occupancy of 1 are denoted as O_1 and O_3; and positions of sulfate oxygen atoms with an occupancy of 1/2 are denoted as O_w and O_4.

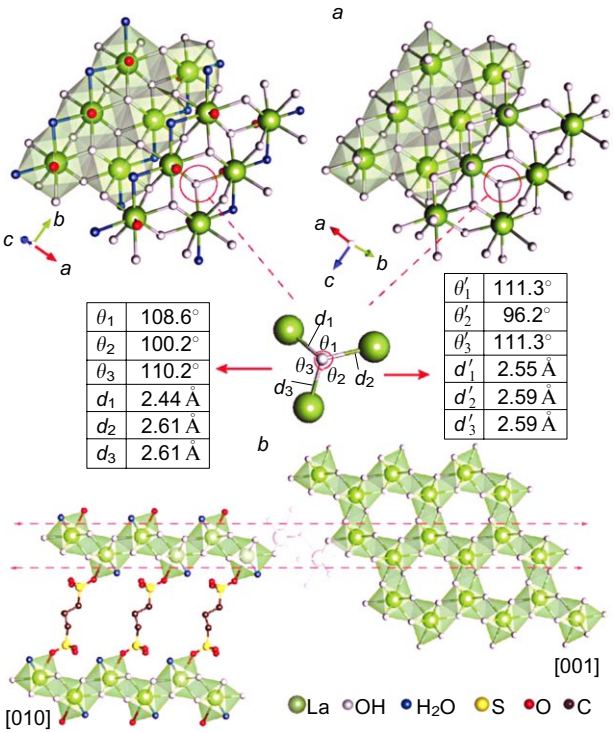


Figure 10. Connection of the coordination polyhedra of the lanthanide atoms (*a*) and projections of the crystal structures of layered lanthanum hydroxide (left) and UCl_3-type $La(OH)_3$ (right) (*b*): a schematic. Panels on the left and on the right present the interatomic distances (d_n) and La – O – La angles (θ_n) in the crystal structures of layered lanthanum hydroxide and UCl_3-type $La(OH)_3$.[148] Dashed lines in Fig. *b* confine similar structural motifs for layered lanthanum hydroxide and $Ln(OH)_3$.

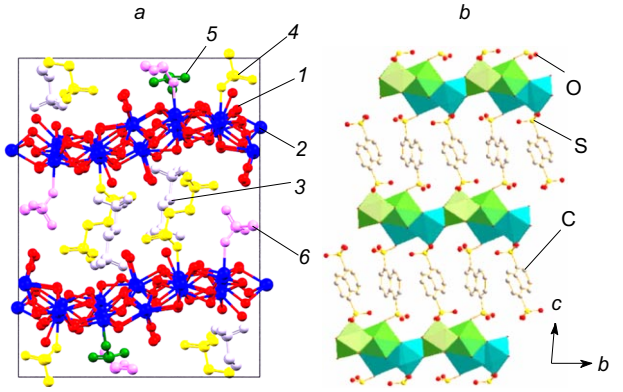


Figure 11. Crystal structures of layered hydroxides $[Er_{12}(OH)_{29}(H_2O)_5][O_3SCH_2CH_2SO_3]_{3.5} \cdot 5\,H_2O$ (*a*)[150] and $Ln_3(OH)_7A$ (Ln = Y, Gd, Er, Yb; A is naphthalene-1,5-disulfonate anion) (*b*).[151] Panel *a*: oxygen (*1*), erbium (*2*), uncoordinated ethanedisulfonate anion (*3*), ethanedisulfonate anion coordinated in monodentate fashion(*4*, *5*) and ethanedisulfonate anion coordinated in bidentate fashion (*6*).

hydroxysulfates except that the metal hydroxide layers are linked by alkanedisulfonate anions rather than sulfate anions. Sulfonate groups are coordinated to the rare-earth cation in monodentate fashion. The structures of the metal hydroxide layers in hydrated rare-earth hydroxysulfates and hydroxysulfonates are derived from the UCl_3-type structures of corresponding hydroxides $Ln(OH)_3$ formed by $[La_nO_9]$ polyhedra (Fig. 10). As the ionic radius of the lanthanide decreases, the structure becomes unstable since the coordination number of the Ln atom decreases from 9 to 7 – 8. For instance, there exists a layered erbium hydroxide intercalated with ethanedisulfonate anion, $[Er_{12}(OH)_{29}(H_2O)_5][O_3SCH_2CH_2SO_3]_{3.5} \cdot 5\,H_2O$.[150]

Layered cerium(III) hydroxysulfates and hydroxyalkyldisulfonates are stable in air. These compounds hold a special position since other cerium hydroxy compounds, such as $Ce(OH)_3$, $Ce_2(OH)_5NO_3 \cdot 2\,H_2O$ and $Ce_2(OH)_5Cl \cdot 2\,H_2O$, are readily oxidized to CeO_2 in air.[149]

4.3. The LREH-III category

The results of recent studies demonstrate that many LRH structures cannot be classified into the LREH-I and LREH-II categories. For instance, the crystal structures of LRHs $[Er_{12}(OH)_{29}(H_2O)_5][O_3SCH_2CH_2SO_3]_{3.5} \cdot 5\,H_2O$ (see Ref. 150) and $Ln_3(OH)_7A$ (Ln = Y, Gd, Er, Yb; A is naphthalene-1,5-disulfonate anion)[151] were determined. In the first structure erbium cations occupy 12 crystallographically independent positions while the ethanedisulfonate anions occupy four positions, which is indicative of rather low symmetry of the structure. The coordination polyhedra of three out of 12 erbium cations are distorted pentagonal bipyramids (CN 7), while those of the other nine Er cations are distorted square antiprisms (CN 8). Ethanedisulfonate anions are coordinated to Er^{3+} in monodentate and bidentate fashion; there are also uncoordinated interlayer ethanedisulfonate anions (Fig. 11 *a*). In the second structure, Ln atoms occupy three independent positions and the eight-vertex coordination polyhedra of these atoms form the metal hydroxide layers. The interlayer naphthalene-1,5-disulfonate anion can be coordinated to the rare-earth cation in bi- and monodentate fashion (Fig. 11 *b*). Thus a third category of layered rare-earth compounds, LREH-III, can be distinguished. The chemical compositions of compounds belonging to this category are intermediate between those of the LREH-I and LREH-II compounds. Anions in the LREH-III structures can occupy several different positions with different denticity with respect to the rare-earth cation.

According to the results of structure determination of recently synthesized layered yttrium hydroxide intercalated with 4-sulfobenzoate anion $Y_3(OH)_7(C_7H_4O_5S) \cdot H_2O$,[152] this compound belongs to the LREH-III category. There are three nonequivalent positions of yttrium cations, each being in the 8-vertex polyhedron formed by oxygens from seven μ_3-OH groups and O atoms of sulfonic and carboxyl groups of the 4-sulfobenzoate anion (Fig. 12 *a*). As mentioned above, a similar structure (seven μ_3-OH groups and an oxygen atom of the anion) and stoichiometry was reported for compounds $Ln_3(OH)_7A$ (Ln = Y, Gd, Er, Yb; A is naphthalene-1,5-disulfonate anion).[151] Three nonequivalent positions of the Ln atoms in the structure of these compounds enable the formation of the simplest structural motif comprising three coordination polyhedra connected through shared OH – OH edges and OH – OH – OH faces. The structural motif in $Y_3(OH)_7(C_7H_4O_5S) \cdot H_2O$ is formed by connecting four polyhedra for each of the three yttrium positions, which gives a total of 12 polyhedra (Fig. 12 *b*). The sulfobenzoate anion is coordinated to yttrium atoms in bidentate fashion by the carboxyl group and in monodentate fashion by the sulfonic group (see Fig. 12 *a*). The Y1 – OD, Y2 – OC and Y3 – OB bond lengths are 2.32,

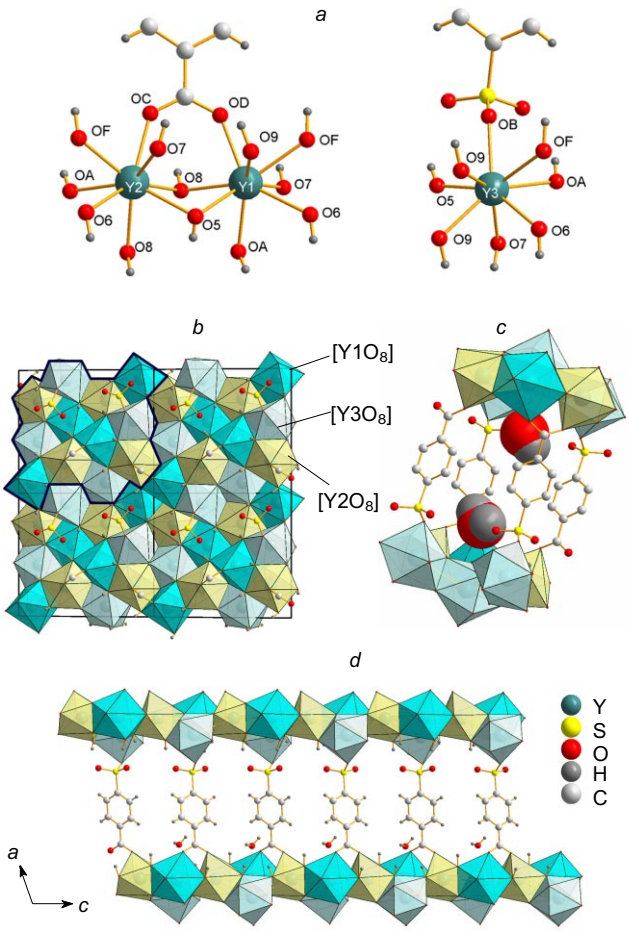


Figure 12. Crystal structure of $Y_3(OH)_7(C_7H_4O_5S)\cdot H_2O$; the colours of the yttrium polyhedra correspond to three different crystallographic positions of Y atoms.[152] Three nonequivalent positions of yttrium atoms (*a*); projection of the structure along the *a* direction, the semi-bold contour specifies the motif forming the metal hydroxide layer (*b*); water molecules in cylindrical pores in the interlayer space (*c*); and projection of the structure along the *b* direction (*d*).
Numbers and letters denote nonequivalent positions of yttrium and oxygen atoms.

2.35 and 2.41 Å, respectively. Four neighbouring 4-sulfobenzoate anions form cylindrical cavities in the interlayer space, filled with two water molecules (Fig. 12 *c*) hydrogen-bonded to the hydroxide layers and sulfonic groups.

Thus, for most compounds belonging to the LREH-I and LREH-II categories the coordination sphere of the Ln atom is a distorted bi- or tricapped trigonal prism (CN 8 or 9, respectively). The coordination polyhedron of the Ln atom is formed by six O atoms of the bridging μ_3-OH groups and O atoms of water molecule and anions coordinated in mono- or bidentate anions. The coordination numbers of the Ln atoms are determined by the electrostatic repulsive force acting between ligands, namely, weak repulsion causes the formation of UCl_3-type structures (CN 9) while strong repulsion leads to $PuBr_3$-type structures (CN 8). The polyhedra of the Ln atoms form chains connected through shared faces (basal planes of trigonal prisms). These chains form layers by sharing edges of the polyhedra of the Ln atoms. Rare-earth cations in these layers are characterized by nearly hexagonal arrangement, which is often followed by the formation of a pseudo-hexagonal sublattice. Layers are held together through either hydrogen bonds involving anions and OH groups (water) or the interaction with anions that constitute the coordination sphere of the rare-earth cations from the adjacent layers. In the latter case such anions act as bridges forming the 3D structure similar to that of metal-organic polymers.[153] Structures containing polydentate anions differently coordinated to the rare-earth cations correspond to new polytypes of these compounds (LREH-III category). Note that heavier rare-earth ions with small ionic radii owing to lanthanide contraction are characterized by smaller CN values (7 – 8).

5. Formation conditions and methods for the synthesis of layered rare-earth hydroxides

The LRHs phases $Ln(OH)_2A\cdot n\,H_2O$ and $Ln_2(OH)_5A\cdot n\,H_2O$ are formed in the system $Ln_2O_3-H_2O-LnA_3$ (Ref. 154), which can be treated as $LnOOH-H_2O-LnOA$ for $A^- = Cl^-$ and NO_3^-. An analysis of the PDF2 crystallographic database and published data[155,156] for the system $LnOOH-H_2O-LnOCl$ revealed the possibility of co-existence of three phases, *viz.*, $Ln(OH)_3$, $Ln_2(OH)_5Cl\cdot n\,H_2O$ and LnOCl; as to the system $LnOOH-H_2O-LnONO_3$, three phases including $Ln(OH)_3$, $Ln_2(OH)_5NO_3\cdot n\,H_2O$ and $Ln_4O(OH)_9NO_3$ are in equilibrium.[156] The synthesis of layered hydroxychlorides and hydroxynitrates is usually accompanied by the formation of impurity phases including $Ln(OH)_3$, LnOCl and $Ln_4O(OH)_9NO_3$. At least equally complex pattern of phase equilibria including the formation of lanthanide complexes should be expected in the case of other anions (*e.g.*, organic ones).

5.1. Precipitation using strong bases

The first detailed physicochemical description of systems $Ln^{3+}-OH^--X^--H_2O$ (Ln is a Sc, Y, La, Ce, Pr, Nd, Sm – Er, Yb , or Lu cation; $X^- = Cl^-$) was reported by Aksel'rud in 1963.[30] Precipitation of hydroxy compounds from rare-earth chlorides was carried out using NaOH at different activity of chloride anions. To determine the composition and formation conditions of rare-earth hydroxides and basic salts, Aksel'rud and Spivakovskii[157] developed an original version of potentiometric method. It was found that the composition of the precipitate depends on the activity of chloride ions and on the synthesis duration, *viz.*, as the activity decreased, the precipitate composition approached that of the corresponding hydroxide. The content of hydroxide anions in the precipitate increased up to transformation of the precipitate to rare-earth hydroxides. Only in the case of yttrium the composition $Y_2(OH)_5Cl\cdot n\,H_2O$ did not change for a long time.

The isobaric potentials of formation (Δz°_{298}) and the activity products (AP) of rare-earth hydroxychlorides $Ln_2(OH)_5Cl$ and $Ln(OH)_2Cl$ and hydroxides $Ln(OH)_3$ are plotted *vs.* atomic numbers of the rare-earth elements in Fig. 13. Both AP and Δz°_{298} of the basic chlorides and hydroxides of scandium, yttrium and lanthanum increase on going from Sc to La, whereas the reverse is observed for lanthanides on going from La to Lu. The curves exhibit a characteristic kink at the point corresponding to gadolinium, which is most pronounced for hydroxides.[158,159] Noteworthy is the increase in absolute values of AP and $\Delta\Delta z^\circ_{298}$ on going from $Ln(OH)_2Cl$ to $Ln(OH)_3$, which is indicative of an increase in the thermodynamic stability of these compounds.

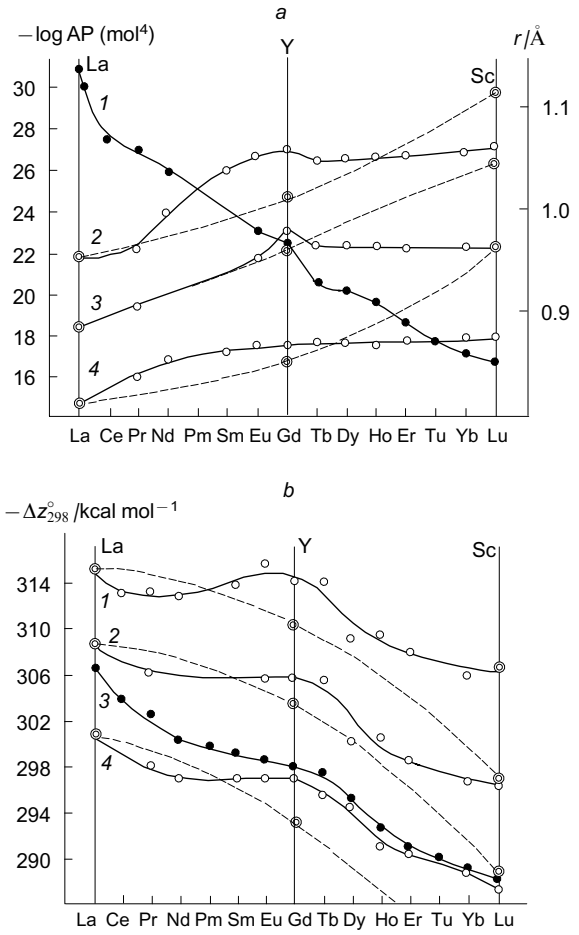


Figure 13. Plots of log AP (*a*) and Δz°_{298} (*b*) for scandium, yttrium and lanthanum compounds (dashed lines) and for lanthanide compounds (solid lines) *vs.* atomic numbers of the elements. Panel *a*: plot of corresponding ionic radii (*r*) (*1*) and the log AP plots for $Ln(OH)_3$ (*2*), $Ln_2(OH)_5Cl$ (*3*) and $Ln(OH)_2Cl$ (*4*). Panel *b*: plots of Δz°_{298} for $Ln(OH)_3$ (*1*), $Ln_2(OH)_5Cl$ (*2*), Ln^{3+} (*3*) and $Ln(OH)_2Cl$ (*4*).[30]

A study[155] on the $LnOCl-Ln_2(OH)_5Cl-Ln(OH)_3$ (Ln = La – Dy, Y) system was much like that reported by Aksel'rud[30] and involved an analysis of the chemical composition of solid-phase products of the interaction between LnOCl and H_2O as function of the $LnOCl:H_2O$ ratio and temperature (Fig. 14). The interaction of the elements of the cerium and yttrium subgroups (*e.g.*, La and Dy, respectively) led to formation of the corresponding hydroxides in the former and oxychlorides in the latter case as major products. Only the interaction of yttrium oxychloride with water in all cases caused the formation of layered hydroxychloride. The addition of sodium chloride was followed by significant increase in the content of layered rare-earth hydroxychlorides for all elements except lanthanum. This is in good agreement with Akselrud's data on the influence of the activity of chloride anions on the stability of layered rare-earth hydroxychlorides and on remarkably high stability of yttrium hydroxychloride.

It follows that, thermodynamically, the stability of layered basic salts of rare-earth elements is governed by the activity of the anion. However, precipitation of the basic salts of rare-earth elements usually proceeds under essentially nonequilibrium conditions, and the chemical composition of the corresponding basic salt being formed will be to a great extent determined by the composition of the complex of the rare-earth element that formed in the course of hydrolysis.

Rare-earth cations exist in aqueous solutions as aqua complexes $Ln(H_2O)_8^{3+}$ (Ln = Er – Lu) and $Ln(H_2O)_9^{3+}$ (Ln = La – Sm) or their mixtures (Ln = Eu – Ho).[160] Usually, counterions are in the second (outer) coordination sphere. At pH > 6, deprotonation of the aqua complexes begins and they are transformed to hydroxo complexes.[160]

$$q\,[Ln(H_2O)_n]^{z+} \rightleftharpoons [Ln_q(H_2O)_{n-p}(OH)]_{aq}^{qz-p} + p\,H^+ \qquad (1)$$

The rate constant for reaction (1) increases with decreasing size of the rare-earth ion;[160] in addition, the basicity of the corresponding cation also decreases.[30, 161] This provides an explanation for the difficulties in the synthesis of layered hydroxides of heavier lanthanides, *e.g.*, lutetium for which the $OH^-:Ln^{3+}$ ratio increases significantly.[140, 162] Main methods for controlling reaction (1) involve variation of pH and temperature.

Layered hydroxides belonging to the LREH-I and LREH-III categories are usually obtained by precipitation from aqueous[151, 162–165] and alcoholic[127, 135, 166] solutions. The $OH^-:Ln^{3+}$ ratio is maintained at 2 : 1, which corresponds to pH 6.5 – 7 for aqueous solutions. A decrease in pH leads to a lower yield of LRHs, whereas an increase in pH causes the formation of $Ln(OH)_3$ impurity.[167, 168] The exception is the yttrium basic salts that can be precipitated without impurity formation at higher pH values.[169, 170] The

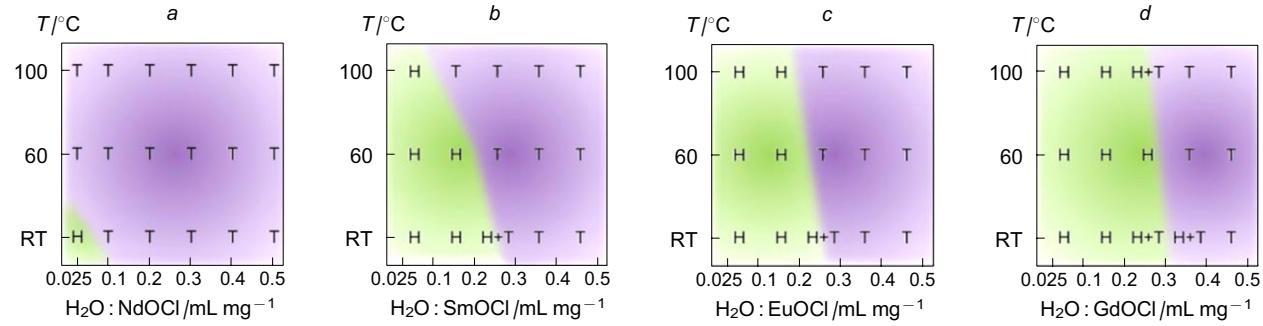


Figure 14. Conditions for $Ln_2(OH)_5Cl$ and $Ln(OH)_3$ formation in the reaction of LnOCl with water.[155] Ln = Nd (*a*), Sm (*b*), Eu (*c*) and Gd (*d*); 'H' stands for $Ln_2(OH)_5Cl\cdot n\,H_2O$ and 'T' stands for $Ln(OH)_3$; RT is room temperature.

most widely used precipitating agents include KOH, NaOH [121, 123, 124, 131, 151, 164, 165, 167, 168, 171–179] or $NH_3 \cdot H_2O$.[132–134, 156, 162, 163, 180–184] In some cases, nitrogen-containing organic bases are used, *e.g.*, oleylamine,[185] triethylamine,[24, 150, 186] polyethyleneimine [127, 135, 166] and tetrabutylammonium hydroxide.[187] A base is mixed with a solution of the lanthanide salt (usually, nitrates or chlorides; the reagent mixing order can be either direct or reverse) and a solution of the salt of the anion to be intercalated into the layered structure of the LRH.[123, 124, 131, 150, 151] The precipitation temperature can also be varied; single-phase layered hydroxides of heavier lanthanides including Lu belonging to the LREH-I category were obtained by decreasing the precipitation temperature to 4 °C.[162]

The LREH-II compounds (first of all, hydroxychlorides and hydroxynitrates) are synthesized at smaller $OH : Ln^{3+}$ ratios [144] or in the absence of precipitating agents (the salt is thus hydrolyzed by water molecules) [141] under hydrothermal [141, 144] or solvothermal [188] conditions. For anions that are readily incorporated into the first coordination sphere of solvated rare-earth cations (*e.g.*, sulfates) [189] the precipitation pH is significantly increased (to 9–11).[140, 148, 190] In this case the equilibrium (1) holds for complexes $[Ln(H_2O)_n(SO_4)_m]^{(z-2m)+}$ instead of aqua complexes $[Ln(H_2O)_n]^{z+}$.[189]

5.1.1. Treatment under pre-hydrothermal conditions

Precipitation of rare-earth hydroxychlorides and hydroxynitrates leads to formation of sediments with low degree of crystallinity. Suspensions formed upon precipitation are often heat treated at 60–220 °C in open or closed (hydrothermal or solvothermal treatment) vessels to increase the degree of crystallinity and the particle size of LRHs.[121, 179]

The first study [191] of the system $K^+ - Y^{3+} - OH^- - NO_3^-$ by the Schreinemakers method revealed that the reaction between potassium hydroxide and yttrium nitrate solutions affords basic yttrium nitrate $Y_2(OH)_5NO_3 \cdot H_2O$ at 25–50 °C as poorly crystallized product (Fig. 15 *a*) and that keeping the reaction mixture at its boiling temperature for a few hours leads to formation of well-crystallized plate-like particles of hexagonal $Y_2(OH)_5NO_3 \cdot H_2O$ (Fig. 15 *b*).

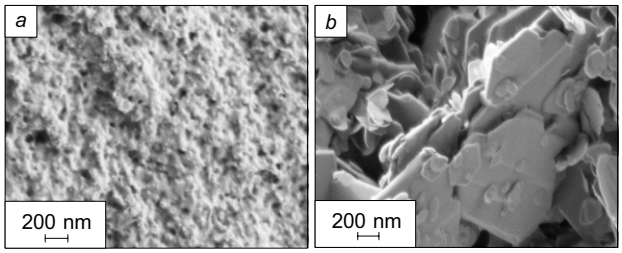


Figure 15. SEM images of $Y_2(OH)_5NO_3 \cdot H_2O$ synthesized at 25 (*a*) and 100 °C (*b*).[191]

An interesting feature of methods involving ageing or boiling of LRH sediments consists in the possibility to obtain very thin plate-like particles (<10 nm). Figure 16 presents the results of atomic force microscopy (AFM) study[172] of layered gadolinium hydroxychloride synthesized using a three-step procedure involving the addition of 0.1 M KOH solution to 0.05 M $GdCl_3$, keeping the suspension thus formed at 60 °C for 12 h and refluxing the suspension for 24 h. The reaction product represented plate-like nanocrystals with a lateral size of about 100 nm. The minimum thickness of the nanocrystals was a few nanometres. The thickness of the plate-like particles can be additionally decreased by carrying out precipitation of LRHs at reduced temperatures.[111, 163] For instance, sols of layered rare-earth hydroxynitrates and solid solutions based on them (plate-like nanocrystals with an average thickness of 3–5 nm) were synthesized by precipitation in the presence of ammonium hydroxide at 4 °C.[111, 162, 163]

5.1.2. Hydro- and solvothermal treatment

In 1974 Haschke [36] for the first time synthesized rare-earth hydroxynitrates $Ln_2(OH)_{6-x}(NO_3)_x$ (Ln = La, Pr, Nd, Sm, Eu, Gd, Tb, Dy, Yb, Y; $x = 0.6–2$) under supercritical conditions (400–800 °C, 1200 atm) in the system $Ln_2O_3 - Ln(NO_3)_3 - H_2O$. This was followed by publications of the results of studies on hydrothermal synthesis of

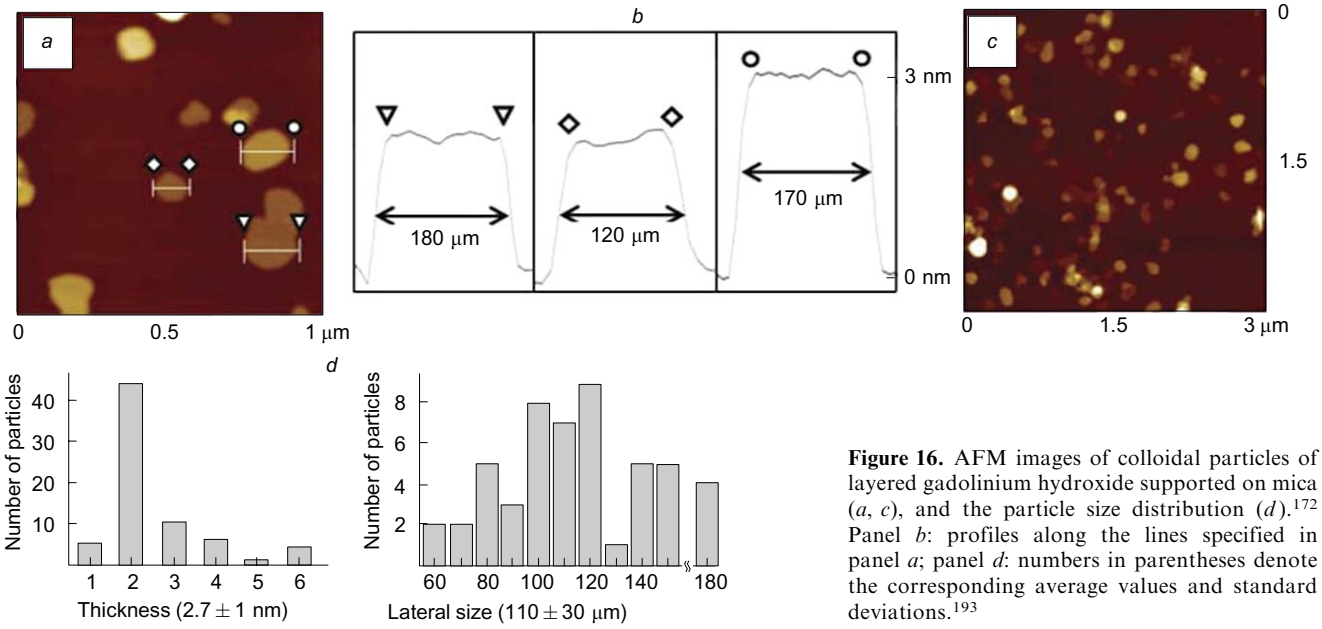


Figure 16. AFM images of colloidal particles of layered gadolinium hydroxide supported on mica (*a*, *c*), and the particle size distribution (*d*).[172] Panel *b*: profiles along the lines specified in panel *a*; panel *d*: numbers in parentheses denote the corresponding average values and standard deviations.[193]

basic salts of rare-earth elements in the systems $LnX_3-NaOH-H_2O$ (Ln = Y, Eu; X = nitrate, chloride or terephthalate anion) under much milder conditions.[45–47] Layered europium terephthalates built of metal hydroxide layers held together by chemical bonds with terephthalate anions were synthesized in 2002 by the hydrothermal method (180–250 °C).[45] In 2006, yttrium hydroxynitrate $Y_2(OH)_{5.06}(NO_3)_{0.94}\cdot 0.32\,H_2O$ was produced by hydrothermal and sonication-assisted hydrothermal treatment at 250 °C.[46]

Usually, crystallization of LRHs under hydrothermal conditions takes 12–120 h at 120–220 °C. Hydrothermal treatment of precipitate using NaOH (KOH) affords rare-earth hydroxynitrates[121, 124, 169, 174] and hydroxychlorides[114, 123, 164, 175] belonging to the LREH-I category. Hydrothermal synthesis of layered gadolinium and heavier lanthanide (Yb, Lu) hydroxynitrates is accompanied by the formation of layered impurity phases with large interlayer spacings.[124] Hydrothermal treatment of layered hydroxynitrates of the elements of the yttrium subgroup produces a mixture of the corresponding oxide, $Ln(OH)_3$ and $Ln(OH)_2NO_3$.[124] Hydrothermal treatment in the presence of NaOH(KOH) was used to obtain not only nitrate- and chloride-containing LRHs, but also the LREH-1 compounds intercalated with porphyrins[165] and molecules of certain biologically active substances (ibuprofen, naproxen, diclofenac),[192] as well as single crystals of LREH-II hydroxynitrates (180–220 °C, 120 h)[144] and the LREH-III layered hydroxides intercalated with organic anions (170 °C, 72 h).[151]

A method was developed for hydrothermal treatment of products of reactions between ammonium hydroxide, rare-earth nitrates and salts containing the anion to be intercalated into LRHs (ammonium sulfate or nitrate) at 100–220 °C.[132–134, 156, 181–184] The influence of the synthesis conditions on the morphology and composition of end products have been thoroughly studied and documented.[156] Various phases with different morphology can form depending on the hydrothermal synthesis conditions, *viz.*, hexagonal platelets of layered hydroxynitrate $Ln_2(OH)_5NO_3\cdot n\,H_2O$ (Ln = Y, Eu), hexagonal prisms and needle-shaped crystals of oxyhydroxynitrate $Ln_4O(OH)_9NO_3$, square platelets of hydroxynitrate $Ln(OH)_{2.94}(NO_3)_{0.06}\cdot n\,H_2O$ and spindle-shaped crystals of hydroxide $Ln(OH)_3$. The method was also used to produce hydrated (100 °C, 24 h)[190] and anhydrous (150 °C, 24 h)[140] layered rare-earth hydroxysulfates; most of them belong to the LREH-II category.

Hydrolysis of lanthanide salts in aqueous solutions can be initiated not only by sodium, potassium and ammonium hydroxides, but also nitrogen-containing organic bases including triethylamine[24, 150, 186] and tetrabutylammonium hydroxide.[187] To obtain well-crystallized compounds, precipitation products of rare-earth salts are exposed to hydrothermal treatment at 120–200 °C for 18–120 h. Hydrothermal treatment in the presence of triethylamine is first of all used to grow single crystals of layered hydroxides and basic salts. This approach was used to synthesize single crystals of layered hydroxides belonging to the LREH-I (Refs 24 and 186) and LREH-III (Ref. 150) categories for subsequent structure determination. The synthesis in the presence of tetrabutylammonium hydroxide produces ultrathin (4–9 nm) plate-like crystals of layered rare-earth hydroxynitrates belonging to the LREH-I category; this feature was explained by adsorption of $Bu^n_4N^+$ cations on the surface of crystals being grown and by blockage of their growth along the [001] direction. Attempts to produce such crystals using other precipitating agents failed.[124, 156, 171]

Layered rare-earth hydroxides are also synthesized by solvothermal treatment in aqueous ethanol[127, 166, 171, 188] or methanol[135] solutions at 120–200 °C for 3–16 h. Compounds $Ln_2(OH)_5NO_3\cdot MNO_3$ (Ln = La, Nd; M = K, Rb, Cs) are synthesized in pure ethanol using various alkalis (KOH, RbOH, CsOH) as precipitating agents. Bringing corresponding reaction mixtures into contact with water causes the formation of colloidal solutions of plate-like crystals of hydroxides $Ln_2(OH)_5NO_3\cdot x\,H_2O$ 2–8 nm thick.[171]

A method has been proposed for the synthesis of LRHs belonging to the LREH-I category in the presence of water–alcohol solutions of polyethyleneimine.[127, 166] Polyethyleneimine is adsorbed on the surface of LRH particles, which does not deteriorate the anion-exchange properties of layered hydroxides and allows one to prepare stable dispersions based on them in organic solvents. This technique was utilized for the first-time preparation of bismuth-[135] and cerium-[127] doped layered yttrium hydroxychlorides.

Solvothermal treatment in the presence of oleylamine[185, 193] is suitable to obtain nanowires (Fig. 17) of LRHs (Pr, Nd, Sm, Eu, Gd) intercalated with acetate, formate or propionate anions. The compositions of the reaction products [*e.g.*, $Gd(OH)_{2.58}(OAc)_{0.42}\cdot 0.29\,H_2O$ and $La(OH)_{1.99}(OAc)_{1.02}\cdot 0.61\,H_2O$] suggest that they can belong to both LREH-I and LREH-II categories. Layered gadolinium hydroxide was for the first time synthesized in reverse microemulsions using oleylamine as hydrophobic component, a base and surfactants (oleylamine, butan-1-ol).[194]

Summing up, precipitation using strong bases allows one to obtain LRHs belonging to any category and to vary their chemical composition, crystal structure and morphology over a wide range. Utilization of nitrogen-containing organic bases provides the possibility to synthesize colloidal solutions of LRHs (first of all, LREH-I compounds) in various solvents.

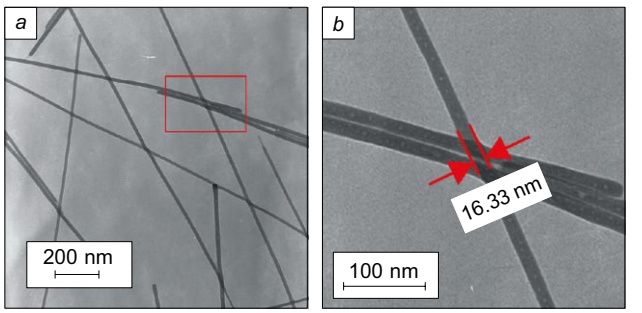


Figure 17. TEM images of layered lanthanum hydroxyacetate nanowires ~16 nm in diameter at different magnitudes.[193]

5.2. Homogeneous hydrolysis

Homogeneous hydrolysis is a method for preparing inorganic materials. It is based on the creation of low and controlled supersaturation using various water-soluble organic reactants capable of undergoing a slow hydrolysis with the formation of hydroxide ions.[195] The technique allows one to avoid the onset of high local concentration gradients and to prepare solid-phase products with specified microstructure (*e.g.*, hydroxides and hydrated oxides).

5.2.1. Homogeneous hydrolysis in the presence of hexamethylenetetramine

Appropriate organic reactants include urea and its analogues, hexamethylenetetramine (HMT), formamide and melamine. Most often, LRHs are synthesized in the presence of HMT. Hydrolysis of this compound begins at 50–60 °C and abruptly accelerates at 140–160 °C.[196–198]

$$(CH_2)_6N_4 + 6\,H_2O \longrightarrow 6\,CH_2O + 4\,NH_3 \quad (2)$$

$$NH_3 + H_2O \longrightarrow NH_3\cdot H_2O \quad (2a)$$

These equations do not give a complete picture of the processes proceeding in the reaction medium.[199] In particular, formaldehyde formed in reaction (2) can be oxidized to formic acid and carbon dioxide.

$$CH_2O + \frac{1}{2}O_2 \longrightarrow HCOOH \quad (3)$$

$$HCOOH + \frac{1}{2}O_2 \longrightarrow CO_2 + H_2O \quad (3a)$$

The formation of formic acid in the course of the synthesis causes a decrease in the yield of the reaction product owing to partial dissolution of the product.[198]

To prepare LRHs, aqueous solutions containing a corresponding salt and HMT mixed in a nearly 1 : 1 mole ratio and the salt with the anion to be intercalated are boiled in nitrogen atmosphere or treated under hydrothermal conditions (at 90–140 °C) for 4–20 h. The hydrolysis of HMT initiates hydrolysis of the salt, which results in the formation of the LRH; this is accompanied by intercalation of the anion present in excess in the reaction mixture into the interlayer space. The processes can be described by the following equation:

$$2\,Ln^{3+} + \frac{7}{4}(CH_2)_6N_4 + 3\,A^{2-} + (15\frac{1}{2} + n)\,H_2O \longrightarrow \quad (4)$$
$$\longrightarrow Ln_2(OH)_5A_{1/2}\cdot(n-2)\,H_2O + 10\frac{1}{2}CH_2O +$$
$$+ 2\frac{1}{2}(NH_4)_2A + 2\,NH_3\cdot H_2O$$

where A^{2-} is the anion to be intercalated. The technique yields the LREH-I compounds containing chloride,[112,114,128,200] nitrate[119,137,138,147,201–212] or dodecyl sulfate anions,[213–215] and the LREH-II compounds containing sulfate[139,145] or alkanedisulfonate anions.[148] Using this method, Gu and co-workers[205] obtained layered europium hydroxide intercalated with octanesulfonate and 8-hydroxypyrene-1,3,6-trisulfonate anions.

The synthesis carried out in the presence of HMT usually produces regularly shaped plate-like microcrystals (Fig. 18); however, the crystal morphology can vary significantly in the presence of amphiphilic anions. In particular, the synthesis using sodium dodecyl sulfate gives conical crystals formed by rolling up flat yttrium hydroxide bilayers (Fig. 19).[215]

The formation of layered hydroxides begins after 1 h of heat treatment of the reaction mixture;[119] however, the duration of the reaction is considerably increased to increase the product yield and the degree of crystallinity. If there is no excess amount of the anion to be intercalated into the interlayer space, the yield of LRHs is low.[119]

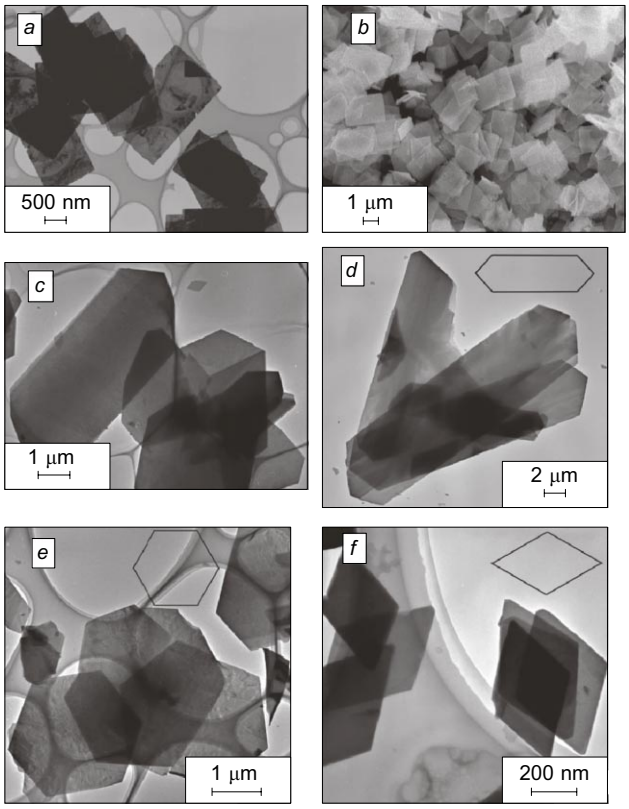


Figure 18. TEM (*a*, *c*–*f*) and SEM (*b*) images of $Eu(OH)_{2.5}Cl_{0.5}\cdot n\,H_2O$ (*a*), $Sm(OH)_{2.5}Cl_{0.5}\cdot n\,H_2O$ (*b*), $Y(OH)_{2.5}Cl_{0.5}\cdot n\,H_2O$ (*c*), $Gd(OH)_{2.5}(NO_3)_{0.5}\cdot n\,H_2O$ (*d*), $Dy(OH)_{2.5}(NO_3)_{0.5}\cdot n\,H_2O$ (*e*), $Er(OH)_{2.5}(NO_3)_{0.5}\cdot n\,H_2O$ (*f*) synthesized by refluxing for 10–12 h in the presence of HMT.[118] Geometric figures in panels *d*–*f* illustrate the predominant shape of crystals.

A new efficient method for the synthesis of the LREH-I compounds including those of yttrium,[120] gadolinium[216] and europium[217] is based on microwave-assisted hydrothermal treatment of lanthanide salts solutions in the presence of HMT. Compared to conventional heating, microwave-assisted hydrothermal treatment is not accompanied by the onset of high temperature gradients and enables much higher heating rate. As a consequence, the LRH synthesis duration decreases from a few hours to nearly a minute at a high yield (~80% and more) and degree of crystallinity of reaction products.

Studies on the influence of the key parameters of the synthesis (temperature and duration of microwave-assisted hydrothermal treatment,[216] ionic strength of the solution,[120] filling factor of the hydrothermal reactor and microwave power[217]) on the composition and morphology of reaction products allowed one to determine the formation conditions of single-phase layered compounds with the lowest content of impurities including carbonate-containing lanthanide phases. These are as follows: the temperature range of 140–180 °C, the filling factor of the hydrothermal reactor <45% and the lanthanide salt concentration <10 mmol L^{-1}.

A distinctive feature of the synthesis of layered rare-earth hydroxynitrates in the presence of HMT, which was not observed earlier for LRHs,[120] is the formation of spheroidal aggregates comprised of plate-like crystals (Fig. 20). The possibility of formation of similar structures

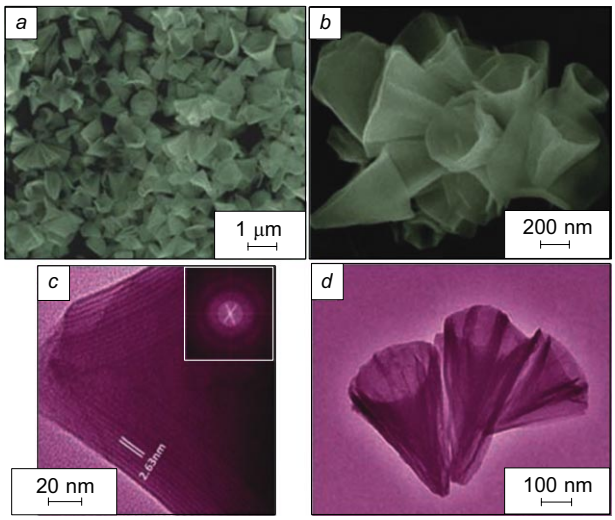


Figure 19. SEM (*a*, *b*) and TEM (*c*, *d*) images of layered yttrium hydroxide synthesized by homogeneous precipitation at 140 °C in the presence of sodium dodecyl sulfate.[215]

was reported for ZnO,[218] $CaCO_3$,[219] CoOOH,[220] and $[Ni(N_2H_4)_3](NO_3)_2$.[221] The mechanism of formation of spheroidal aggregates is usually treated as self-assembly and oriented attachment of nuclei in the initial stages of synthesis.[222]

Precipitation and homogeneous hydrolysis in the presence of the salt of the intercalating anion seem to be especially promising for the preparation of LRHs with bulky interlayer anions. For instance, homogeneous hydrolysis under microwave-assisted hydrothermal treatment conditions was used to synthesize the first representative of a new category of LRHs containing cluster anions, *viz.*, layered yttrium hydroxide intercalated with *closo*-dodecaborate anion.[223]

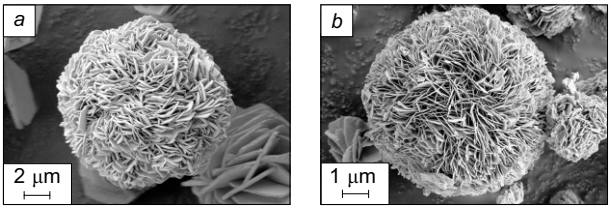


Figure 20. SEM images of layered yttrium (*a*) and gadolinium (*b*) hydroxynitrates synthesized using microwave-assisted hydrothermal treatment in the presence of HMT (unpublished working materials for Refs 120 and 219).

5.2.2. Homogeneous hydrolysis in the presence of urea

Studies on the synthesis of LRHs by homogeneous hydrolysis in the presence of urea are scarce. For instance, a LREH-I-type layered yttrium hydroxide was synthesized in the presence of urea in the heterophase systems xylene – water and butanol – water at 80 °C.[224] Urea and yttrium nitrate were dissolved in the aqueous phase, while the carboxylic (benzoic, sebacic or lauric) acid was dissolved in the organic phase. Owing to the presence of excess amount of the acid in the organic phase the concentration of the organic anions A in the aqueous phase is maintained at a desired value throughout the synthesis, which allows one to obtain crystalline products in one step. The corresponding reaction scheme is as follows:

$$2\,Ln^{3+} + \frac{5}{2}(NH_2)_2CO + 6\,A^- + (7\frac{1}{2} + n)\,H_2O \longrightarrow \quad (5)$$
$$\longrightarrow Ln_2(OH)_5A \cdot n\,H_2O + 2\frac{1}{2}CO_2 + 5\,NH_4A$$

5.2.3. Homogeneous hydrolysis in the presence of melamine

The list of slowly hydrolyzing reactants for the synthesis of layered hydroxides using homogeneous precipitation under hydrothermal conditions[225] is not limited to urea and HMT. An example is provided by melamine (1,3,5-triazino-2,4,6-triamine), which was for the first time proposed[226] and used[226] for the synthesis of metal hydroxides and oxides (including LRHs) using homogeneous hydrolysis under microwave-assisted hydrothermal treatment conditions. Melamine is a weak base that can undergo a slow hydrolysis with the formation of ammonium hydroxide under hydrothermal conditions.[227, 228] The amino groups of melamine are replaced by OH groups with the formation of ammonia and certain melamine derivatives including ammeline (4,6-diamino-2-hydroxy-sym-triazine), ammelide (6-amino-2,4-dihydroxy-*sym*-triazine) and cyanuric acid (2,4,6-trihydroxy-*sym*-triazine). Melamine or products of its hydrolysis can undergo condensation with the formation of melam, melem and melon.[228 – 230]

Hydrolysis of melamine under microwave-assisted hydrothermal treatment conditions begins at temperatures above 130 °C (Fig. 21). In this case the process involving europium nitrate affords $Eu_2(OH)_5NO_3 \cdot n\,H_2O$ and can be described as follows:

$$2\,Ln^{3+} + 1\frac{2}{3}C_3N_6H_6 + 6\,NO_3^- + (10 + n)\,H_2O \longrightarrow \quad (6)$$
$$\longrightarrow Ln_2(OH)_5NO_3 \cdot n\,H_2O + 1\frac{2}{3}C_3N_3O_3H_3 + 5\,NH_4NO_3$$

The technique allows one to control the microstructure of the product by varying the melamine : europium nitrate ratio. At high melamine concentrations, weakly aggregated plate-like crystals are formed, whereas the process conducted at low melamine concentrations produces spheroidal aggregates of plate-like crystals.[226]

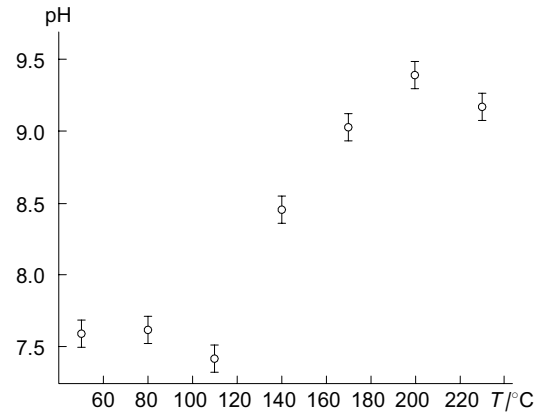


Figure 21. Temperature dependence of pH values of aqueous melamine solutions (0.05 mol L^{-1}) exposed to 60-min microwave-assisted hydrothermal treatment at different temperatures (50 – 230 °C).[226]

Summing up, methods for the synthesis of LRHs have been well developed to date and enable the preparation of various categories of LRHs intercalated with organic and inorganic anions and variation of their microstructure from nanoparticles to large single crystals. The decisive role in the synthesis of LRHs is played by the type of the precipitating agent, the temperature and the duration of heat treatment. Precipitation using strong bases offers prospects for the preparation of various LRHs of different composition; however, the corresponding procedures are time-consuming, some of them require high temperatures and do not ensure control of the product morphology. Homogeneous precipitation (especially its microwave-assisted version) accelerates the synthesis of LRHs and allows one to obtain products with specified composition and morphology. Methods of synthesis of intercalated LRHs are not limited to the one-step techniques described above and involve anion-exchange reactions that will be thoroughly considered below.

6. Modification of layered rare-earth hydroxides

A distinctive feature of LRHs is the possibility to vary their composition over a wide range with retention of the main structural motif. The crystal structure of LRHs enables the following:

— variation of the cationic composition of the host layers through replacement of certain rare-earth cations by some other rare-earth cations;

— variation of the anionic composition by carrying out anion-exchange reactions including simultaneous intercalation of different-type anions with specific functions;

— exfoliation of layered hydroxides and subsequent reassembly of multilayer structures;

— replacement of OH groups in the host layers by fluoride or phosphate ions; and

— synthesis of rare-earth oxo compounds by heat treatment of layered hydroxides.

Such a compositional variability with retention of the structural motif significantly differs LRHs from other compounds. Layered rare-earth compounds can be considered as occupying an intermediate position between molecular complexes and ionic crystals (coordination polymers, *etc*.). This Section is devoted to main methods of modification of LRHs, *viz*., anion-exchange reactions, modification of the host layers, as well as exfoliation and subsequent assembly of layers.

6.1. Anion-exchange reactions

Layered rare-earth hydroxides belong to anion exchangers and are characterized by record-high surface charge density (SCD) values among layered ion-exchangeable inorganic materials (Table 2), which is indicative of high ion-exchange capacity (C) of these materials.

$$C \approx \frac{\rho_m}{\rho_a}$$

where ρ_m is the SCD of the layered material and ρ_a is the anion-charge-to-anion-size ratio. The SCD (ρ_{LRH}) values for LRHs are determined from crystallographic data for rare-earth hydroxychlorides[112] for the LREH-I category and from the data for rare-earth hydroxysulfates[145] for the LREH-II compounds. Lanthanide contraction causes the ρ_{LRH} value to slightly increase throughout the lanthanide series from 0.041 to 0.045 e Å^{-2} for the LREH-I compounds and from 0.075 to 0.087 e Å^{-2} for the LREH-II compounds.

Table 2. Surface charge density for metal hydroxide layers in inorganic layered ion-exchangeable compounds.

Material	SCD /e Å^{-2}	Ref.
Natural materials		
Laponite $Na[(Si_8Mg_{5.5}Li_{0.4})O_{20}(OH)_4]$	0.014	231, 232
Hectorite $Na_{0.3}(Mg,Li)_3(Si_4O_{10})(F,OH)_2$	0.008 – 0.010	233
Montmorillonite $(Na,Ca)_{0.33}(Al,Mg)_2(Si_4O_{10})(OH)_2 \cdot n\,H_2O$	0.011 – 0.017	233
Layered double hydroxides		
Mg_3Al-NO_3	0.031	234, 235
Zn_2Al-NO_3	0.041	234
Ca_2Al-Cl	0.035	234
$LiAl_2-NO_3$	0.041	234
Zn_2Cr-NO_3	0.040	234
Ni_2Al-NO_3	0.040	234
Layered rare-earth hydroxides		
LREH-I	0.041 – 0.045	56, 112, 119
LREH-II	0.075 – 0.087	145

A comparison of the ρ_{LRH} and ρ_a values provides information on the packing of interlayer anions, namely, anions form a monolayer if $\rho_{LRH} < \rho_a$ and a bilayer if $\rho_{LRH} > \rho_a$.[214]

Anion exchange involving LRHs can be described by the following scheme:

$$Ln_2(OH)_{6-x}(A^{a-})_{x/a} \cdot n\,H_2O + \frac{y}{b}B^{b-} + (m-n)\,H_2O \longrightarrow \quad (7)$$

$$\longrightarrow Ln_2(OH)_{6-y}(B^{b-})_{y/b} \cdot m\,H_2O + \frac{x}{a}A^{a-} + (y-x)\,OH^-$$

where A^{a-} and B^{b-} are the exchanging anions and x and y take values from 1 to 2.

Different classes of LRHs manifest their anion-exchange properties in different manner owing to structural differences between them. The proportion of anions that form covalent bonds with metal hydroxide layers increases in the order LREH-I, LREH-III, LREH-II and therefore the anion exchangeability (at least at room temperature) decreases. Indeed, anion-exchange reactions involving the LREH-I and LREH-III compounds proceed at room temperature,[114, 150] whereas the LREH-II compounds react only at elevated temperatures.[236] The vast majority of anion-exchange reactions are carried out using rare-earth hydroxynitrates and hydroxychlorides from the LREH-I category.[114, 124] Layered yttrium, dysprosium, erbium and ytterbium hydroxybromides[123] as well as LRHs intercalated with dodecyl sulfate[215] or ethanedisulfonate anions[150] also exhibit anion-exchange properties at room temperature.

Intercalation of anions into the interlayer space of LRHs is most often confirmed by powder X-ray diffraction data. Positions of the 00l reflections are used to determine the basal interplanar distance. Changes in this parameter provide information not only on the fact of intercalation of the anion into the LRH structure, but also on the arrangement of the anion in the interlayer space.[124, 167] However, if

the sizes of the anions being exchanged are close along at least one direction, the interplanar distance can remain unchanged in the course of the anion-exchange reaction.[164] This parameter is evaluated by subtracting the average thickness of a metal hydroxide layer (5.5–6.5 Å) from the basal interplanar distance.[112, 114, 223, 237] By comparing the size of the anion with the interplanar distance one can assess the character of localization of the anion in the interlayer space, namely, the packing type (anionic mono- or bilayer), orientation of anions relative to the metal hydroxide layers, *etc.*[137, 238]

The basal interlayer distances (d_{002}) in rare-earth hydroxynitrates and products of their anion-exchange reactions with potassium fluoride and ammonium sulfate are plotted *vs.* ionic radii of the lanthanide in Fig. 22.[111] Intercalation of fluoride anions in all cases leads to a considerable decrease in d_{002}. Shortening of the basal interlayer distance throughout the lanthanide series can be explained by an increase in the charge density on the metal hydroxide layers and, therefore, by strengthening of the interaction between fluoride anions and the host layers of LRHs. Among layered rare-earth hydroxysulfates, this behaviour is observed only for heavier lanthanides and yttrium. Layered rare-earth hydroxynitrates do not obey this trend. An increase in the basal interlayer distance for layered yttrium hydroxynitrates can be explained by rotation of the nitrate anion plane by 90° relative to the host layers.[111]

Anion-exchange reactions with LRHs are carried out in aqueous, water–alcohol[174, 215, 239] and aqueous formamide[202] solutions containing excess amounts of the intercalating ion (A^{n-} : LRHs = 2–15). Usually, organic solvents are used since salts and intercalating acid residues are poorly soluble or unstable in aqueous media. The reactions take from 30 min to several days to complete at room temperature or under hydrothermal conditions (70–140 °C). As a rule, anion-exchange reactions are conducted in neutral media (pH ≈ 7 and higher), where the corresponding acid is fully deprotonated. When using polybasic acids, various acid anions can exist, and each type of anions is intercalated at specific pH value.[205, 207] By varying

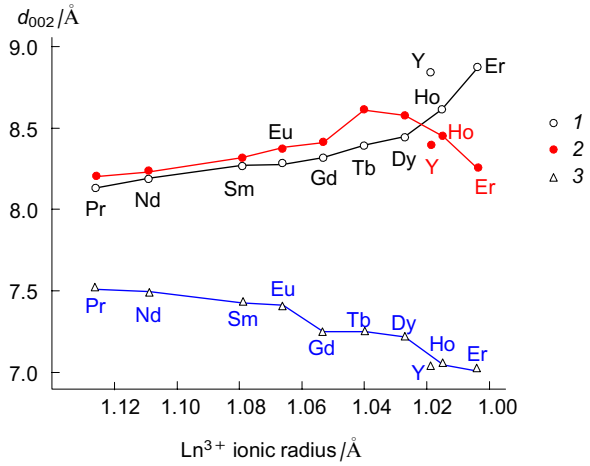


Figure 22. Basal interlayer distances in layered rare-earth hydroxynitrates (*1*), hydroxysulfates (*2*) and hydroxyfluorides (*3*) plotted *vs.* lanthanide ionic radii.[111]

the anion : lanthanide ratio one can vary the arrangement of anions in the interlayer space of LRHs.[210] For instance, anion-exchange reactions between layered europium hydroxynitrate and naproxen taken in different ratios resulted in products with different interlayer distances; this can be due to different anion arrangement patterns in the interlayer space (Fig. 23).[210]

Main criteria for the possibility of intercalating LDHs with anions are known.[17, 86] This is not the case for LRHs; however, similarity between LRHs and LDHs gives grounds to assume that such criteria can exist. In particular, anions can be arranged as follows with respect to their ability to participate in the ion-exchange reactions with LDHs:[85, 86, 111, 240]

$$CO_3^{2-} > SO_4^{2-} > OH^- > F^- > HPO_4^{2-} > Cl^- > Br^- > NO_3^- > I^-$$

This sequence was established using the results of comparison of the equilibrium constants of anion-exchange

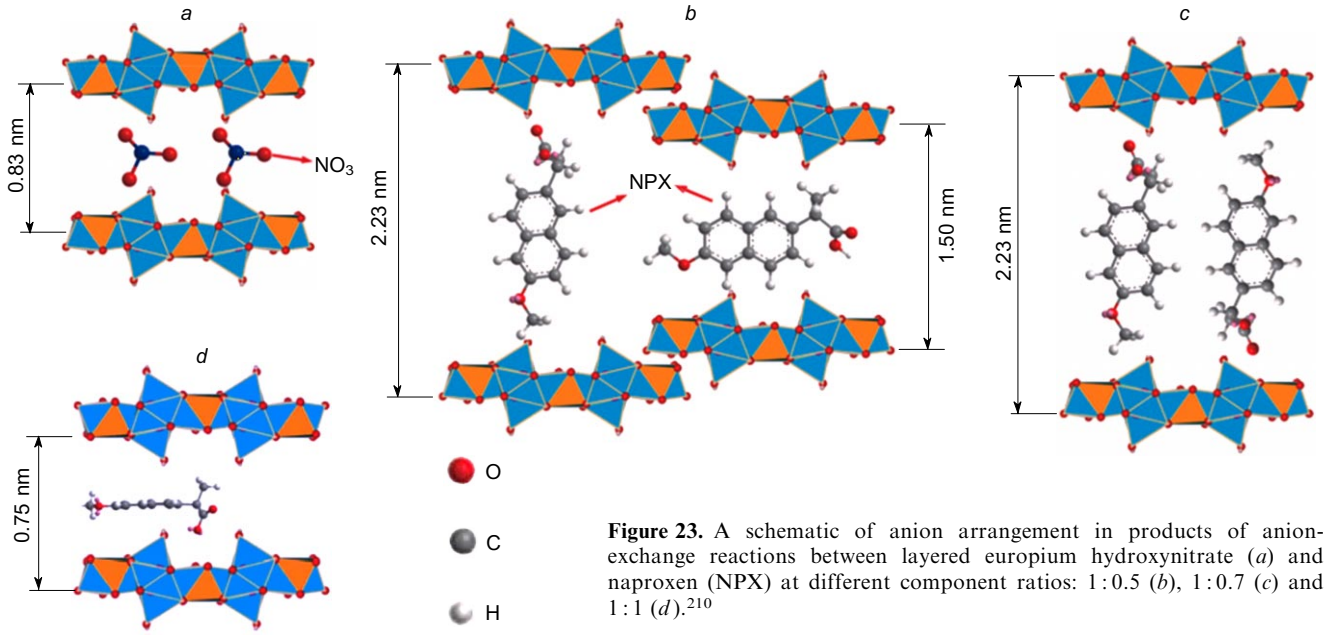


Figure 23. A schematic of anion arrangement in products of anion-exchange reactions between layered europium hydroxynitrate (*a*) and naproxen (NPX) at different component ratios: 1 : 0.5 (*b*), 1 : 0.7 (*c*) and 1 : 1 (*d*).[210]

reactions determined from the sorption isotherms of ion exchangers.[241] Since the equilibria of similar reactions of LRHs were not studied, an analysis is restricted to the following series of anions arranged with respect to their ability to coordinate to rare-earth ions:[242]

$$PO_4^{3-} > CO_3^{2-} > HPO_4^{2-} > SO_4^{2-} > OH^- > F^- > H_2PO_4^- >$$
$$> NCS^- > NO_3^- > Cl^- > ClO_4^-$$

The leftmost positions of carbonate ions in the series indicate that they are with certainty intercalated into LRHs.

The kinetics of anion-exchange reactions of LRHs has been very poorly studied. Anion-exchange reactions of LDHs are successfully investigated using methods of solid-phase kinetics [87] that also seem to be applicable in the case of LRHs. Kinetic studies of ion exchange in the LREH-I compounds involved sampling followed by analysis of solid and liquid samples using X-ray diffraction analysis,[243] high-performance liquid chromatography,[207] as well as UV-vis [210] and luminescence spectroscopies.[243] For instance, from powder X-ray diffraction and luminescence spectroscopy data [243] it follows that exchange of Cl^- anions for NO_3^- in Tb- or Ce-intercalated layered gadolinium hydroxide proceeds much slower than the exchange of NO_3^- anions for Cl^-. UV-vis spectroscopy data revealed that (S)-6-methoxy-α-methyl-2-naphthaleneacetate anion (naproxen) is released from layered europium hydroxide in phosphate buffer simulating physiological conditions (Na_2HPO_4–NaH_2PO_4, pH 6.86, 37 °C) at high rate (91% after 135 min).[210] The release rate of acetylsalicylate anion from layered terbium hydroxide under identical conditions is 90% after 36 h.[207] Different rates of these anion-exchange reactions are probably indicative of different abilities of the released anions to form hydrogen bonds. The kinetic analysis of anion-exchange reactions was for the first time carried out taking exchange of various pharmaceuticals (naproxen, diclofenac, ibuprofen) by carbonate anion in layered gadolinium hydroxide as an example. The kinetic curves were described within the framework of the Avrami–Erofeev and Bhaskar diffusion models.[192] Both models correctly describe experimental data, thus substantiating that ion exchange is a diffusion-controlled process.[192]

Recently, there has been an increasing number of studies on the synthesis of LRH-based hybrid structures containing two types of anions [137, 138, 201, 205, 211, 212, 238, 244] with different properties. For instance, octanesulfonate anion is co-intercalated with organic luminophores,[137, 244] Eu^{3+} luminescence sensitizers,[138, 201] and pharmaceuticals.[212] The presence of octanesulfonate anion enables subsequent exfoliation of the hybrid structures and their transformation to colloids. The octanesulfonate anion is the structure-forming component of the compounds, while the content of the second anion is usually a few per cent (mol/mol). A hybrid LRH ($Gd:Tb_{0.5-x}Eu_x$, $x = 0-0.5$) containing a bulky luminophore and a small sensitizer ion (salicylate anion) was reported.[238]

In addition to anion-exchange reactions, layered structures with different interlayer anions are often prepared by hydrolysis of rare-earth elements in the presence of the intercalating anion (see Section 5). Quasi-2D particles of exfoliated LRHs are formed by self-assembly (see below). Methods for the preparation of such particles (exfoliation) are described in the next Section. The synthesis of layered europium hydroxide intercalated with the heteropolyanion $[EuW_{10}O_{36}]^{9-}$ through self-assembly is schematically shown in Fig. 24.[245] A similar procedure was used to synthesize layered europium and gadolinium hydroxides modified with molybdenum compounds.[246] Colloidal solutions of layered europium and gadolinium hydroxides were mixed with a sodium molybdate solution at different pH values (from 4 to 10). At pH > 5, $Gd_2(OH)_5(MoO_4)_{0.5} \cdot n H_2O$ with a Mo:Gd ratio of 0.25 was prepared. As pH decreased to 5, the Mo:Gd ratio increased to ~1.3 due to the formation of layered gadolinium hydroxide intercalated with the heptamolybdate ion ($Mo_7O_{24}^{6-}$).

Surface modification of LRHs is also possible (for exfoliated LRHs the surface and the interlayer space coincide). This can be done using various compounds including, *e.g.*, folic acid [247] and 2-thenoyltrifluoroacetone.[248] Folic acid increases the biocompatibility of LRHs, while 2-thenoyltrifluoroacetone is an efficient sensitizer of Eu^{3+} luminescence in the layered yttrium–europium hydroxide.

To date, LRHs have been intercalated with the following types of interlayer anions:

— inorganic anions: Cl^-,[128] Br^-,[123] I^-,[243] NO_3^-,[122] SO_4^{2-},[145] CrO_4^{2-},[179] ClO_3^-,[243] MoO_4^{2-};[246]

— polyoxometallates and heteropolyanions: $Mo_7O_{24}^{6-}$,[246] $[H_2W_{12}O_{42}]^{10-}$,[249] $[EuW_{10}O_{36}]^{9-}$;[245]

— cluster anion: *closo*-dodecaborate anion $[B_{12}H_{12}]^{2-}$;[223]

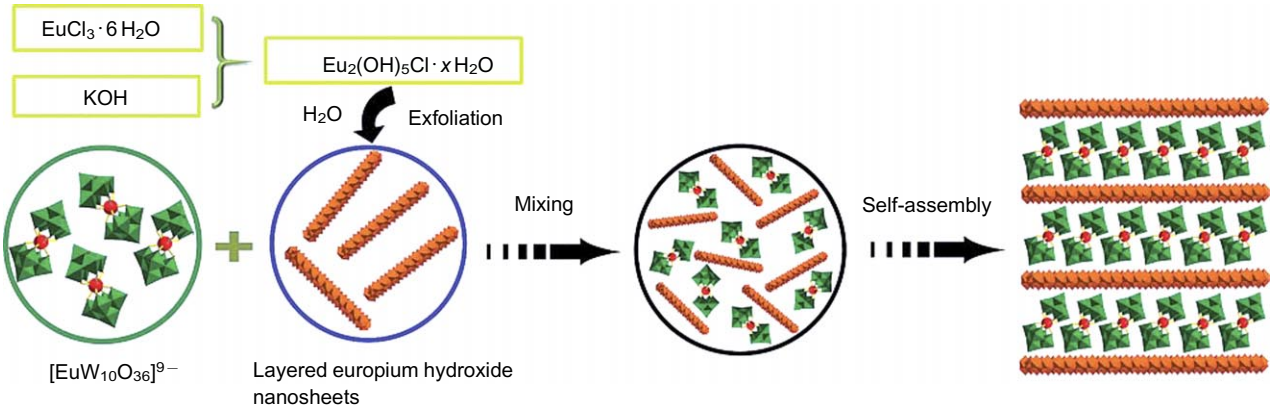


Figure 24. Hybrid structure comprising layered europium hydroxide and $[EuW_{10}O_{36}]^{9-}$ anions: a schematic of self-assembly.[245]

— organic anions (molecules): oleate,[178] aliphatic sulfates,[167] aliphatic sulfonates,[167] aliphatic carboxylates [171] and dicarboxylates,[124] acetylacetonates,[248] porphyrins,[127, 165] ethylene glycol and glycerol;[174] amino acid anions,[208] benzenecarboxylic acid anions [206, 237] and more complex carboxylic and sulfonic acid anions;[168]

— coordination compounds: complexes of carboxyethyl-substituted azacrown ether with various cations,[204] a palladium complex with a porphyrin,[165] lanthanide complexes with picolinic acid [250] and hexafluoroacetone.[251]

Summing up, the arrangement of anions in the interlayer space of LRHs is determined by the anion size, shape, charge and by the fashion of their coordination to the metal hydroxide layer. For instance, dodecyl sulfate anions form a bilayer packing when coordinated to the metal centres of the host layers (LREH-II compounds) and a monolayer packing when uncoordinated (LREH-I compounds).[214] The coordination fashion can be controlled by varying the anion-exchange reaction conditions or using one-step methods for the synthesis of intercalated LRHs. Bulky anions (in particular, polyoxometallates and heteropolyanions, cluster anions) cannot be intercalated into LRHs using anion-exchange reactions; self-assembly [249] and synthesis of LRHs in the presence of the intercalating anion [223] are used instead.

6.2. Exfoliation

Many layered compounds are prone to exfoliation to monoatomic layers or their stacks. The best-known examples are provided by graphite, molybdenum sulfide and boron nitride.[49, 252] The discovery of graphene led to the development of various exfoliation techniques (from simple peeling to chemical methods) aimed at breaking weak van der Waals interactions in the layered substances.[49, 252, 253] Electrostatic interactions between layers are much stronger; nevertheless, they can also be broken. Among layered compounds with charged layers, cation-exchangeable clays (laponite, hectorite, montmorillonite) can be exfoliated most readily. In their structure adjacent layers are largely separated, weakly charged and are therefore loosely bound to the interlayer anions. An increase in the surface charge density in the hydroxide layers and a decrease in the interlayer distance (see Table 2) make exfoliation more difficult. Considering LDHs and LRHs, not only electrostatic forces between anions and host layers, but also hydrogen bonds between the host layers and the interlayer anions (water molecules) should be broken.

The most widely used method of exfoliation of LRHs is based on the interaction with FM [254] and involves intercalation of layered rare-earth hydroxynitrates [162] or hydroxychlorides (Fig. 25, line *1*) with dodecyl sulfate anions [147, 254] or one-step synthesis of LRHs intercalated with these anions.[214] As a result, one gets layered phases with a basal interplanar distance of about 2.5 – 3.5 nm (line *2*). Dispersion of the LRH thus prepared in FM (0.5 – 3 g L^{-1}) causes the basal interplanar distance to increase to nearly 3.5 nm (line *3*) due to the intercalation of FM molecules into the interlayer space. Intense mixing at 25 °C for 2 – 24 h leads to complete breakdown of the layered structure (line *4*) and formation of a colloidal solution. The yield of the exfoliation product is at most 50%.[254]

Exfoliation of LRHs is confirmed using AFM (Fig. 26 *a*,*b*) and transmission electron microscopy (TEM) data (Fig. 26 *c*).[162, 254] Two-dimensional particles thus formed are nearly 16 – 17 Å thick (*cf.* 9.3 Å for the crystallographic thickness of the metal hydroxide layer). The difference between these values is due to the presence of the surface dodecyl sulfate anions.[254] Electron diffraction data for 2D particles and bulky samples of hydroxychlorides (hydroxynitrates) are mutually consistent (Fig. 26 *d*).

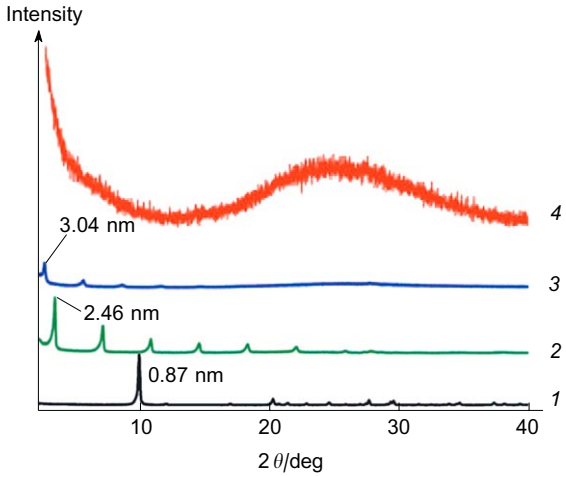


Figure 25. X-Ray diffraction patterns of layered europium hydroxychloride (*1*), layered europium hydroxide intercalated with sodium dodecyl sulfate (*2*), primary product of dispersion of the latter system in formamide (*3*) and exfoliated product obtained by centrifugation (*4*).[254]

Recently, the 'FM' technique is widely used for exfoliation of doubly intercalated LRHs containing octanesulfonate anion (Fig. 27).[137, 138, 201, 211, 212]

Although no long-term stability studies of LRH sols (within a few days) in FM were carried out, one can assume that hydrolysis of FM will proceed [255] provided that LRHs contain water. The products of such a hydrolysis include formic acid;[255] we believe it will react with LRHs to give lanthanide formates, *e.g.*, $[Ln(HCOO)_3 \cdot 2(HCONH_2)]$.[256]

The second most frequently used method for exfoliation of LRHs is the exfoliation in toluene.[178] This is the case for LRHs intercalated with oleate anions; often, the process is conducted under sonication. Intercalation of LRHs with amphiphilic ions increases the basal interplanar distance to 4.7 nm (Fig. 28 *a*,*b*) and to minimize electrostatic interaction between the charged layers. Interaction with toluene causes solvation of hydrophobic fragments of the intercalated anions and weakening of van der Waals interactions between them. Intense stirring and sonication of suspensions thus prepared facilitate the formation of colloidal solutions containing exfoliated particles (Fig. 28 *c*). The colloidal solutions remain stable over a period of a month or more. Two-dimensional particles are 5 nm thick (AFM data, see Fig. 28 *d*,*e*), which is comparable with the basal interlayer distance in the LRHs intercalated oleate anions and confirms that exfoliation did occur. These colloidal solutions can be used to fabricate rare-earth oxide thin films.[126, 180, 184, 257]

A new method [258] for exfoliation of LRHs intercalated with dodecylsulfate anion is based on the increase in the interlayer distance (by 20%) in layered yttrium hydroxide intercalated with dodecylsulfate anion through penetration of supercritical CO_2 into the interlayer space. The product of the interaction with CO_2 was exfoliated in toluene under sonication.

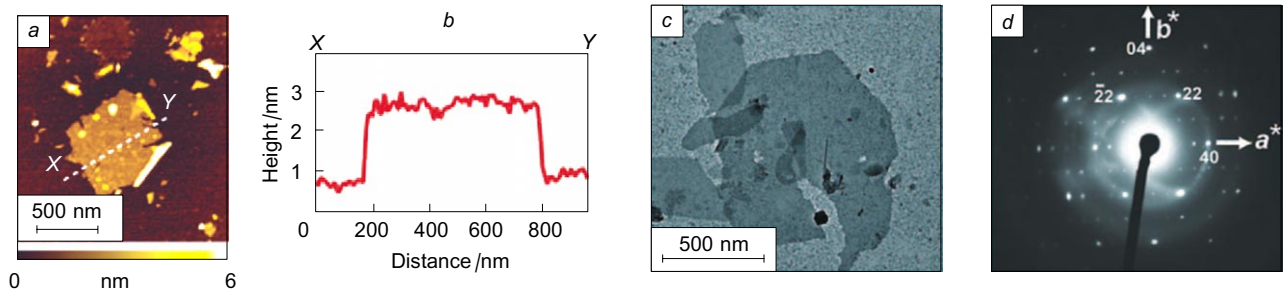


Figure 26. AFM image (*a*), height profile along the $X-Y$ line (*b*), TEM image (*c*) and selected area electron diffraction pattern (*d*) of exfoliated layered europium hydroxide nanosheets.[254]

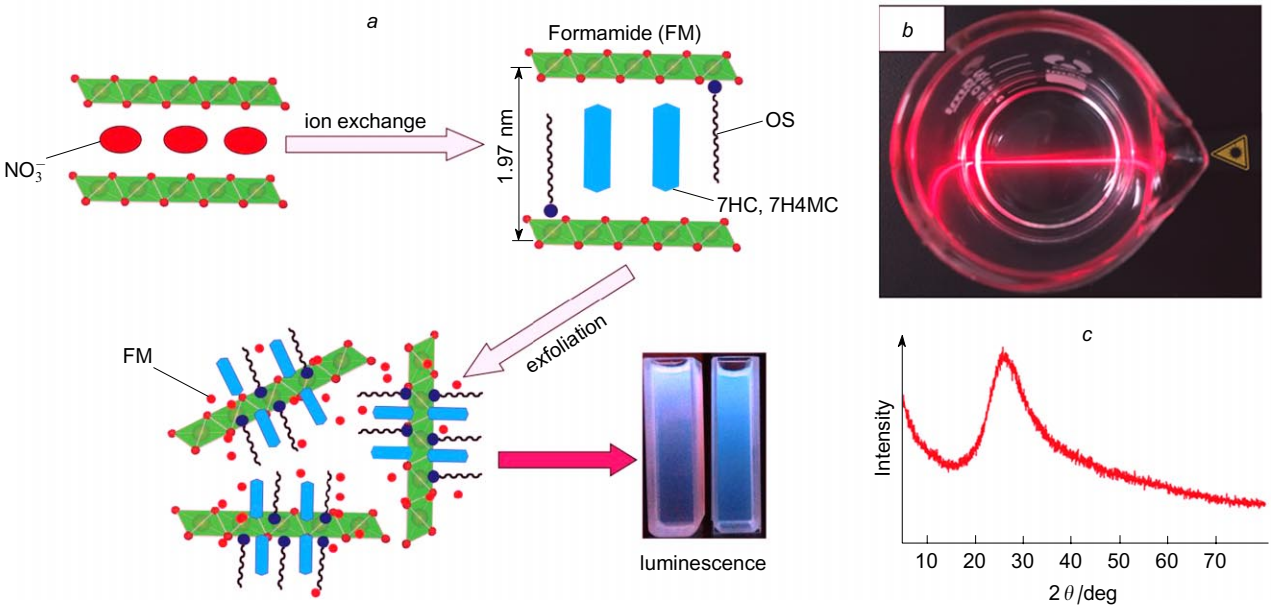


Figure 27. Preparation of sols of layered europium hydroxide intercalated with octanesulfonate (OS) anions, 7-hydroxycoumarin (7HC) and 7-hydroxy-4-methylcoumarin (7H4MC) (*a*),[30] a 1 : 1 photograph of colloidal solution (*b*) and X-ray diffraction pattern of exfoliated layered europium hydroxide intercalated with OS anions and coumarin-3-carboxylate (*c*).[201]

Other solvents for exfoliation of LRHs[129, 130, 248] are also used for exfoliation of LDHs.[76] For instance, exfoliation of layered europium hydroxynitrate in butan-1-ol was reported.[248] Layered hydroxynitrate $Y_{1.9}Eu_{0.1}(OH)_5NO_3 \cdot 2\,H_2O$ was dispersed in butan-1-ol (5 g L^{-1}) and sonicated for 30 min. The colloidal solution thus produced (Fig. 29 *a*) was stable over a period of a month and more. According to AFM data (Fig. 29 *b*,*c*), 2D nanosheets were ~1 nm thick, being indicative of complete exfoliation of the layered hydroxide to monolayers.

Exfoliation of LRHs in aqueous media is also possible.[129, 130] Dispersion of layered rare-earth hydroxynitrates in 1 M glycine solution under sonication produced colloidal solutions with concentrations to 10 g L^{-1}.[129, 130]

6.3. Reactions involving host layers of layered rare-earth hydroxides

Layered rare-earth hydroxides act as precursors of other lanthanide compounds including fluorides, phosphates, peroxides and oxides. These compounds are formed by the topotactic mechanism or by dissolution–precipitation. Topotactic reactions enable more reliable control of the phase composition and microstructure of the compounds formed. In addition, the ratio and homogeneous distribution of rare-earth cations characteristic to mixed layered hydroxides remain unchanged.

Rare-earth phosphates are products of reactions between LRHs and solutions of phosphates including NaH_2PO_4,[259] $(NH_4)_2HPO_4$;[242] in particular, the reaction with the phosphate buffer $Na_2HPO_4-NaH_2PO_4$ is used for drug release from LRHs.[207, 210] Taking $(NH_4)_2HPO_4$ and layered yttrium hydroxynitrate as an example, the process can be described as follows:[242]

$$Y_2(OH)_5NO_3 \cdot n\,H_2O + 2\,(NH_4)_2HPO_4 \longrightarrow \quad (8)$$

$$\longrightarrow 2\,YPO_4 \cdot (n+2)\,H_2O + 3\,NH_3 \cdot H_2O + NH_4NO_3$$

The reaction results in hexagonal yttrium phosphate h-YPO_4 with the rhabdophane structure (Fig. 30 *a*). It is assumed that the reaction proceeds by the topotactic mechanism involving transformation from the [001] planes of layered yttrium hydroxynitrate with pseudohexagonal arrangement of yttrium cations to the [0001] planes of

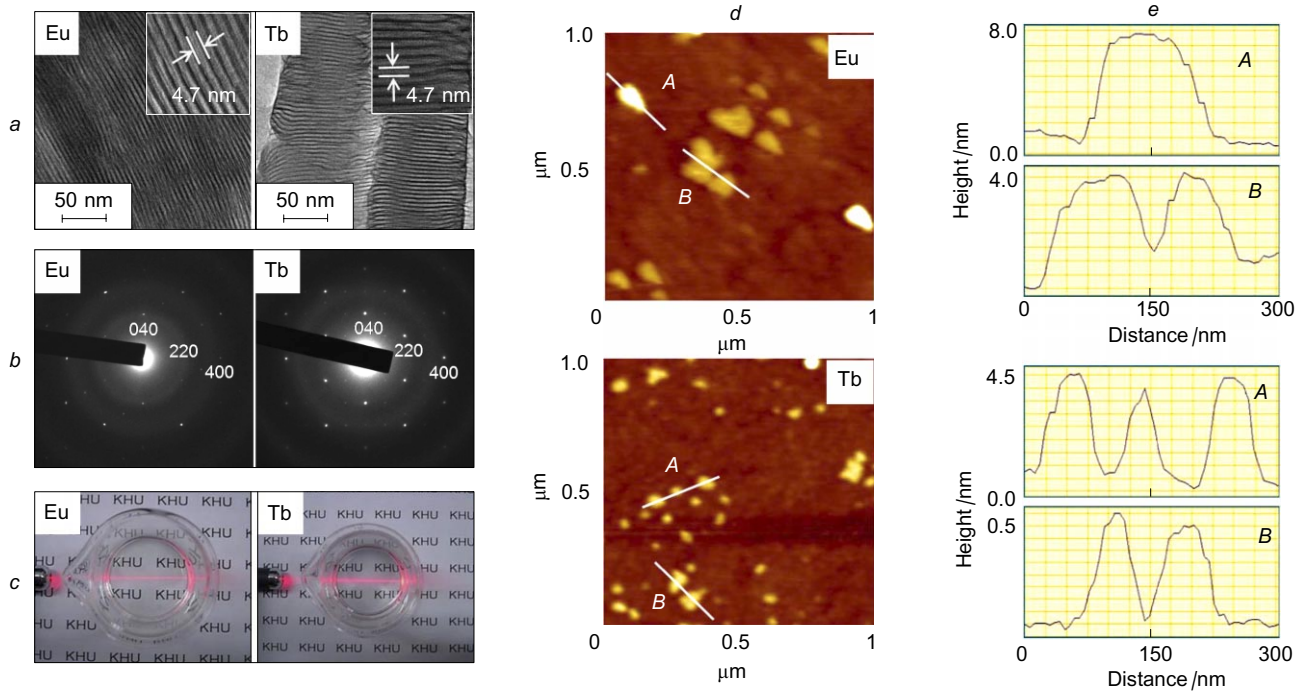


Figure 28. TEM images (*a*) and electron diffraction patterns (*b*) of layered europium and terbium hydroxides intercalated with oleate anions; photographs (*c*), AFM images (*d*) and height profiles along the *A* and *B* lines (*e*) of films prepared from exfoliated layered europium and terbium hydroxides intercalated with oleate anions.[178]

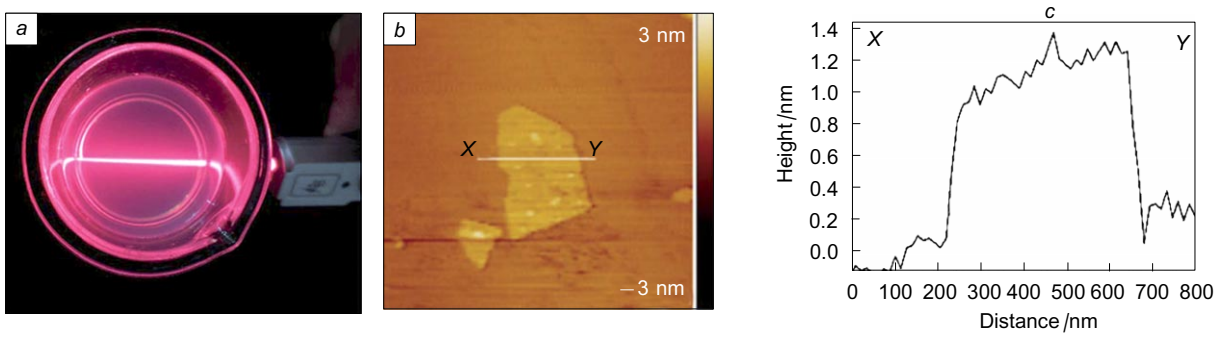


Figure 29. A 1 : 1 photograph of colloidal solution (*a*) and an AFM image of nanosheets of layered hydroxynitrate $Y_{1.9}Eu_{0.1}(OH)_5NO_3 \cdot 2\,H_2O$ dispersed in butan-1-ol (*b*).[248] Panel *c*: height profile along the *X* – *Y* line in panel *b*.

hexagonal yttrium phosphate.[259] Interestingly, the reaction of amorphous yttrium hydroxycarbonate with ammonium hydroxyphosphate affords tetragonal yttrium phosphate t-YPO_4 (Fig. 30 *b*).

Fluorination of LRHs was for the first time considered taking the interaction of layered rare-earth ($Y_{0.95}Eu_{0.05}$ and $Y_{0.78}Yb_{0.20}Er_{0.02}$) hydroxynitrates with aqueous NH_4F solutions at room temperature as an example.[163] The chemical composition of the reaction product was determined by the fluorine : lanthanide mole ratio in the reaction mixture.[163]

$$Ln_2(OH)_5NO_3 \cdot n\,H_2O + NH_4F \longrightarrow \longrightarrow Ln_2(OH)_5F \cdot n\,H_2O + NH_4NO_3 \quad (9)$$

$$Ln_2(OH)_5NO_3 \cdot n\,H_2O + NH_4F \longrightarrow \longrightarrow Ln(OH)_{1.57}F_{1.43} \cdot n\,H_2O + OH^- + NH_4NO_3 + n\,H_2O \quad (10)$$

$$Ln_2(OH)_5NO_3 \cdot n\,H_2O + \frac{20}{3}NH_4F \longrightarrow \longrightarrow \frac{2}{3}NH_4Ln_3F_{10} + 5\,NH_3 \cdot H_2O + NH_4NO_3 + n\,H_2O \quad (11)$$

$$Ln_2(OH)_5NO_3 \cdot n\,H_2O + 7\,NH_4F \longrightarrow \longrightarrow NH_4Ln_2F_7 + 5\,NH_3 \cdot H_2O + NH_4NO_3 + n\,H_2O \quad (12)$$

The reaction of layered rare-earth hydroxynitrate with NH_4F proceeding at F : Ln = 3 results in layered rare-earth hydroxyfluoride [reaction (9)]. An increase in the F : Ln ratio to 6 leads to amorphization of the layered hydroxide due to breakdown of the layered structure upon replacement of OH groups by fluoride anions. At F : Ln = 7, hexagonal hydroxyfluoride $Ln(OH)_{1.57}F_{1.43}$ is formed [reaction (10)]. Further increase in the F : Ln ratio leads to formation of double ammonium/rare-earth fluorides [see

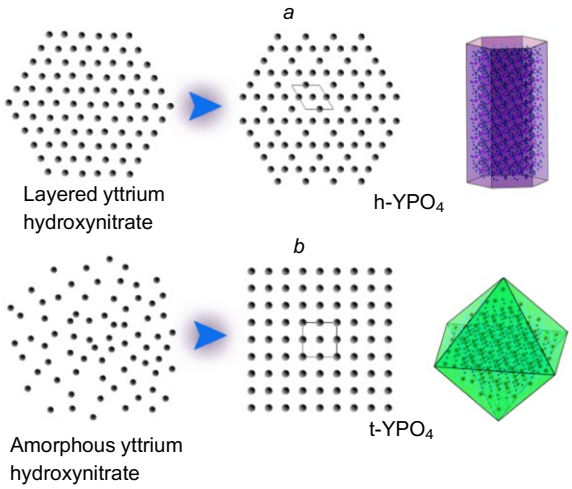


Figure 30. Schematic illustration of topotactic transformation mechanism from layered yttrium hydroxynitrate to hexagonal yttrium phosphate (h-YPO_4) (*a*) and from amorphous yttrium hydroxycarbonate to tetragonal yttrium phosphate (t-YPO_4) (*b*).[259]

reactions (11) and (12)], which can be calcined to obtain pure rare-earth fluorides.

To prepare oxides, LRHs are heat treated; the process is accompanied by decomposition and breakdown of the layered structure. Layered rare-earth hydroxynitrates, hydroxychlorides and hydroxysulfates act as precursors of corresponding oxides;[128, 177, 200, 261] oxychlorides [188, 260] and oxysulfates.[262] Heat treatment of LRHs containing different-type anions is also utilized; for instance, a small impurity of sulfate in layered yttrium hydroxynitrate provides better sinterability of yttria-based ceramics.[170]

Thermolysis of the LREH-I hydroxynitrates involves three main stages:[46]

— loss of physically bound water and water from the interlayer space at temperatures below 200°C; in this step, the high-hydration LRH phase can undergo transition to the low-hydration one;

— removal of chemically bound water and nitrate ions (and impurity carbonate ions) mainly by the pyrohydrolysis mechanism in the temperature range of 200 – 400°C; and

— removal of nitrate ions mainly by the pyrolysis mechanism in the temperature range of 400 – 700°C with the formation of rare-earth oxides.

Decomposition of the LREH-I hydroxynitrates proceeds *via* the formation of $Ln_2O_2(OH)_{2-x}(NO_3)_x$ (Ln = La – Nd), $Ln_2(OH)_5NO_3$ (Ln = Eu, Gd) and $Ln_4O_5(NO_3)_2$ (Ln = Dy – Yb) as intermediate.[36] Decomposition of the LREH-II hydroxynitrates proceeds analogously; however, in this case the intermediates are $LnONO_3$ (Ln = La – Gd) and $Ln_4O_5(NO_3)_2$ (Ln = Dy – Yb).[36]

Often, decomposition of layered hydroxynitrates proceeds with retention of their microstructure. The effect is used to obtain rare-earth oxide particles of specific shape. For instance, the synthesis of LRHs by homogeneous hydrolysis in the presence of dodecylsulfate anions produces particles with cone-like morphology [215] that can act as precursors of cone-shaped oxide particles (precursor is intercalated with nitrate anion and then heat treated).[215]

Thermal decomposition of a peroxo derivative of layered yttrium hydroxynitrate at 580 °C produces 6-nm yttria

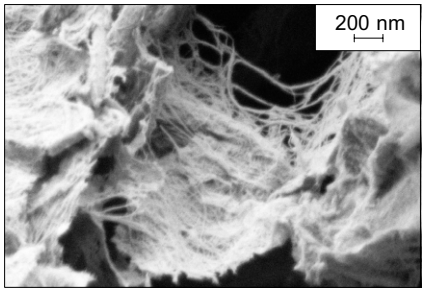


Figure 31. SEM image of yttria prepared from layered yttrium hydroxynitrate treated with 87% aqueous H_2O_2 by annealing at 580 °C.[263]

nanoparticles with filamentary structure atypical of this compound (Fig. 31).

The most interesting precursors of rare-earth oxides are thin (up to 10 nm) plate-like particles of layered rare-earth hydroxynitrates,[187, 264] hydroxychlorides [128, 177, 200] and exfoliated hydroxides intercalated with oleate anions.[126, 180, 257] Heat treatment of films fabricated from such particles causes the formation of corresponding oxide films oriented along the [111] direction. It is assumed that transformation of the LRH to the oxide proceeds by the quasi-topotactic mechanism, *viz*., the (001) plane of the LRH is transformed to the (111) plane of the oxide with slight variation of the mutual arrangement of the in-plane rare-earth cations in the course of heat treatment (Fig. 32).[128, 200]

The thermal decomposition pattern of layered rare-earth hydroxynitrates is determined by the initial crystal structure and by the nature of the rare-earth element. As to the layered rare-earth hydroxychlorides, heating to 600 – 700 °C in most cases (Ln = Y, La – Dy) leads to formation of PbFCl-type rare-earth oxychlorides.[155, 260] Many oxychlorides thus produced can again form LRHs when brought in contact with water (Fig. 33).[155, 265, 266] Such a behaviour is also typical of LDHs and is called the 'memory effect'.

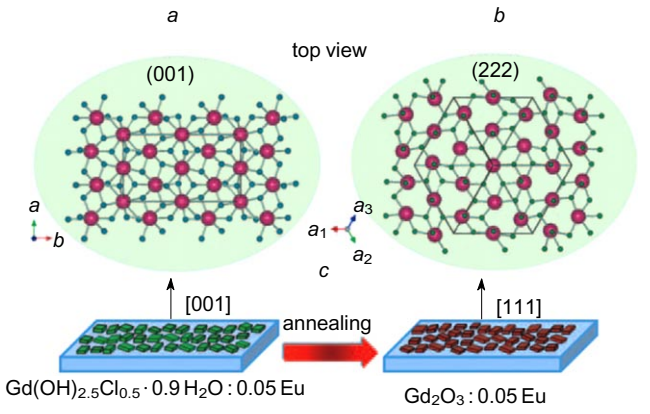


Figure 32. Projections of crystallographic planes (00*l*) for orthorhombic $Gd(OH)_{2.5}Cl_{0.5} \cdot 0.9\,H_2O : 0.05$ Eu (*a*) and (222) for cubic $Gd_2O_3 : 0.05$ Eu (*b*); a schematic of structural transformation from $Gd(OH)_{2.5}Cl_{0.5} \cdot 0.9\,H_2O : 0.05$ Eu film into $Gd_2O_3 : 0.05$ Eu film (*c*).[200] Rare-earth metal cations are given in red, OH groups are given in blue and oxygen atoms are given in green. Preferential crystallographic orientation normal to the film surface is given in parentheses.

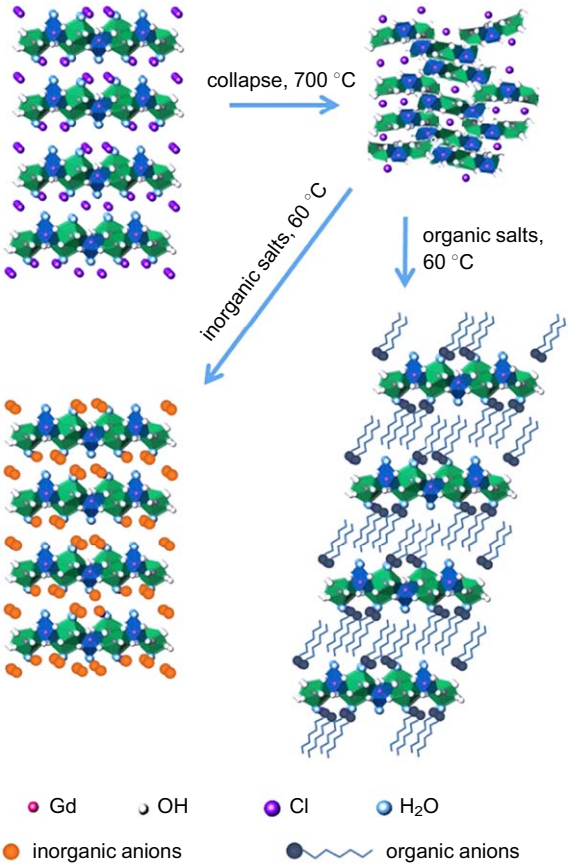


Figure 33. Schematic illustration of the recovery of the crystal structure of layered gadolinium hydroxychloride after annealing at 700 °C followed by hydrolysis in salt solutions containing inorganic and organic anions.[265,266]

Hydrolysis of layered rare-earth oxychlorides is also suitable for preparation of LRHs with specified anionic composition including organic anions.[265]

Thermal decomposition of rare-earth hydroxysulfates $Ln_2(OH)_4SO_4 \cdot n\,H_2O$ belonging to the LREH-II category has been thoroughly studied since these compounds are precursors of efficient phosphors Ln_2O_2S (when decomposition occurs in reductive atmosphere) and $Ln_2O_2SO_4$.[140,190,262,267,268] Decomposition in air involves three main stages, *viz*., dehydration (200–300 °C), dehydroxylation (300–400 °C) and desulfation (1200–1450 °C), which can be described by the following reactions: [140,262]

$$Ln_2(OH)_4SO_4 \cdot n\,H_2O \xrightarrow{200-300\ ^\circ C} Ln_2(OH)_4SO_4 + n\,H_2O \quad (13)$$

$$Ln_2(OH)_4SO_4 \xrightarrow{300-400\ ^\circ C} Ln_2O_2SO_4 + 2\,H_2O \quad (14)$$

$$Ln_2O_2SO_4 \xrightarrow{1200-1450\ ^\circ C} Ln_2O_3 + SO_3 \quad (15)$$

The dehydroxylation temperature increases from ~360 to ~400 °C (Fig. 34),[140,262] while the desulfation temperature decreases from ~1450 to ~1200 °C throughout the lanthanide series.[262]

Rare-earth oxysulfides are obtained from layered rare-earth hydroxysulfates by annealing in hydrogen stream at 1200 °C.[140,190,267]

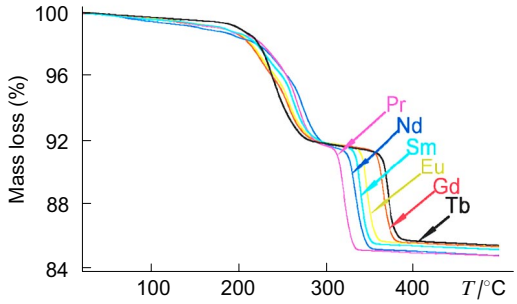


Figure 34. Results of thermogravimetric analysis of $Ln_2(OH)_4SO_4 \cdot n\,H_2O$ (Ln = Pr–Tb).[262]

$$Ln_2O_2SO_4 + 4\,H_2 \xrightarrow{>550\ ^\circ C} Ln_2O_2S + 4\,H_2O \quad (16)$$

Decomposition of layered rare-earth hydroxysulfates with the formation of oxo compounds proceeds without retention of the microstructure (Fig. 35) since gas evolution causes breakdown of plate-like crystals and formation of smaller spheroidal particles. As the treatment temperature increases, these particles are sintered.[190,267,268]

Intercalation of organic anions into LRHs can enhance the thermal stability of the anions.[203,207,210–212,269] In particular, intercalation of aspirin[207] and naproxen[210] molecules into LRHs was followed by the shift of the first stage of thermal decomposition of these compounds by 2 and 5 °C, respectively. Thermogravimetric analysis and differential thermal analysis data for intercalates were significantly different from corresponding data obtained for potassium or sodium salts of the intercalating anions.[211,212]

Structural and morphological features of LRHs are used for targeted solid-phase synthesis of various compounds.[270,271] For instance, the use of yttrium hydroxynitrate as precursor of $CuYO_2$ made it possible to essentially simplify the synthetic procedure, to reduce the temperature from 1000 to 900 °C and shorten the synthesis time from 10 to 4 h. In addition, this technique allows one to carry out targeted synthesis of the 3R-type polymorph of $CuYO_2$ due to structural similarity between $CuYO_2$ and layered yttrium hydroxide.[270] Solid-state reactions can also be utilized to prepare composite inorganic materials including those with complex 3D architectures. For instance, heat treatment of exfoliated layered gadolinium–europium hydroxide supported on silica microbeads with methylphosphonate-modi-

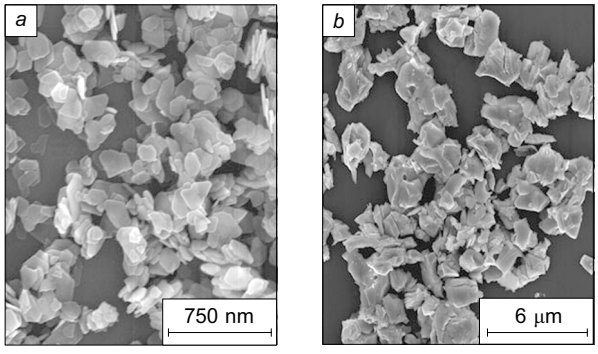


Figure 35. SEM images of samples prepared by annealing $(La_{0.95}Eu_{0.05})_2(OH)_4SO_4 \cdot 2\,H_2O$ at 400 (*a*) and 1300 °C (*b*).[268]

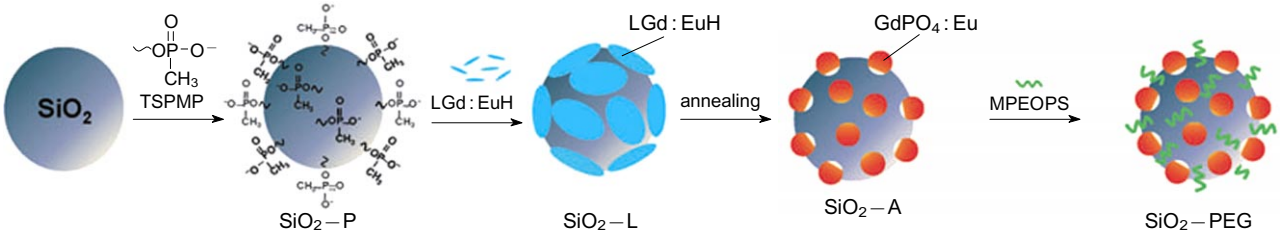


Figure 36. Fabrication of a composite material based on silica microspheres and europium-doped gadolinium phosphate nanoparticles: a schematic.[271] Notations: TSPMP stands for sodium 3-(trihydroxysilyl)propylmethylphosphonate, SiO_2-P stands for silica particles modified with methylphosphonate groups; SiO_2-L stands for silica particles modified with methylphosphonate groups and coated with layered gadolinium–europium hydroxide nanosheets (LGd : EuH); SiO_2-A stands for silica microspheres coated with $GdPO_4$: Eu particles; MPEOPS stands for 2-[methoxy(polyethyleneoxy)propyl]trimethoxysilane; SiO_2-PEG stands for particles modified with poly(ethylene glycol) (PEG) and coated with $GdPO_4$: Eu particles.

fied surface afforded a composite material representing silica beads coated with Eu-doped gadolinium phosphate nanoparticles (Fig. 36).[271]

7. Luminescent and magnetic properties of layered rare-earth hydroxides

7.1. Luminescent properties

All lanthanides except Lu^{3+} are characterized by radiative f–f transitions with energies in the UV (Gd^{3+}), visible (Pr^{3+}, Sm^{3+}, Eu^{3+}, Tb^{3+}, Dy^{3+}, Tm^{3+}) or near-IR (Pr^{3+}, Nd^{3+}, Ho^{3+}, Er^{3+} and Yb^{3+}) spectral regions.[272] Certain lanthanides can emit in the visible and IR regions (Pr^{3+}, Sm^{3+}, Eu^{3+}, Ho^{3+}, Er^{3+}, Tm^{3+}). Transitions from radiative levels can cause both fluorescence (spin-allowed process) and phosphorescence (spin-forbidden process) of lanthanides.[272] Since the lanthanide f-orbitals are shielded and almost not involved in the formation of chemical bonds, the bonding geometry remains unchanged in the ground and excited states. This underlies the distinctive features of the luminescence spectra of lanthanides, namely, narrow bands and large Stokes shifts (provided intrinsic excitation). It should also be noted that the strongest radiative electric dipole transitions of lanthanides are forbidden by the selection rules. However, in the crystal field this prohibition is partially removed due to mixing of the wavefunctions of the 4f-electrons.[272]

The efficiency of transition to excited state provided intrinsic excitation of lanthanides is rather low owing to low extinction coefficients ($\varepsilon < 12.5$ L cm^{-1} mol^{-1}).[273] To increase the efficiency of lanthanide luminescence, excitation energy is transferred to the lanthanide cation *via* an organic ligand characterized by high extinction coefficient. This is the sensitization of luminescence or the 'antenna effect'.[272,273] There are also methods based on sensitization of lanthanide cations using transition-element cations,[272] other lanthanide cations[272] and on excitation *via* charge-transfer bands.[274]

The luminescent properties of LRHs were first of all studied for trivalent europium and terbium compounds since the strongest luminescence bands of these systems (red for europium, green for terbium) are in the visible spectral range. There are a few studies on luminescent materials based on LRHs doped with Ce^{3+} and Dy^{3+} cations (see, *e.g.*, Refs 127 and 214, respectively). In addition, the influence of the anionic composition from simple (chloride and nitrate) to more complex inorganic (polyoxometallate) and organic (aromatic carboxylate) anions on the luminescent properties of LRHs has been widely investigated.

The excitation and emission spectra of layered europium and terbium hydroxychlorides are shown in Fig. 37. The luminescence spectra exhibit the $^5D_0-{}^7F_J$ ($J = 0-4$) and $^5D_4-{}^7F_J$ ($J = 3-6$) bands characteristic of Eu^{3+} and Tb^{3+}, respectively. The Stark splitting and intensities of these bands are indicative of centrosymmetric position of lanthanide cation in the low-symmetry environment, which is in good agreement with crystallographic data (point symmetry groups C_1 and C_{4v} for the lanthanide cation).[92]

The character of luminescence of layered europium and terbium hydroxynitrates is somewhat different from that of luminescence of layered rare-earth hydroxychlorides.[243] In particular, the excitation spectrum of layered terbium hydroxynitrate demonstrates no $4f^8 \rightarrow 4f^75d^1$ bands in the region of 250–300 nm. The reason is the filter effect of nitrate anion, which absorbs in this region.[243]

The luminescent properties of LRHs intercalated (or surface-modified) with F^-,[163] SO_4^{2-},[262] $Mo_7O_{24}^{6-}$,[246] $[H_2W_{12}O_{42}]^{10-}$ (Ref. 249) and VO_4^{3-} anions[275] have been studied. Fluoride and sulfate anions replace OH groups and water molecules in the coordination environment of lanthanide atoms, which leads to weaker quenching of the luminescence of rare-earth cations (higher luminescence intensity).[276] Luminescence of polyoxo and oxo compounds can be sensitized *via* charge-transfer bands. Similar hybrid LDHs were also reported.[277–279]

The luminescence intensity of layered europium hydroxide intercalated with $Mo_7O_{24}^{6-}$ much exceeds that of original layered europium hydroxychloride (see Fig. 38).[246] The intensity of the $^5D_0-{}^7F_2$ transition (excitation at 394 nm) is comparable with that of commercially available phosphor Y_2O_3 : Eu (excitation at 260 nm). A broad band near 287 nm appears in the absorption spectrum of the hybrid compound in addition to the narrow strong bands of f–f-transitions of the Eu^{3+} ion. Excitation at this wavelength causes a $^5D_0-{}^7F_2$ radiative transition at 613 nm. The band in the UV region of the absorption spectrum originates from energy transfer from the heptamolybdate anion to Eu^{3+}. A similar effect, *viz.*, sensitization of the Eu^{3+} and Tb^{3+} luminescence was observed for LRHs intercalated with $[H_2W_{12}O_{42}]^{10-}$ (Ref. 249) and $[EuW_{10}O_{36}]^{9-}$.[245]

The sensitization mechanism of lanthanide luminescence by organic ligands is schematically shown in Fig. 39. The ligand initially goes to singlet excited state and then to a triplet excited state through intersystem crossing. Excitation energy is transferred from the triplet level of the ligand to a

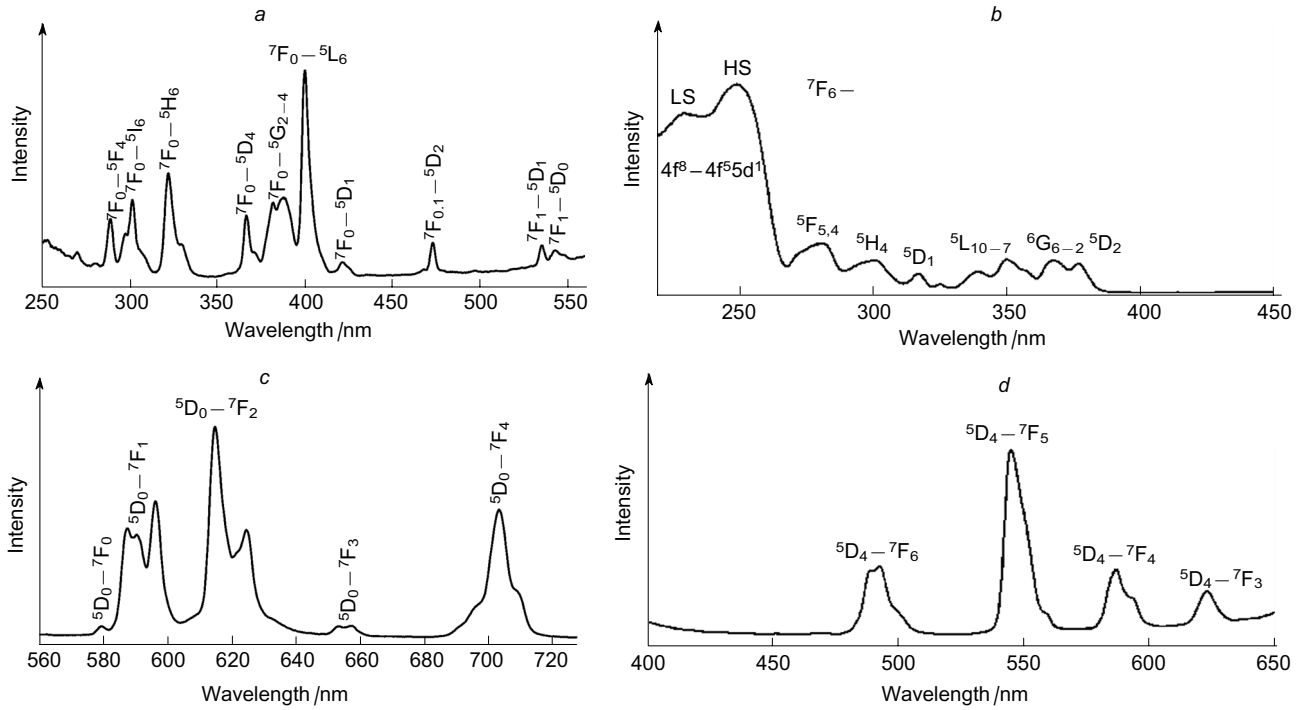


Figure 37. Excitation spectra (*a*, *b*) and emission spectra (*c*, *d*) of layered europium hydroxychloride (*a*, *c*) [114] and terbium hydroxychloride (*b*, *d*).[112] LS and HS denote the high- and low-spin excited states of terbium cation ($4f^75d^1$ configuration).

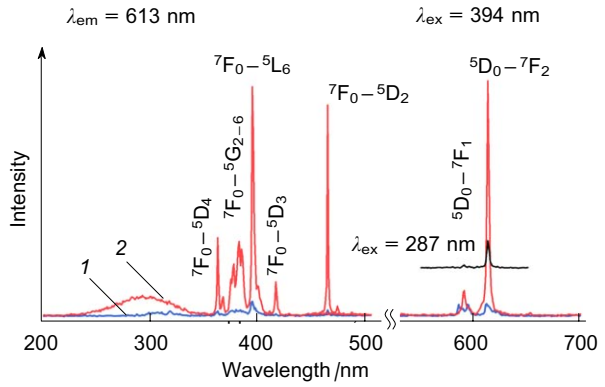


Figure 38. Excitation spectra (left) and emission spectra (right) of layered europium hydroxide intercalated with Cl^- (*1*) and $Mo_7O_{24}^{6-}$ anions (*2*).[246] λ_{em} is the emission wavelength hand λ_{ex} is the excitation wavelength.

radiative level of the lanthanide. Charge-transfer transitions can also be involved.

Luminescence of lanthanide ions can be sensitized using β-diketonates, acylpyrazolonates, phosphorylphenolates, complexes with Schiff bases and aromatic carboxylates.[273] Sensitization of Eu^{3+} luminescence in corresponding LRHs can be achieved by intercalation with anions of the following organic acids: benzoic,[224, 280] benzene-1,3,5-tricarboxylic,[206, 209] biphenyl-2,2′-dicarboxylic,[209] biphenyl-4-carboxylic,[237] benzene-1,4-dicarboxylic,[202, 203, 237, 243] benzene-1,2,4,5-tetracarboxylic [206] and naphthalene-2-carboxylic.[243] Intercalation of LRHs with anions of benzoic,[280] 2-aminobenzoic,[269] benzene-1,4-dicarboxylic,[243] 2-hydroxybenzoic [238] and 2,2′-{[(2,4,6-trimethyl-1,3-phenylene)di(methylene)]dioxy}dibenzoic acids [168, 239] causes sensitization of the luminescence of Tb^{3+}. Most of these anions belong to aromatic carboxylates whose complexes with Tb^{3+} and Eu^{3+} cations are characterized by high stability and bright luminescence.[273] In addition, the luminescent properties of

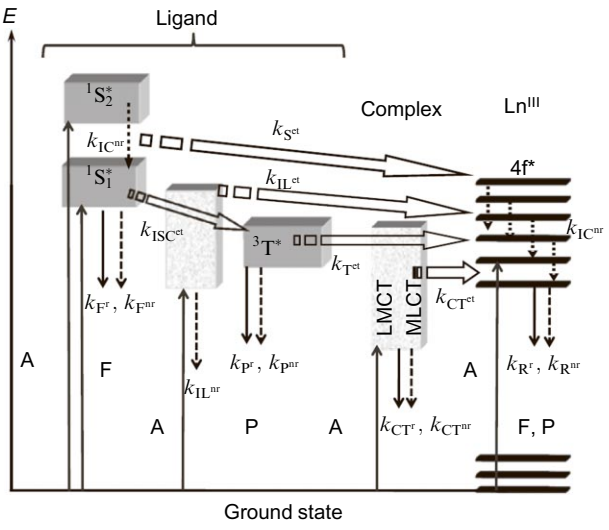


Figure 39. A schematic of energy absorption, transfer, emission (solid lines) and dissipation (dashed lines) in lanthanide complexes. $^1S^*$ or S denotes a singlet state, $^3T^*$ and T denote triplet states, A denotes absorption, F denotes fluorescence, P denotes phosphorescence, *k* is rate constant, et denotes electron transfer, r denotes radiative transition, nr denotes nonradiative transition, IC denotes internal conversion, R denotes f–f transition, ISC denotes intersystem crossing, ILCT (IL) denotes inter-ligand charge transfer, LMCT denotes ligand-to-metal charge transfer and MLCT (CT) denotes metal-to-ligand charge transfer.[272]

lanthanide carboxylates can be varied with ease by incorporating substituents and heteroatoms into the aromatic ring of the ligand.[273] According to Latva's empirical rule for the Eu^{3+} and Tb^{3+} complexes, efficient sensitization of luminescence requires that the triplet level of the ligand be $\sim 2500-3500$ cm^{-1} (for Eu^{3+}) and $\sim 2500-4000$ cm^{-1} (for Tb^{3+}) higher than the excited state of lanthanide [$E(^5D_0\ Eu^{3+}) = 17\,200$ cm^{-1} and $E(^5D_4\ Tb^{3+}) = 20\,400$ cm^{-1}].[273] This rule is applicable not only to complexes, but also to LRHs containing Tb^{3+} and Eu^{3+} cations. Consider an example. The triplet levels of biphenyl-4-carboxylate and terephthalate lie at 22 083 and 25 160 cm^{-1}, respectively. The narrower gap between the former and the $^5D_0$ radiative level of europium cation lying at 17 200 cm^{-1} (Fig. 40) favours enhancement of the Eu luminescence intensity and an increase in the luminescence lifetime from 0.166 to 0.433 ms for europium in the layered hydroxide intercalated with biphenyl-4-carboxylate compared to the luminescence of europium in the layered hydroxide intercalated with terephthalate.[237] A similar situation was observed for the luminescence of terbium as dopant in the layered hydroxides intercalated with terephthalate, phenyl-1,3,5-tricarboxylate and phenyl-1,2,4,5-tetracarboxylate anions. The corresponding luminescence intensities are in a 1 : 5 : 12 ratio, while the luminescence lifetimes are 0.32, 0.58 and 0.64 ms, respectively.[281]

The optical properties of anions are significantly changed upon intercalation into LRHs. Often, shifts of their absorption bands and enhancement of phosphorescence are observed. The latter effect is most pronounced for anions intercalated into LRHs doped with paramagnetic gadolinium cation.[238] The excitation bands of many ligands are shifted relative to those of corresponding complexes. For instance, the excitation band edge of Eu-doped lanthanide terephthalates is at ~ 325 nm and shifts to 300 nm for LRHs.[202] This can be due to violation of Kasha's rule for terephthalate anions intercalated into LRHs, *i.e.*, energy transfer occurs not from the lowest excited level of terephthalate anion. Consequently, the determination of positions of triplet levels and extinction coefficients of aromatic anions intercalated into LRHs seems to be interesting and practically valuable. Probably, the mechanism of energy transfer from the sensitizer anion to the radiative levels of europium and terbium differs from the mechanism described for corresponding lanthanide complexes. Changes in the sensitization mechanism can be due to an increase in the distance between the rare-earth cation and carboxylate anions in LRHs compared to the distance in molecular complexes and to the shielding of rare-earth cations by OH groups. In this case energy transfer can proceed by the multistep exchange mechanism[237] or by the Förster mechanism (due to the Coulomb interaction).[273]

An interesting structure-dependent feature of the luminescent properties of LRHs is the possibility of intra- and interlayer energy transfer between rare-earth cations (*e.g.*, $Tb^{3+} \rightarrow Eu^{3+}$ and $Ce^{3+} \rightarrow Tb^{3+}$). For instance, Tb^{3+}/Eu^{3+}-doped solid solutions often exhibit sensitization of the Eu^{3+} luminescence by Tb^{3+} cation.[133,238] This effect is also typical of fluorides,[282] certain oxo compounds[283] and metal-organic polymers based on rare-earth elements.[284] To increase the luminescence intensity and the lifetimes of europium and terbium cations in the excited state, the concentration of active centres Eu^{3+} and Tb^{3+} is decreased through the synthesis of solid solutions doped with yttrium[131–133,202] or gadolinium.[168,238,243] Unlike yttrium, gadolinium provides more efficient (compared to intrinsic absorption of europium) excitation of europium luminescence using the $^8S_{7/2} \rightarrow {}^6I_J$ transition of Gd^{3+} ion (273 nm).[92] Gadolinium also allows one to significantly increase the quantum yield of luminescence through stabilization of the excited triplet level of the ligand (Fig. 41).[168,273]

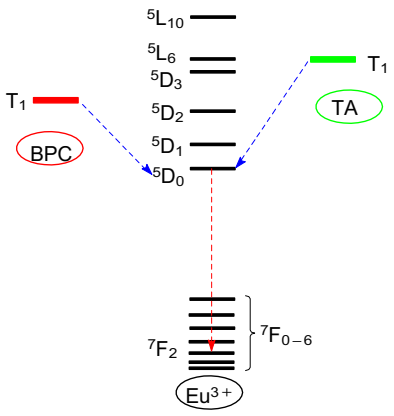


Figure 40. A schematic of energy transfer from triplet levels of terephthalate (TA) and biphenyl-4-carboxylate (BPC) anions to radiative f-levels of Eu^{3+}.[237]

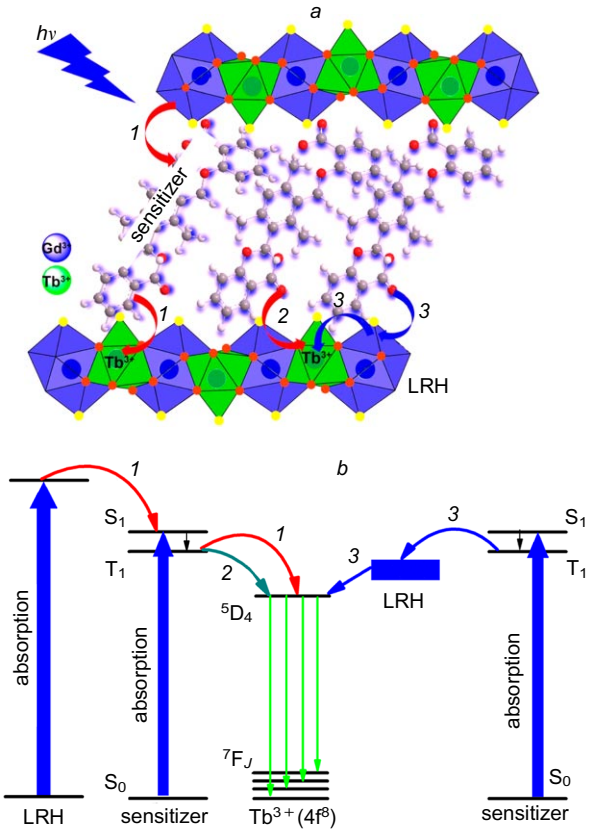


Figure 41. Schematic representation of the structure of sensitized layered gadolinium hydroxide doped with terbium (*a*) and the energy transfer mechanism in this material (*b*).[168] Arrows *1–3* denote electron transfer processes.

A study[285] on solid solutions of layered europium–terbium hydroxides with different interlayer distances showed that energy transfer from Tb^{3+} cation to Eu^{3+} cation is mainly inter- rather than intra-layer process (*cf.* Fig. 42 *a*, *2* and Fig. 42 *a*, *1* where excitation energy dissipates on OH groups). It follows that energy transfer between lanthanides can be controlled by varying the interlayer distance in LRHs. Corresponding changes in the luminescence spectrum can be used as analytical signal in sensors.

Energy transfer between rare-earth cations from the host metal hydroxide layers and interlayer lanthanide complexes[250,251] is also possible. For instance, energy transfer $Tb^{3+} \rightarrow Eu^{3+}$ from a terbium complex with hexafluoroacetylacetone to layered yttrium–europium hydroxide (Fig. 42 *b*) was reported.[251]

No record-high luminescent properties of LRHs should be expected since water molecules and hydroxyl groups considerably decrease the quantum yield of luminescence due to vibrational nonradiative relaxation of excited states of lanthanides.[274] The maximum quantum efficiency of luminescence of sensitized LRHs is 33%.[168] However, not only rare-earth elements, but also intercalated anions can luminesce. Hydroxyl groups are efficient quenchers of singlet oxygen (key component of photodegradation reactions of organic luminophores); however, intercalation of organic luminophores into LRHs significantly increases their photostability.[286]

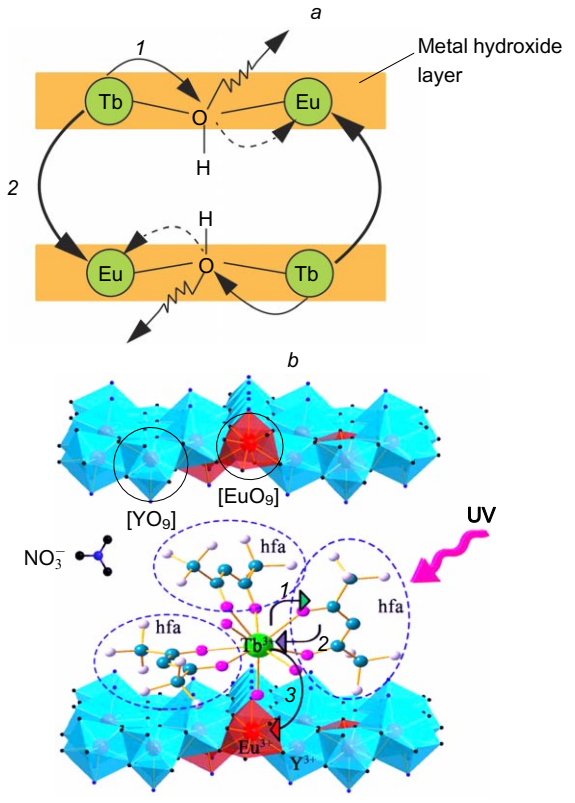


Figure 42. Schematic illustration of excitation energy transfer between Eu^{3+} and Tb^{3+} cations in LRHs (*a*)[285] and between terbium complex with hexafluoroacetone (hfa) and layered yttrium–europium hydroxide (*b*).[251] Panel *a*: (*1*, *2*) see text, dashed arrows denote the hardly probable energy transfer pathways; panel *b*: *1* and *2* respectively denote direct and back transfer of luminescence excitation energy between hexafluoroacetone and Tb^{3+}; (*3*) excitation energy transfer from terbium complex to europium cation intercalated into LRH.

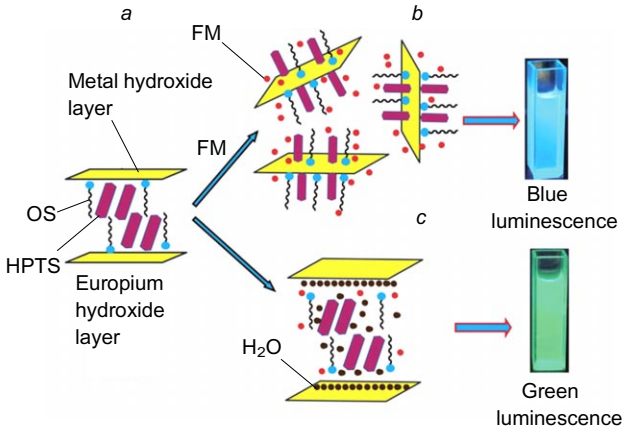


Figure 43. Luminescence of layered europium hydroxide/HPTS hybrid in different states: a schematic.[205] Quenching of luminescence in solid phase (*a*), luminescence upon exfoliation in formamide (*b*) and luminescence upon partial self-assembly of particles in aqueous formamide solution (*c*).

Layered rare-earth hydroxides were successfully intercalated with the following organic luminophores: coumaric acid anions[287] and their derivatives (7-hydroxy- and 7-hydroxy-4-methylcoumarin),[211] niflumate anion,[212] 4,4′-distyrylbiphenyl sulfonate anion (Tinopal CBS),[238,250] 8-hydroxypyrene-1,3,6-trisulfonate anion (HPTS)[205] and fluorescein anion.[176,244] Intercalation of luminophores into LRHs is followed by shifts of their excitation and emission bands, *i.e.*, by changes in the Stokes shifts of corresponding molecules.[287] Concentration quenching of the luminescence of intercalated luminophores and its quenching by Eu^{3+} or Tb^{3+} cations in the interlayer space was reported.[137,205] In some studies LRHs were doubly intercalated with organic luminophores and octanesulfonate anion for exfoliation of hybrid compounds,[211,244] or salicylate anion for sensitization of the europium and terbium luminescence (Fig. 43).[238] It was found that quenching of the luminescence of organic luminophores weakens and the quantum yield of their luminescence increases.[244] The luminescent properties of bulk and delaminated LRHs are significantly different (Fig. 43 *b*,*c*); they are sensitive to the presence of water[205,244] and transition-metal cations[244] in the environment, which can be used for fabrication of sensors.

Thus, rigid metal hydroxide hosts make LRHs unique objects for studies of lanthanide–lanthanide and lanthanide–ligand energy transfer processes. Besides, LRHs are convenient matrices for organic luminophores that significantly change the luminescent properties of intercalants.

7.2. Magnetic properties of layered rare-earth hydroxides

Taking account of numerous experimental studies on the design of novel magnetic materials based on LDHs[288,289] including those for targeted drug delivery,[289] it is of paramount interest to investigate the magnetic properties of LRHs, which are mainly determined by the unfilled f-shell of the rare-earth ions. Gadolinium ion Gd^{3+} has a half-filled f-shell with seven unpaired electrons and exhibits strong magnetic properties. Most gadolinium compounds are paramagnetic. Among them, there are layered gadolinium hydroxides,[151,173] which are widely used as key

components of contrast agents for MRI.[172, 176, 271] In the temperature range of 1.5–7 K, materials based on layered gadolinium hydroxide (including those intercalated with dodecyl sulfate anions) demonstrate pronounced magnetocaloric effect comparable with that of the gadolinium compounds used as components of cryogenic magnetic coolers.[290]

There has been intensive research into magnetic properties of other rare-earth hydroxides (Tb, Dy, Ho, Er, Yb).[151, 291–293] In particular, it was shown that layered dysprosium hydroxychloride is the first condensed system demonstrating the properties of a single-molecule magnet.[293] Studies on low-temperature Ln–Ln magnetic interactions in layered Tb, Dy, Ho and Er hydroxides showed that these interactions can be varied by preparing solid solutions containing a diamagnetic rare-earth element (*e.g.*, yttrium) and by varying the interlayer distance.[291, 292]

8. Functional materials based on layered rare-earth hydroxides

Functional materials based on LRHs include luminescent materials, biomaterials and catalysts. Luminescent materials can be divided into luminophores *per se* (in particular, white light sources) and sensors that change the luminescence signal upon changes in external conditions (temperature, presence of certain molecules and ions). Biomaterials based on LRHs demonstrate multiple functionalities ranging from materials for targeted drug delivery systems to contrast agents for MRI and X-ray computed tomography and even to luminescence detection. Catalysts based on LRHs represent hybrid materials demonstrating synergistic effect of the host and anionic components. They are first of all used when conducting low-temperature reactions.

8.1. Luminescent materials

8.1.1. Phosphors

Since intercalated LRHs contain luminescent rare-earth cations and organic luminophores, one can develop methods for fabrication of LRH-based white light sources (*i.e.*, materials whose emission spectra span the entire visible region). They can be prepared by combining different rare-earth elements in the metal hydroxide host and by blocking energy transfer between them through exfoliation or dilution with heterocations. For instance, a phosphor that generates white light under simultaneous excitation at 284, 318 and 377 nm was prepared by mixing colloidal suspensions of delaminated layered terbium, europium and dysprosium hydroxide nanosheets.[214] A similar material was fabricated using exfoliated layered (terbium and europium) hydroxide.[285] More efficient phosphors are based on LRHs intercalated with sensitizers or lanthanide complexes. For instance, a mixed layered gadolinium, europium and terbium hydroxide intercalated with salicylate and 4,4′-distyrylbiphenyl sulfonate anions generates white light with a quantum efficiency of 11% (Fig. 44).[238] Yet another example is provided by layered gadolinium hydroxide intercalated with heteroligand complexes of terbium and europium with 4,4′-distyrylbiphenyl sulfonate anion; the quantum efficiency of this luminophore reaches a value of 16%.[250]

Luminophores based on LRHs can be encapsulated into polymeric matrices, thus producing hydrogels or flexible films (Fig. 44) for certain practical applications. Luminescent polymer films based on polyvinyl alcohol[294] and poly(methyl methacrylate),[238, 250] as well as hydrogels based on polyacrylamide[129, 130] were reported.

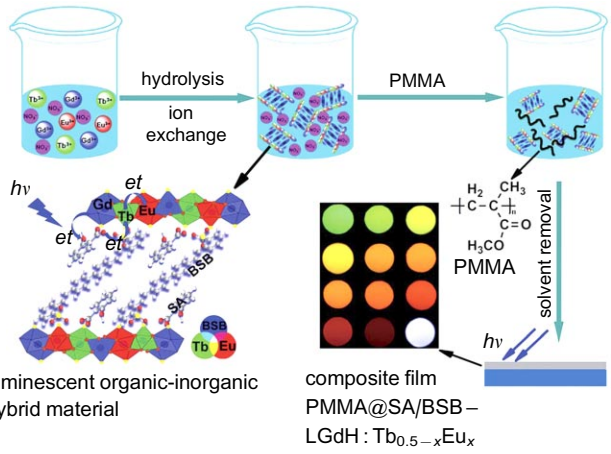


Figure 44. Fabrication of composite luminescent material based on mixed layered gadolinium, terbium and europium hydroxide ($LGdH:Tb_{0.5-x}Eu_x$), encapsulated into poly(methyl methacrylate) matrix.[238] SA is salicylate anion and BSB is 4,4′-biphenyldistyrylsulfonate anion.

8.1.2. Sensor materials

Sensor materials based on LRHs utilize the intensity of the luminescence of Tb^{3+} and Eu^{3+} cations or organic luminophores intercalated into LRHs as analytical signal. There are two types of sensor materials. Analytical signal increases with increasing the analyte content in type-I materials and decreases in type-II materials. An example of type-I materials is provided by exfoliated layered gadolinium–europium hydroxide (1 g L^{-1}) suitable for the determination of the concentration of vanadate ions down to 10^{-5} mol L^{-1} at pH 7–9 from sensitization of the luminescence of Eu^{3+}; the limit of detection of vanadate ions is 4.5×10^{-8} mol L^{-1}.[275] Yet another example is layered europium hydroxide intercalated with MoS_4^{2-} anion (Fig. 45). When exfoliated, the material is highly sensitive to the presence of water, which hydrolyzes MoS_4^{2-} with the formation of $[MoS_{4-x}O_x]^{2-}$ anion acting as sensitizer of the luminescence of Eu^{3+} ion. In both cases sensitization of Eu^{3+} is attained through charge-transfer transitions $O \rightarrow V$ and $O \rightarrow Mo$, respectively. LRH-based sensor materials utilizing luminescence of the intercalating anion as analytical signal can be exemplified by layered europium hydroxide intercalated with naphthalenedicarboxylate anion.[295] Its interaction with aqueous solutions of phosphates (concentration is at least 10^{-6} mol L^{-1}) is accompanied by the release of the naphthalenedicarboxylate anion; by analyzing its luminescence one can determine the concentration of phosphate anions in the aqueous solution.

The second type of LRH-based sensors utilizes selective quenching of the luminescence of Tb^{3+} and Eu^{3+} by different anions.[179] Thus, luminescence of Tb^{3+} in the hydroxychlorides $Y_{1-x}Tb_x$ is efficiently quenched by $HCrO_4^-$ and CrO_4^{2-} ions[179] sorbed on their surface. The limit of detection of Cr^{VI} compounds is $<10^{-6}$ mol L^{-1} and the sorption capacity is in the range of 80–100 mg g^{-1} depending on the pH value. Selective quenching of the luminescence of Tb^{3+} (see Fig. 46) is due to the overlap

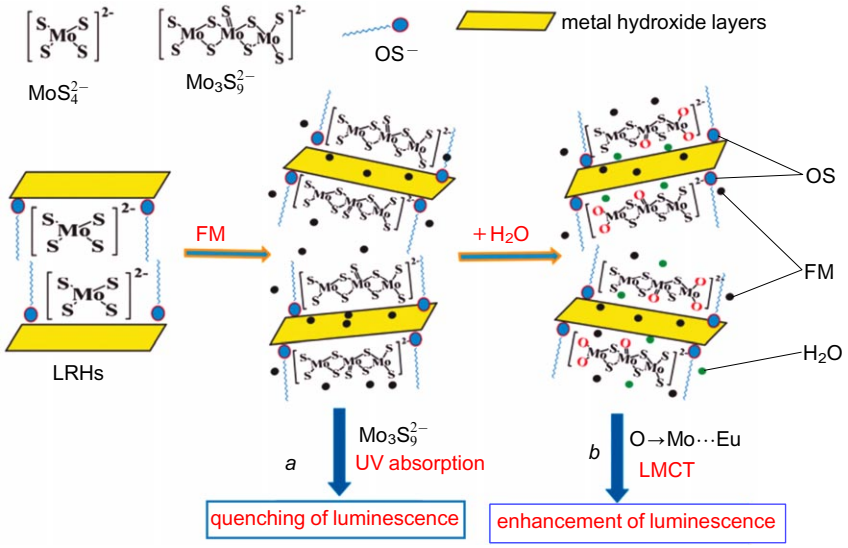


Figure 45. A schematic of the operation of sensor material based on exfoliated layered europium hydroxide intercalated with MoS_4^{2-} and octanesulfonate anions.[138] Quenching of Eu^{3+} luminescence in neat formamide (*a*) and sensitization of Eu^{3+} luminescence in the presence of water molecules (*b*).

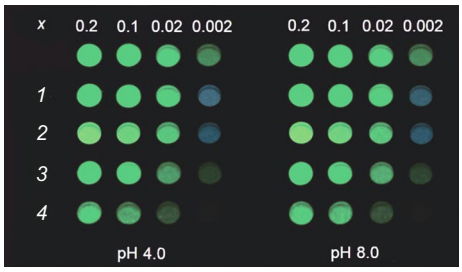


Figure 46. Photographs under UV irradiation at 254 nm of layered $Y_{1-x}Tb_x$ hydroxide samples ($x = 0.002-0.2$) and products of their interaction with aqueous Cr^{VI} solutions for 10 min at pH 4.0 and 8.0 .[179] Chromium concentration /μmol L^{-1}: 1 (*1*), 5 (*2*), 10 (*3*) and 100 (*4*).

between the band corresponding to the $^5D_4 \rightarrow {}^7F_5$ radiative transition of Tb^{3+} and the absorption bands of Cr^{VI}.

Materials based on layered cerium hydroxide represent a particular type of LRhH-based sensor materials. Cerium has two stable oxidation states, Ce^{3+} and Ce^{4+}. The electrode potential of $Ce^{3+} \rightleftharpoons Ce^{4+}$ transition is relatively low. This feature is widely used in, *e.g.*, titrimetric determination of reducing agents (cerimetry); however, it makes the preparation of layered cerium(III) hydroxides difficult.[149] Blue luminescence of Ce^{3+} cation can be used as analytical signal.[127, 149] The addition of oxidizing agent (*e.g.*, potassium permanganate) to layered yttrium–cerium hydroxide induces the $Ce^{3+} \rightarrow Ce^{4+}$ transition and subsequent quenching of the luminescence of Ce^{3+}.[127] As a reducing agent (ascorbic acid) is added, the reverse transition occurs, followed by luminescence. The sensor can be repeatedly switched on and off (Fig. 47 *a*). A photoluminescence feature of the sensor material $(Tb_xCe_{1-x})_2(OH)_4SO_4 \cdot n\,H_2O$ consists in the possibility to significantly enhance the luminescence of terbium, which plays the role of analytical signal, using the band corresponding to energy transfer from Ce^{3+} to Tb^{3+} (Fig. 47 *b*).[149]

The change in the luminescence intensity due to the $Tb^{3+} \rightarrow Eu^{3+}$ energy transfer between the complex of terbium with hexafluoroacetylacetone and layered yttrium–europium hydroxide can be used as analytical signal.[251] The composite is a chameleon luminophore emitting in the range from green to pink depending on temperature (77–450 K). This is the first example of application of LRHs as luminophores for contactless thermometry.

Chemiluminescence sensors based on LRHs were also reported. Heterogeneous catalytic oxidation reactions can be accompanied by chemiluminescence due to the formation of emitting intermediates in excited states. The intensity of the chemiluminescence signal is proportional to the concentration of the substance being oxidized. Lanthanide oxides also catalyze these reactions, but their selectivity is low. Layered yttrium–europium hydroxide was found to be a selective catalyst of the oxidation of diethyl ether in the presence of other widely used volatile organic compounds. The oxidation is accompanied by chemiluminescence that can be used as analytical signal for the determination of diethyl ether in the concentration range of 1–100 mmol L^{-1}.[169] The process can be described by the following equations:[169]

$$MeCH_2OCH_2Me + O_2 \longrightarrow MeCHO^* \quad (17)$$

$$MeCHO^* + Eu^{3+} \longrightarrow MeCHO + Eu^{3+*} \quad (18)$$

$$Eu^{3+*} \longrightarrow Eu^{3+} + h\nu \quad (19)$$

8.2. Biomaterials

The design of biomaterials based on LRHs is a very promising avenue of research since they are analogues to widely used LDHs.[103] The potential of LRHs as multifunctional materials can be even more extended by utilizing specific features of lanthanide cations. Being low toxic, LRHs seem to be promising drug delivery systems, sensor materials, contrast agents for MRI and X-ray computed tomography, as well as fluorescence microscopy.

The design of biomaterials requires clear understanding of the concentration ranges corresponding to safe applica-

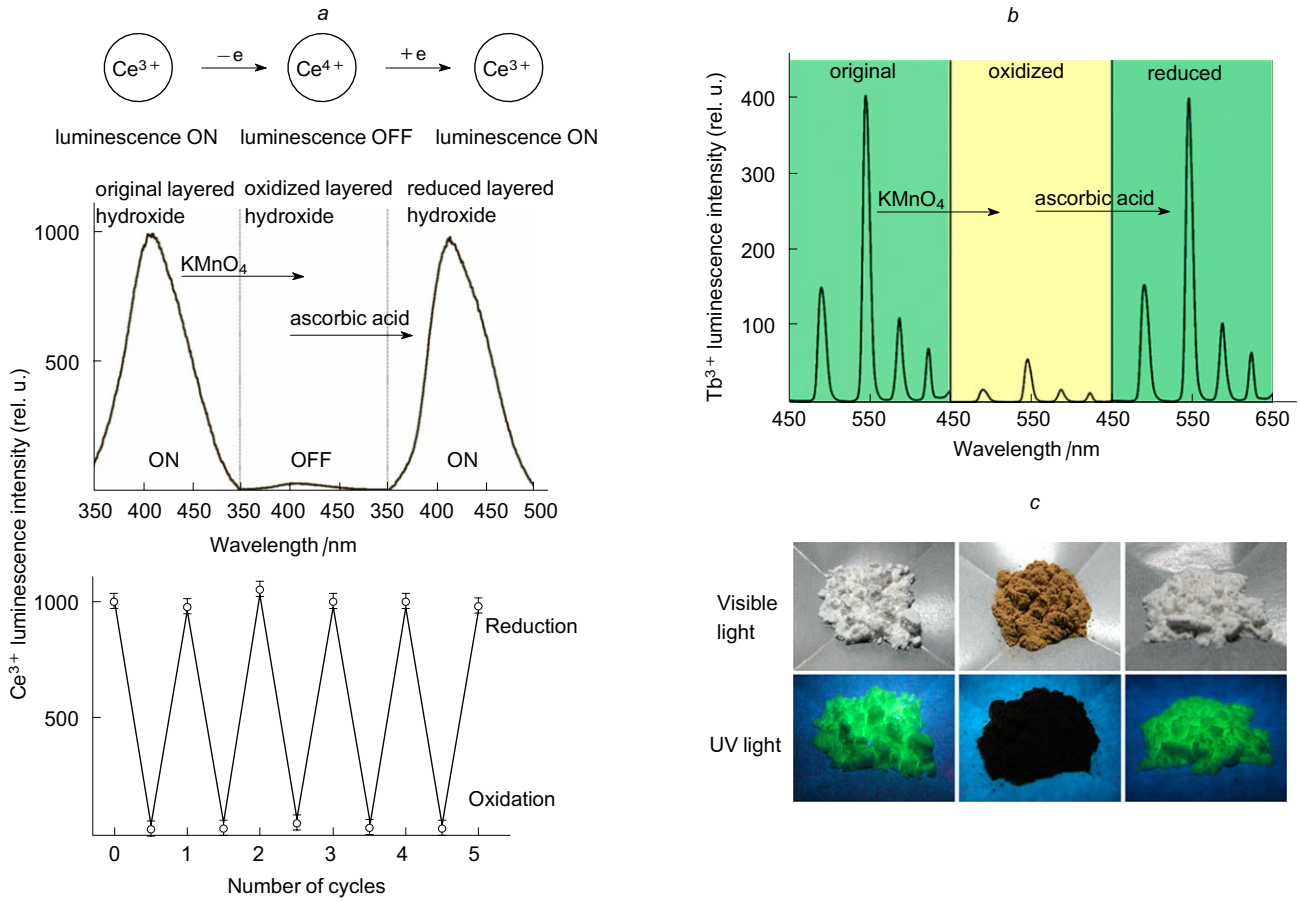


Figure 47. Layered yttrium – cerium hydroxide (*a*)[127] and layered terbium – cerium hydroxide (*b*)[149] as sensor materials. The luminescent properties of these materials are sensitive to the oxidation state of cerium. Appearance of the layered terbium – cerium hydroxide samples before and after the oxidation – reduction cycle under visible light and under UV light (*c*).

tion. Rare-earth cations are toxic to living organisms, but their toxicity is minimized by using poorly soluble LRHs. Mention should be made that the solubility of LRHs increases in acidic media (pH < 5). Surface modification of LRHs with surfactant molecules enhances their stability to dissolution in acidic media.[176]

Biocompatibility of LRHs in concentrations up to 500 μg mL^{-1} was tested *in vitro* using different cell lines and tissues [164, 166, 176, 192] including human cells.[207, 210] Most LRHs are characterized by weak cytotoxic effects (Fig. 48 *a* – *d*);[210] in some cases they stimulate cell growth.[192] Long-term (up to 30 days) *in vivo* action of layered Gd : Ce,Tb hydroxide on various mice organs was not followed by pathological changes.[166] Further *in vivo* experiments should reveal the accumulation and excretion pathways of LRHs for better understanding of prospects for their clinical applications.

The efficiency of most pharmaceuticals can be increased using targeted delivery and controlled release. To this end, various inorganic and organic compounds are used as drug containers. Layered rare-earth hydroxides are intercalated with many anions that are widely used in pharmacology. These are amino acid anions (aspartate,[173] glutamate,[173] phenylalaninate,[208, 209] tyrosinate [208, 209]), nalidixic acid anions,[173] porphyrins [127] (*S*)-6-methoxy-α-methyl-2-naphthaleneacetate anion (naproxen),[192, 210] acetylsalicylate anion (aspirin),[207] (*RS*)-2-[4-(2-methylpropyl)phenyl]propanecarboxylate (ibuprofen),[192] 2-[2-(2,6-dichlorophenylamino)phenyl]acetate (diclofenac),[192] microRNA.[164] Studies on the kinetics of release of certain compounds listed above in phosphate and carbonate buffers simulating physiological fluids (Fig. 48 *e* – *h*) revealed that the time of complete (> 90%) drug release varies from 2 to 36 h and increases in the order naproxen (1 – 2 h), diclofenac (4 h), ibuprofen (24 h), aspirin (36 h).

LRH-based materials are suitable for not only targeted drug delivery, but also as contrast agents for various kinds of biovisualization. Layered gadolinium hydroxides are used as contrast agents for MRI to obtain both T_1-weighted (fatty tissue is highlighted) [164, 172] and T_2-weighted (water in, *e.g.*, tumours is highlighted) [166, 176, 192] images, in contrast to commercially available gadolinium complexes, which are only used to obtain the T_1-weighted images. Unfortunately, reproducible results on layered gadolinium hydroxide enhancement of MRI signals have not been reported so far since local magnetic fields produced by the layered gadolinium hydroxide particles depend on the particle morphology and on the properties of anions that were intercalated or adsorbed on their surface.[176, 192] T_2-Weighted images of different organs of rats taken in specified time intervals after injection of layered gadolinium hydroxide particles are presented in Fig. 49.[166] Accumulation of layered gadolinium hydroxide particles in fatty tissues of liver and kidneys reduces the image contrast. Contrary to this, layered gadolinium hydroxide particles in water-rich bladder and tumour enhance the image contrast.

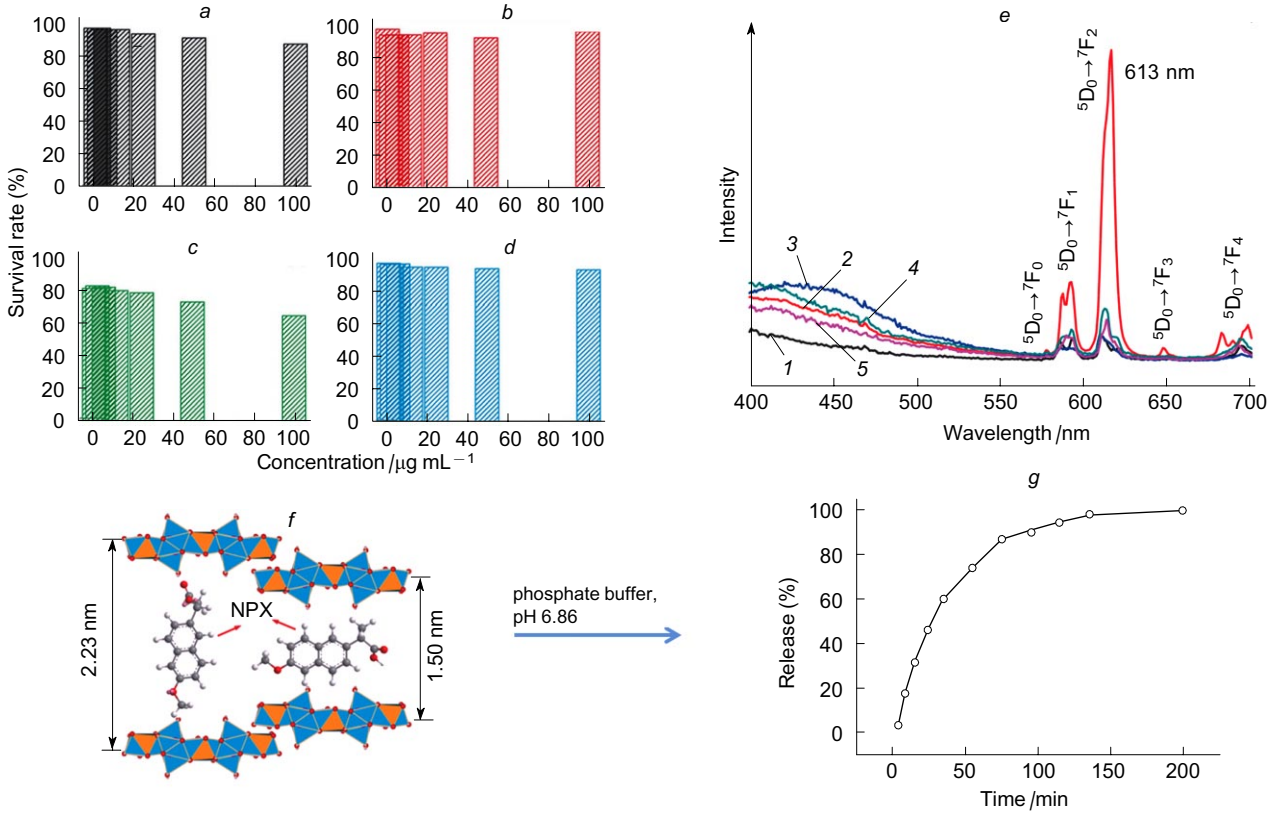


Figure 48. Cytotoxic effect of different concentrations of layered europium hydroxide intercalated with naproxen (in suspensions) on different cells based on a cell survival assay (*a*–*d*), luminescence spectra of layered europium hydroxynitrate and products of anion-exchange reaction of this compound with naproxen (*e*), arrangement of naproxen (NPX) molecule in the structure of layered europium hydroxide (*f*) and kinetics of naproxen release from the structure of layered europium hydroxide in phosphate buffer (*g*).[210]
Brain glioma U87MG cells (*a*), breast cancer MDA-MB-435S cells (*b*), murine brain microvascular endothelial cells (BMVECs) (*c*) and human umbilical vein endothelial cells (HUVECs) (*d*). Luminescence spectra: NO–LEuH (*1*), NPX : LEuH = 1 : 0.5 (*2*), NPX : LEuH = 1 : 0.7 (*3*), NPX : LEuH = 1 : 1 (*4*) and NPX : LEuH = 1 : 1.2 (*5*).

Layered rare-earth hydroxides can also act as contrast agents for X-ray computed tomography since lanthanides more efficiently absorb X-ray radiation than soft tissues of living organisms. For instance, *in vivo* studies on mice showed that LRH nanoparticles (Ln = Gd, Ce and Tb) are accumulated in kidneys and liver one hour after injection, as was confirmed by MRI data (see Fig. 49).[166] Layered rare-earth hydroxides containing Tb^{3+} and Eu^{3+} cations can be used in fluorescence microscopy, which allows one to monitor the distribution of particles in the body. However, the luminescence signal from layered terbium and europium hydroxychlorides is too weak to be detected *in vivo*; application of LRHs intercalated with sensitizers of the luminescence of Tb^{3+} and Eu^{3+}, as well as LRH-based IR emitters seems to be more efficient.

Thus, biomaterials based on LRHs offer multiple functionalities since they combine the anion-exchange properties of LRHs with the luminescent and magnetic properties of lanthanide cations. Layered rare-earth hydroxides are low toxic; therefore, the design of biomaterials is one of the most promising fields of application of these compounds.

8.3. Catalysts

By analogy with metal-organic polymers based on rare-earth elements, LRHs can be treated as bifunctional (acid–base) heterogeneous catalysts of low-temperature processes. Their intercalates with naphthalene-2,6-disulfonate and anthraquinone-2,6-disulfonate anions are used as catalysts of hydrodesulfurization of thiophene, oxidation of alkylbenzenethiol to sulfoxides and oxidation of linalool to furanoids and pyranoids.[24, 186] In some cases these catalysts demonstrated higher activity and selectivity than related metal-organic polymers.[186]

Layered rare-earth hydroxides are also used as components of complex multicomponent catalytic systems. In particular, a system including an ionic liquid 1-methyl-3-octylimidazolium hexafluorophosphate, hydrogen peroxide and layered europium hydroxide intercalated with europium-containing heteropolytungstate anion ($[EuW_{10}O_{36}]^{9-}$) appeared to be a highly efficient and recyclable catalyst of hydrodesulfurization reactions.[245] A tentative reaction mechanism is presented in Fig. 50. In this case, LRHs are necessary to form peroxide intermediates acting as oxidizing agents.

Layered rare-earth hydroxides can exhibit photocatalytic activity. For instance, layered yttrium–cerium [127] and europium–terbium[165] hydroxides intercalated with 5,10,15,20-tetrakis(4-sulfonatophenyl)porphyrin (TPPS) can generate singlet oxygen, an important component of many photocatalytic processes. Note that OH groups of LRHs are efficient quenchers of singlet oxygen; therefore, TPPS-intercalated LRHs are less efficient generators of singlet oxygen under irradiation compared to metal-organic polymers based on TPPS and lanthanides.[165]

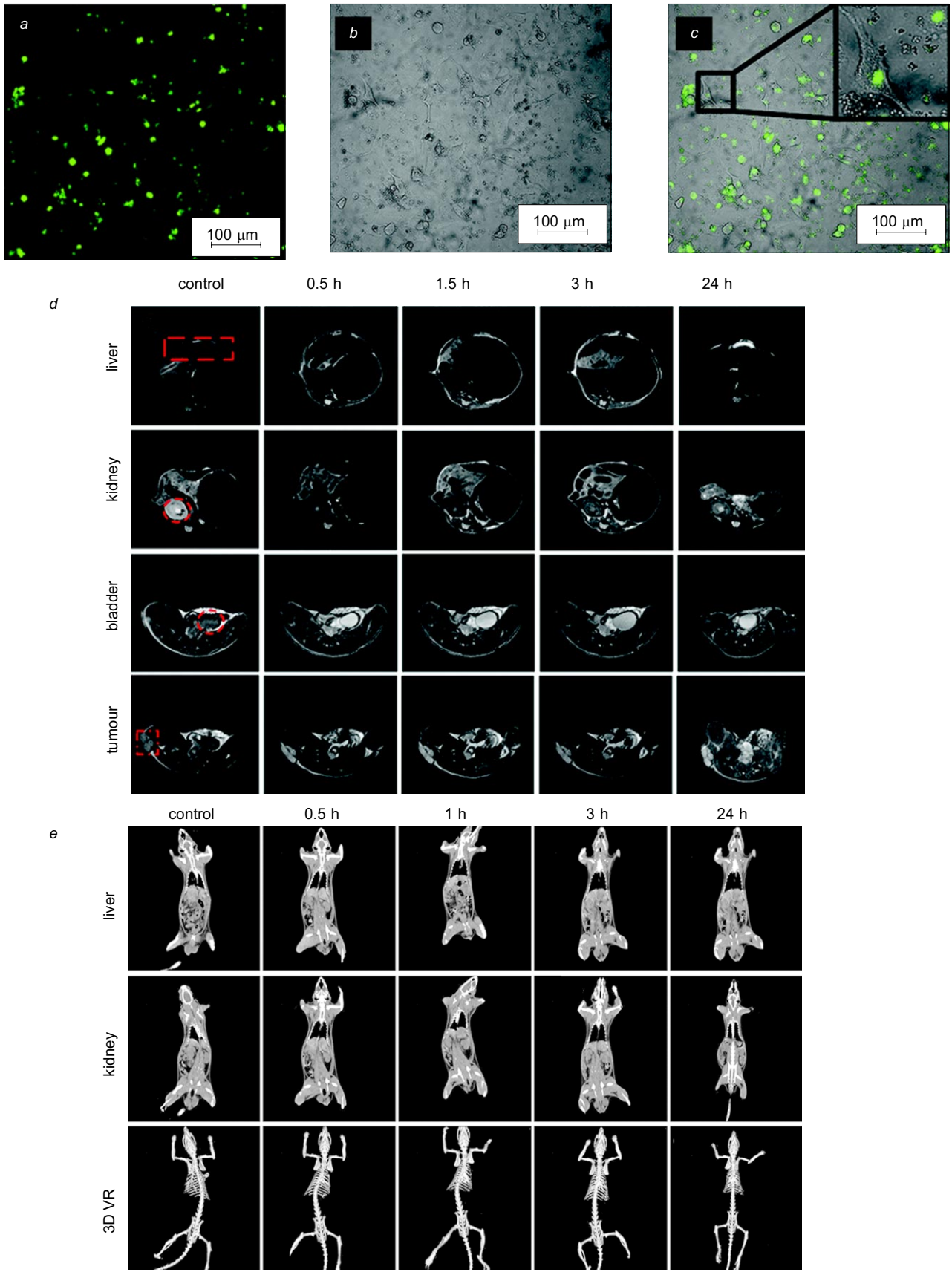


Figure 49. Fluorescence image (*a*), bright-field image (*b*) and superimposed image of human umbilical vein endothelial cells (HUVECs) after incubation with layered Gd : Ce,Tb hydroxide nanoparticles for 48 h obtained using confocal microscopy (*c*), *in vivo* T_2-weighted magnetic resonance images of a mouse body after injection of layered Gd : Ce,Tb hydroxide nanoparticles (10 mg per kg of body mass) (*d*) and X-ray computed tomography images of rats (*e*) after injection of layered Gd : Ce,Tb hydroxide nanoparticles (10 mg per kg of body mass).[166] 3D VR is 3D volume rendering.

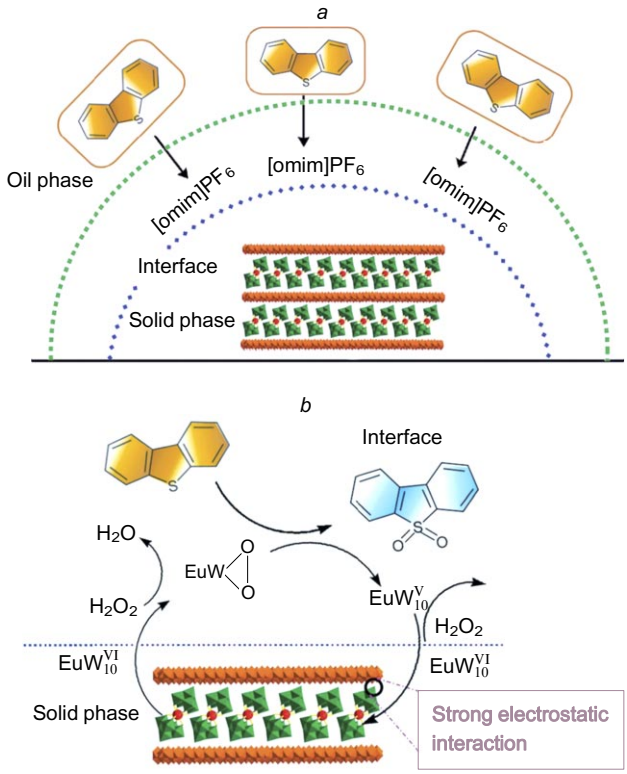


Figure 50. Hydrodesulfurization mechanism of dibenzothiophene using the catalytic system 'ionic liquid [1-methyl-3-octylimidazolium hexafluorophosphate (omim)]/hydrogen peroxide/layered europium hydroxide intercalated with europium-containing heteropolytungstate anion ($[EuW_{10}O_{36}]^{9-}$)': first (*a*) and second (*b*) steps.[245]

9. Conclusion

Layered rare-earth hydroxides represent a new family of layered inorganic compounds. Unique structure of LRHs built of alternating rigid host layers of rare-earth elements and labile anion layers between them underlies versatility of structure-sensitive properties.

Methods for the synthesis of LRHs have been well developed and allow one to obtain compounds of different stoichiometry (LREH-I, LREH-II and LREH-III categories) intercalated with both organic and inorganic anions and to vary their microstructure over a wide range from quasi-2D nanoparticles to millimetre-size single crystals. Structural features of LRHs enable the preparation of continuous series of lanthanide-based solid solutions and chemical modification of the host metal hydroxide layers using substitution reactions involving hydroxyl groups. Layered LRHs can be exfoliated to quasi-2D crystals, a convenient substrate for layer-by-layer assembly of hybrid organic-inorganic structures.

Layered rare-earth hydroxides with unusual luminescent and magnetic properties are unique matrices for basic research into electronic transitions between different rare-earth ions, as well as between rare-earth ions and ligands coordinated to them. Layered rare-earth hydroxides have a great potential for the design of multifunctional materials including biomaterials that simultaneously exhibit the luminescent, magnetic, catalytic and sensor properties.

This review has been prepared within the framework of the State Assignment to the Kurnakov Institute of General and Inorganic Chemistry of the Russian Academy of Sciences and financially supported by the Russian Foundation for Basic Research (Project No. 18-33-00117).

Figures 1, 12, 16, 18, 22, 23, 27, 29, 36, 38, 40, 43, 44, 45, 46 and 47 are courtesy of The Royal Society of Chemistry. Figures 2, 3, 24 – 26, 32, 33, 42 and 50 are courtesy of John Wiley and Sons. Figures 5, 6, 8, 11, 14, 17, 30, 34 and 41 are courtesy of the American Chemical Society. Figures 7, 15 and 31 are courtesy of Springer Nature. Figure 35 is courtesy of Cambridge University Press. Figure 39 is courtesy of Elsevier. Figures 4, 9, 11, 37, 47 and 49 were compiled by the authors of this review.

References

1. N.G.Vasil'ev, F.D.Ovcharenko. *Russ. Chem. Rev.*, **46**, 775 (1977)
2. M.I.Rozengart, G.M.V'yunova, G.V.Isagulyants. *Russ. Chem. Rev.*, **57**, 115 (1988)
3. E.V.Kukharskaya, A.D.Fedoseev. *Russ. Chem. Rev.*, **32**, 490 (1963)
4. A.A.Krasilin, D.P.Danilovich, E.B.Yudina, S.Bruyere, J.Ghanbaja, V.K.Ivanov. *Appl. Clay Sci.*, **173**, 1 (2019)
5. V.V.Aksenov, V.M.Vlasov, G.N.Shnitko. *Russ. Chem. Rev.*, **59**, 738 (1990)
6. G.S.Petrov, A.S.Skoropanov, A.A.Vecher. *Russ. Chem. Rev.*, **56**, 701 (1987)
7. Y.N.Novikov, M.E.Vol'pin. *Russ. Chem. Rev.*, **40**, 733 (1971)
8. A.M.Abakumov, M.G.Rozova, E.I.Ardashnikova, E.V.Antipov. *Russ. Chem. Rev.*, **71**, 383 (2002)
9. E.V.Antipov, A.M.Abakumov. *Physics-Uspekhi*, **51**, 180 (2008)
10. V.S.Kravchenko. *Russ. Chem. Rev.*, **80**, 473 (2011)
11. M.W.Barsoum. *Prog. Solid State Chem.*, **28**, 201 (2000)
12. B.Anasori, M.R.Lukatskaya, Y.Gogotsi. *Nat. Rev. Mater.*, **2**, 16098 (2017)
13. T.W.Scharf, S.V.Prasad. *J. Mater. Sci.*, **48**, 511 (2013)
14. W.Guo, J.Yin, H.Qiu, Y.Guo, H.Wu, M.Xue. *Friction*, **2**, 209 (2014)
15. K.-H.Goh, T.-T.Lim, Z.Dong. *Water Res.*, **42**, 1343 (2008)
16. S.R.J.Oliver. *Chem. Soc. Rev.*, **38**, 1868 (2009)
17. A.V.Radha, P.Vishnu Kamath, C.Shivakumara. *Solid State Sci.*, **7**, 1180 (2005)
18. V.Rives, M.del Arco, C.Martín. *Appl. Clay Sci.*, **88 – 89**, 239 (2014)
19. H.Chen, W.Zhang. *Sci. China Chem.*, **53**, 1273 (2010)
20. H.Chen, W.-G.Zhang. *J. Am. Ceram. Soc.*, **93**, 2305 (2010)
21. D.R.Martínez Vargas, M.J.Oviedo, F.da Silva Lisboa, F.Wypych, G.A.Hirata, G.G.Carbajal Arizaga. *J. Nanomater.*, 730153 (2013)
22. Á.Monge, F.Gándara, E.Gutiérrez-Puebla, N.Snejko. *CrystEngComm*, **13**, 5031 (2011)
23. M.P.Yutkin, D.N.Dybtsev, V.P.Fedin. *Russ. Chem. Rev.*, **80**, 1009 (2011)
24. F.Gándara, J.Perles, N.Snejko, M.Iglesias, B.Gómez-Lor, E.Gutiérrez-Puebla, M.Á.Monge. *Angew. Chem., Int. Ed.*, **45**, 7998 (2006)
25. C.E.Holcombe. *J. Am. Ceram. Soc.*, **61**, 481 (1978)
26. V.Natadze, N.Mzareulishvili, E.Davitashvili. *Soobshch. Akad. Nauk Gruz. SSR*, **49**, 85 (1968)
27. N.V.Aksel'rud, V.B.Spivakovskii. *Zh. Neorg. Khim.*, **5**, 348 (1960)
28. N.Mzareulishvili, E.Davitashvili. *Soobshch. Akad. Nauk Gruz. SSR*, **50**, 357 (1968)
29. N.Mzareulishvili, E.Davitashvili. *Soobshch. Akad. Nauk Gruz. SSR*, **50**, 619 (1968)
30. N.V.Aksel'rud. *Russ. Chem. Rev.*, **32**, 353 (1963)
31. N.V.Aksel'rud, V.B.Spivakovskii. *Zh. Neorg. Khim.*, **4**, 56 (1959)
32. N.V.Aksel'rud, V.B.Spivakovskii. *Zh. Neorg. Khim.*, **5**, 547 (1960)

33. N.V.Aksel'rud, V.I.Ermolenko. *Zh. Neorg. Khim.*, **6**, 777 (1961)
34. N.V.Aksel'rud, V.B.Spivakovskii. *Zh. Neorg. Khim.*, **5**, 327 (1960)
35. N.V.Aksel'rud, V.B.Spivakovskii. *Zh. Neorg. Khim.*, **5**, 340 (1960)
36. J.M.Haschke. *Inorg. Chem.*, **13**, 1812 (1974)
37. P.V.Klevtsov, V.M.Bembel', Z.A.Grankina. *J. Struct. Chem.*, **10**, 543 (1969)
38. P.V.Klevtsov. *J. Struct. Chem.*, **10**, 411 (1969)
39. T.N.Tarkhova, N.N.Mironov, I.A.Grishin. *J. Struct. Chem.*, **11**, 515 (1970)
40. R.F.Klevtsova, L.A.Glinskaya. *J. Struct. Chem.*, **10**, 408 (1969)
41. P.V.Klevtsov, T.G.Lysenina, L.Y.Kharckenko. *J. Struct. Chem.*, **14**, 76 (1973)
42. P.V.Klevtsov, R.F.Klevtsova, L.P.Sheina. *J. Struct. Chem.*, **6**, 449 (1966)
43. R.F.Klevtsova, P.V.Klevtsov. *J. Struct. Chem.*, **7**, 524 (1967)
44. F.L.Carter, S.Levinson. *Inorg. Chem.*, **8**, 2788 (1969)
45. C.Serre, F.Millange, J.Marrot, G.Férey. *Chem. Mater.*, **14**, 2409 (2002)
46. A.E.Baranchikov, V.K.Ivanov, A.V.Dmitriev, E.A.Tkachenko, P.P.Fedorov, Y.D.Tret'yakov, V.V.Osiko. *Russ. J. Inorg. Chem.*, **51**, 1689 (2006)
47. C.Jouve, J.Marrot, D.Riou. *Acta Crystallogr., Sect. C*, **58**, i14 (2002)
48. H.O.Pierson. In *Handbuch Carbon, Graph. Diamonds Fullerenes*. (Park Ridge, NJ: Neyes Publications, 1993). P. 43
49. S.Z.Butler, S.M.Hollen, L.Cao, Y.Cui, J.A.Gupta, H.R.Gutierrez, T.F.Heinz, S.S.Hong, J.Huang, A.F.Ismach, E.Johnston-Halperin, M.Kuno, V.V.Plashnitsa, R.D.Robinson, R.S.Ruoff, S.Salahuddin, J.Shan, L.Shi, M.G.Spencer, M.Terrones, W.Windl, J.E.Goldberger. *ACS Nano*, **7**, 2898 (2013)
50. J.W.Steed, J.L.Atwood. *Supramolecular Chemistry*. (Chechester: Wiley, 2009)
51. O.Palamarciuc, E.Delahaye, P.Rabu, G.Rogez. *New J. Chem.*, **38**, 2016 (2014)
52. S.Si, A.Taubert, A.Mantion, G.Rogez, P.Rabu. *Chem. Sci.*, **3**, 1945 (2012)
53. B.Zhang, Y.Liu, S.Agarwal, M.-L.Yeh, H.E.Katz. *ACS Appl. Mater. Interfaces*, **3**, 4254 (2011)
54. I.A.Rodionov, I.A.Zvereva. *Russ. Chem. Rev.*, **85**, 248 (2016)
55. K.Kalantar-zadeh, J.Z.Ou, T.Daeneke, A.Mitchell, T.Sasaki, M.S.Fuhrer. *Appl. Mater. Today*, **5**, 73 (2016)
56. F.Geng, R.Ma, T.Sasaki. *Acc. Chem. Res.*, **43**, 1177 (2010)
57. C.H.Swanson, H.A.Shaikh, D.L.Rogow, A.G.Oliver, C.F.Campana, S.R.J.Oliver. *J. Am. Chem. Soc.*, **130**, 11737 (2008)
58. M.F.Brigatti, E.Galan, B.K.G.Theng. In *Handbook of Clay Science*. (Eds F.Bergaya, B.K.G.Theng, G.Lagaly). (Amsterdam, Oxford: Elsevier, 2006). P. 19
59. J.H.Rayner, H.M.Powell. *J. Chem. Soc.*, 3412 (1958)
60. R.S.Pease. *Nature (London)*, **165**, 722 (1950)
61. J.D.Bernal. *Proc. R. Soc. A: Math. Phys. Eng. Sci.*, **106**, 749 (1924)
62. L.A.Chernozatonskii, A.A.Artyukh. *Phys.-Uspekhi*, **61**, 2 (2018)
63. K.Beneke, G.Lagaly. *Inorg. Chem.*, **22**, 1503 (1983)
64. *Layered Double Hydroxides*. (Eds X.Duan, D.G.Evans). (Berlin, Heidelberg: Springer-Verlag, 2006)
65. G.Rogez, C.Massobrio, P.Rabu, M.Drillon. *Chem. Soc. Rev.*, **40**, 1031 (2011)
66. N.B.Allou, P.Saikia, A.Borah, R.L.Goswamee. *Colloid Polym. Sci.*, **295**, 725 (2017)
67. J.Yu, Q.Wang, D. O'Hare, L.Sun. *Chem. Soc. Rev.*, **46**, 5950 (2017)
68. S.Omwoma, W.Chen, R.Tsunashima, Y.-F.Song. *Coord. Chem. Rev.*, **258** – **259**, 58 (2014)
69. G.Fan, F.Li, D.G.Evans, X.Duan. *Chem. Soc. Rev.*, **43**, 7040 (2014)
70. K.Yan, G.Wu, W.Jin. *Energy Technol.*, **4**, 354 (2016)
71. J.Qu, Q.Zhang, X.Li, X.He, S.Song. *Appl. Clay Sci.*, **119**, 185 (2016)
72. J.He, M.Wei, B.Li, Y.Kang, D.G.Evans, X.Duan. In *Layered Double Hydroxides*. (Eds X.Duan, D.G.Evans). (Berlin, Heidelberg: Springer-Verlag, 2005). P. 89
73. F.L.Theiss, G.A.Ayoko, R.L.Frost. *Appl. Surface Sci.*, **383**, 200 (2016)
74. P.Benito, M.Herrero, C.Barriga, F.M.Labajos, V.Rives. *Inorg. Chem.*, **47**, 5453 (2008)
75. S.Mallakpour, M.Dinari, V.Behranvand. *RSC Adv.*, **3**, 23303 (2013)
76. Q.Wang, D.O'Hare. *Chem. Rev.*, **112**, 4124 (2012)
77. N.Mao, C.H.Zhou, D.S.Tong, W.H.Yu, C.X.C.Lin. *Appl. Clay Sci.*, **144**, 60 (2017)
78. H.Yin, Z.Tang. *Chem. Soc. Rev.*, **45**, 4873 (2016)
79. Y.Cao, G.Li, X.Li. *Chem. Eng. J.*, **292**, 207 (2016)
80. M.Daud, M.S.Kamal, F.Shehzad, M.A.Al-Harthi. *Carbon*, **104**, 241 (2016)
81. G.B.B.Varadwaj, V.O.Nyamori. *Nano Res.*, **9**, 3598 (2016)
82. L.Mohapatra, K.Parida. *J. Mater. Chem. A*, **4**, 10744 (2016)
83. S.Mallakpour, M.Hatami. *Eur. Polym. J.*, **90**, 273 (2017)
84. J.Zhao, J.Chen, S.Xu, M.Shao, Q.Zhang, F.Wei, J.Ma, M.Wei, D.G.Evans, X.Duan. *Adv. Funct. Mater.*, **24**, 2938 (2014)
85. S.Miyata. *Clays Clay Miner.*, **31**, 305 (1983)
86. U.Costantino, R.Vivani, M.Bastianini, F.Costantino, M.Nocchetti. *Dalton Trans.*, **43**, 11587 (2014)
87. G.R.Williams, A.I.Khan, D.O'Hare. In *Layered Double Hydroxides*. (Eds X.Duan, D.G.Evans). (Berlin, Heidelberg: Springer-Verlag, 2005). P. 161
88. B.Zümreoglu-Karan, A.Ay. *Chem. Pap.*, **66**, 1 (2012)
89. R.Tian, R.Liang, M.Wei, D.G.Evans, X.Duan. In *50 Years of Structure and Bonding — The Anniversary Volume*. (Eds D.M.P.Mingos). (Cham: Springer, 2016). P. 65
90. M.Zubair, M.Daud, G.McKay, F.Shehzad, M.A.Al-Harthi. *Appl. Clay Sci.*, **143**, 279 (2017)
91. M.Sajid, C.Basheer. *TrAC Trends Anal. Chem.*, **75**, 174 (2016)
92. J.Liang, R.Ma, T.Sasaki. In *Photofunctional Layered Materials*. (Eds M.Yan, D.Wei). (Cham: Springer, 2015). P. 69
93. N.G.Zhuravleva, A.A.Eliseev, A.V.Lukashin, U.Kynast, Y.D.Tret'yakov. *Dokl. Chem.*, **396**, 87 (2004)
94. G.Abellán, C.Martí-Gastaldo, A.Ribera, E.Coronado. *Acc. Chem. Res.*, **48**, 1601 (2015)
95. P.Rabu, E.Delahaye, G.Rogez. *Nanotechnol. Rev.*, **4**, 557 (2015)
96. T.Li, H.N.Miras, Y.-F.Song. *Catalysts*, **7**, 260 (2017)
97. K.Takehira. *Appl. Clay Sci.*, **136**, 112 (2017)
98. M.Shao, M.Wei, D.G.Evans, X.Duan. In *Photofunctional Layered Materials* (Eds D.Yan, M.Wei). (Cham: Springer, 2015). P. 105
99. S.Nakagaki, K.M.Mantovani, G.S.Machado, K.A.Dias de Freitas Castro, F.Wypych. *Molecules*, **21**, 291 (2016)
100. D.-H.Park, G.Choi, J.-H.Choy. In *Photofunctional Layered Materials* (Eds D.Yan, M.Wei). (Cham: Springer, 2015). P. 137
101. Y.Kuthati, R.K.Kankala, C.-H.Lee. *Appl. Clay Sci.*, **112** – **113**, 100 (2015)
102. J.-M.Oh, D.-H.Park, S.-J.Choi, J.-H.Choy. *Recent Pat. Nanotechnol.*, **6**, 200 (2012)
103. X.Bi, H.Zhang, L.Dou. *Pharmaceutics*, **6**, 298 (2014)
104. M.S.Usman, M.Z.Hussein, S.Fakurazi, F.F.Ahmad Saad. *Chem. – Cent. J.*, **11**, 47 (2017)
105. K.Zhang, Z.Xu, J.Lu, Z.Tang, H.Zhao, D.Good, M.Wei. *Int. J. Mol. Sci.*, **15**, 7409 (2014)
106. X.Li, D.Du, Y.Zhang, W.Xing, Q.Xue, Z.Yan. *J. Mater. Chem. A*, **5**, 15460 (2017)
107. S.-D.Xie, Y.Liu, Z.-Y.Wu, G.-L.Shen, R.-Q.Yu. *Chin. J. Anal. Chem.*, **43**, 1648 (2015)

108. Y.D.Tretyakov, A.V.Lukashin, A.A.Eliseev. *Russ. Chem. Rev.*, **73**, 899 (2004)
109. M.P.Nikiforov, M.V.Chernysheva, A.A.Eliseev, A.V.Lukashin, Y.D.Tretyakov, Y.V.Maksimov, I.P.Suzdalev, P.Goernert. *Mater. Sci. Eng. B*, **109**, 226 (2004)
110. J.Zhong, Z.Yuan, C.Lu. *Anal. Bioanal. Chem.*, **408**, 8731 (2016)
111. X.Wu, J.-G.Li, Q.Zhu, W.Liu, J.Li, X.Li, X.Sun, Y.Sakka. *J. Mater. Chem. C*, **3**, 3428 (2015)
112. F.Geng, Y.Matsushita, R.Ma, H.Xin, M.Tanaka, F.Izumi, N.Iyi, T.Sasaki. *J. Am. Chem. Soc.*, **130**, 16344 (2008)
113. L.J.McIntyre, T.J.Prior, A.M.Fogg. *Chem. Mater.*, **22**, 2635 (2010)
114. F.Geng, H.Xin, Y.Matsushita, R.Ma, M.Tanaka, F.Izumi, N.Iyi, T.Sasaki. *Chem. – Eur. J.*, **14**, 9255 (2008)
115. G.S.Thomas, P.V.Kamath. *J. Chem. Sci.*, **118**, 127 (2006)
116. N.Li, K.Yanagisawa. *J. Solid State Chem.*, **181**, 1738 (2008)
117. F.Sato, S.Hitoshi, Y.Yano, M.Sigura, R.Takahashi. *J. Ceram. Soc. Jpn*, **125**, P10 (2017)
118. J.Liang, R.Ma, T.Sasaki. *Dalton Trans.*, **43**, 10355 (2014)
119. F.Geng, Y.Matsushita, R.Ma, H.Xin, M.Tanaka, N.Iyi, T.Sasaki. *Inorg. Chem.*, **48**, 6724 (2009)
120. A.D.Yapryntsev, A.E.Baranchikov, L.S.Skogareva, A.E.Goldt, I.P.Stolyarov, O.S.Ivanova, V.V.Kozik, V.K.Ivanov. *CrystEngComm*, **17**, 2667 (2015)
121. S.A.Hindocha, L.J.McIntyre, A.M.Fogg. *J. Solid State Chem.*, **182**, 1070 (2009)
122. L.J.McIntyre, L.K.Jackson, A.M.Fogg. *J. Phys. Chem. Solids*, **69**, 1070 (2008)
123. L.Poudret, T.J.Prior, L.J.McIntyre, A.M.Fogg. *Chem. Mater.*, **20**, 7447 (2008)
124. L.J.McIntyre, L.K.Jackson, A.M.Fogg. *Chem. Mater.*, **20**, 335 (2008)
125. L.McIntyre. *Synthesis and Characterisation of Layered Hydroxy Anion Exchange Materials*. (University of Liverpool, 2009)
126. Q.Zhu, X.Zhang, J.-G.Li, X.Li, X.Sun. *J. Nanosci. Nanotechnol.*, **17**, 2471 (2017)
127. Y.Xiang, X.-F.Yu, D.-F.He, Z.Sun, Z.Cao, Q.-Q.Wang. *Adv. Funct. Mater.*, **21**, 4388 (2011)
128. L.Hu, R.Ma, T.C.Ozawa, T.Sasaki. *Inorg. Chem.*, **49**, 2960 (2010)
129. L.Wu, C.Gao, Z.Li, G.Chen. *J. Mater. Chem. C*, **5**, 5207 (2017)
130. L.Wu, G.Chen, Z.Li. *Small*, **13**, 1604070 (2017)
131. L.Wang, D.Yan, S.Qin, S.Li, J.Lu, D.G.Evans, X.Duan. *Dalton Trans.*, **40**, 11781 (2011)
132. X.Wu, J.G.Li, Q.Zhu, J.G.Li, R.Ma, T.Sasaki, X.Li, X.Sun, Y.Sakka. *Dalton Trans.*, **41**, 1854 (2012)
133. X.Wu, J.-G.Li, Q.Zhu, X.Li, X.Sun, Y.Sakka. *Sci. Technol. Adv. Mater.*, **14**, 15006 (2013)
134. X.L.Wu, J.G.Li, J.K.Li, S.H.Liu, X.D.Li, X.D.Sun, Y.Sakka. *Key Eng. Mater.*, **544**, 252 (2013)
135. T.Watanabe, Y.Iso, T.Isobe, K.Higashi, Y.Watanabe, Y.Iso, T.Isobe. *RSC Adv.*, **7**, 14107 (2017)
136. M.Jobbágy, N.Iyi. *J. Phys. Chem. C*, **114**, 18153 (2010)
137. F.Su, C.Liu, Y.Yang, S.Ma, G.Sun, X.Yang. *J. Colloid Interface Sci.*, **496**, 353 (2017)
138. L.Xie, C.Liu, L.Ma, C.Xiao, S.Ma, G.Sun, H.Li, X.Yang. *Dalton Trans.*, **46**, 3110 (2017)
139. T.Ye, W.Huang, L.Zeng, M.Li, J.Shi. *Appl. Catal. B: Environ.*, **210**, 141 (2017)
140. X.Wang, M.S.Molokeev, Q.Zhu, J.-G.Li. *Chem. – Eur. J.*, **23**, 16034 (2017)
141. R.A.Zehnder, D.L.Clark, B.L.Scott, R.J.Donohoe, P.D.Palmer, W.H.Runde, D.E.Hobart. *Inorg. Chem.*, **49**, 4781 (2010)
142. D.Louër, M.Louër. *J. Solid State Chem.*, **68**, 292 (1987)
143. D.F.Mullica, E.L.Sappenfield, D.A.Grossie. *J. Solid State Chem.*, **63**, 231 (1986)
144. Y.Song, M.Luo, C.Lin, N.Ye. *Chem. Mater.*, **29**, 896 (2017)
145. F.Geng, R.Ma, Y.Matsushita, J.Liang, Y.Michiue, T.Sasaki. *Inorg. Chem.*, **50**, 6667 (2011)
146. X.Wang, J.-G.Li, M.S.Molokeev, Q.Zhu, X.Li, X.Sun. *Chem. Eng. J.*, **302**, 577 (2016)
147. P.Feng, B.Shao, X.Wang, X.Yang. *Eur. J. Inorg. Chem.*, 4861 (2017)
148. J.Liang, R.Ma, Y.Ebina, F.Geng, T. Sasaki. *Inorg. Chem.*, **52**, 1755 (2013)
149. J.Wu, J.Liang, R.Ma, T.Sasaki. *J. Phys. Chem. C*, **119**, 26229 (2015)
150. K.M.Sergo, C.S.Han, M.R.Bresler, S.C.Citrak, Y.Abdollahian, H.Fei, S.R.J.Oliver. *Inorg. Chem.*, **54**, 3883 (2015)
151. H.Li, T.Sheng, Z.Xue, X.Zhu, S.Hu, Y.Wen, R.Fu, C.Zhuo, X.Wu. *CrystEngComm*, **19**, 2106 (2017)
152. A.Yapryntsev, B.Abdusatorov, I.Yakushev, R.Svetogorov, A.Gavrikov, A.Rodina, Y.Fatyushina, A.Baranchikov, Y.Zubavichus, V.Ivanov. *Dalton Trans.*, **48**, 6111 (2019)
153. V.V.Butova, M.A.Soldatov, A.A.Guda, K.A.Lomachenko, C.Lamberti. *Russ. Chem. Rev.*, **85**, 280 (2016)
154. B.H.T.Chai, S.Mroczkowski. *J. Cryst. Growth*, **44**, 84 (1978)
155. B.-I.Lee, H.Jeong, S.-H.Byeon. *Inorg. Chem.*, **53**, 5212 (2014)
156. Q.Zhu, J.-G.Li, R.Ma, T.Sasaki, X.Yang, X.Li, X.Sun, Y.Sakka. *J. Solid State Chem.*, **192**, 229 (2012)
157. N.V.Aksel'rud, V.B.Spivakovskii. *Zh. Inorg. Khim.*, **2**, 2709 (1957)
158. G.V.Ionova. *Russ. Chem. Rev.*, **59**, 39 (1990)
159. S.A.Stepanchikova, R.P.Biteikina, G.P.Shironosova, G.R.Kolonin. *Russ. Geol. Geophys.*, **55**, 941 (2014)
160. E.N.Rizkalla, G.R.Choppin. In *Handbook on the Physics and Chemistry of Rare Earths*. Vol.18. (Eds K.A.Gschneidner Jr., L.Eyring, G.R.Choppin, G.H.Lander). (Amsterdam, Oxford: Elsevier, 1994). P. 529
161. E.N.Rizkalla, G.R.Choppin. *J. Alloys Compd.*, **180**, 325 (1992)
162. J.-G.Li, J.Li, X.Wang, Q.Zhu, X.Li, B.-N.Kim, X.Sun. *Dalton Trans.*, **46**, 12683 (2017)
163. J.Li, J.-G.Li, Q.Zhu, X.Sun. *Mater. Design.*, **112**, 207 (2016)
164. S.S.Yoo, R.Razzak, E.Bédard, L.Guo, A.R.Shaw, R.B.Moore, W.H.Roa. *Nanotechnology*, **25**, 425102 (2014)
165. J.Demel, P.Kubat, F.Millange, J.Marrot, I.Cisařová, K.Lang. *Inorg. Chem.*, **52**, 2779 (2013)
166. M.Wu, L.Li, X.Yu, D.Zhang, T.Sun, X.Li, L.Sun, S.Lui, X.Huang, F.Bi, H.Wang, H.Zhu, Q.Gong. *J. Biomed. Nanotechnol.*, **10**, 3620 (2014)
167. K.-H.Lee, S.-H.Byeon. *Eur. J. Inorg. Chem.*, 929 (2009)
168. L.Liu, Q.Wang, C.Gao, H.Chen, W.Liu, Y.Tang. *J. Phys. Chem. C*, **118**, 14511 (2014)
169. S.Wang, W.Shi, C.Lu. *Anal. Chem.*, **88**, 4987 (2016)
170. B.Lu, J.-G.Li, T.S.Suzuki, M.Estili, W.Liu, X.Sun, Y.Sakka. *J. Am. Ceram. Soc.*, **98**, 1413 (2015)
171. K.-H.Lee, S.-H.Byeon. *Eur. J. Inorg. Chem.*, 4727 (2009)
172. B.I.Lee, K.S.Lee, J.H.Lee, I.S.Lee, S.H.Byeon. *Dalton Trans.*, **14**, 2490 (2009)
173. D.Stefanakis, D.F.Ghanotakis. *J. Nanopart. Res.*, **12**, 1285 (2010)
174. Y.Xi, R.J.Davis. *Inorg. Chem.*, **49**, 3888 (2010)
175. L.Zhu, L.Zhang, J.Li, D.Zhang, L.Chen, D.Sheng, S.Yang, C.Xiao, J.Wang, Z.Chai, T.E.Albrecht-Schmitt, S.Wang. *Environ. Sci. Technol.*, **51**, 8606 (2017)
176. Y.Yoon, B.-I.Lee, K.S.Lee, G.H.Im, S.-H.Byeon, J.H.Lee, I.S.Lee. *Adv. Funct. Mater.*, **19**, 3375 (2009)
177. B.-I.Lee, E.Lee, S.-H.Byeon. *Adv. Funct. Mater.*, **22**, 3562 (2012)
178. B.-I.Lee, J.-S.Bae, E.-S.Lee, S.-H.Byeon. *Bull. Korean Chem. Soc.*, **33**, 601 (2012)
179. H.Kim, B.I.Lee, S.H.Byeon. *Chem. Commun.*, **51**, 725 (2015)
180. Q.Zhu, X.Sun, J.-G.Li, X.Li, Y.Qi, X.Sun. *RSC Adv.*, **5**, 64588 (2015)
181. X.Wu, J.-G.Li, D.-H.Ping, J.Li, Q.Zhu, X.Li, X.Sun, Y.Sakka. *J. Alloys Compd.*, **559**, 188 (2013)

182. Q.Zhu, J.-G.Li, C.Zhi, X.Li, X.Sun, Y.Sakka, D.Golberg, Y.Bando. *Chem. Mater.*, **22**, 4204 (2010)
183. Q.Zhu, J.-G.Li, X.Li, X.Sun, Y.Qi, M.Zhu, Y.Sakka. *Sci. Technol. Adv. Mater.*, **15**, 014203 (2014)
184. Q.Zhu, X.D.Li, X.D.Sun. *Key Eng. Mater.*, **602 – 603**, 1017 (2014)
185. P.P.Wang, B.Bai, L.Huang, S.Hu, J.Zhuang, X.Wang. *Nanoscale*, **3**, 2529 (2011)
186. F.Gándara, E.G.Puebla, M.Iglesias, D.M.Proserpio, N.Snejko, M.A.Monge. *Chem. Mater.*, **21**, 655 (2009)
187. Q.Zhu, J.G.Li, C.Zhi, R.Ma, T.Sasaki, J.X.Xu, C.H.Liu, X.D.Li, X.D.Sun, Y.Sakka. *J. Mater. Chem.*, **21**, 6903 (2011)
188. S.-S.Lee, C.-H.Joh, S.-H.Byeon. *Mater. Sci. Eng. B*, **151**, 163 (2008)
189. L.Niinistö, M.Leskelä. In *Handbook on the Physics and Chemistry of Rare Earths*. Vol. 9. (Eds K.A.Gschneidner Jr., L.Eyring). (Amsterdam, Oxford: Elsevier, 1987). P. 91
190. J.-G.Li, X.Wang, W.Liu, Q.Zhu, X.Li, X.Sun. *Nanoscale Res. Lett.*, **12**, 508 (2017)
191. E.A.Frolova, D.F.Kondakov, A.D.Yapryntsev, A.E.Baranchikov, V.K.Ivanov, V.P.Danilov. *Russ. J. Inorg. Chem.*, **60**, 259 (2015)
192. Y.Xu, A.Goyanes, Y.Wang, A.J.Weston, P.-W.So, F.G.C.Geraldes, A.M.Fogg, A.W.Basit, G.R.Williams. *Dalton Trans.*, **47**, 3166 (2018)
193. P.P.Wang, B.Bai, S.Hu, J.Zhuang, X.Wang. *J. Am. Chem. Soc.*, **131**, 16953 (2009)
194. Y.Xu, J.Suthar, R.Egbu, A.J.Weston, A.M.Fogg, G.R.Williams. *J. Solid State Chem.*, **258**, 320 (2018)
195. H.H.Willard, N.K.Tang. *J. Am. Chem. Soc.*, **59**, 1190 (1937)
196. H.Tada. *J. Am. Chem. Soc.*, **82**, 255 (1960)
197. J.M.Dreyfors, S.B.Jones, Y.Sayed. *Am. Ind. Hyg. Assoc. J.*, **50**, 579 (1989)
198. E.A.Dolgopolova, O.S.Ivanova, V.K.Ivanov, F.Y.Sharikov, A.E.Baranchikov, A.B.Shcherbakov, Y.D.Trietyakov. *Russ. J. Inorg. Chem.*, **57**, 1303 (2012)
199. C.A.Antonyraj, P.Koilraj, S.Kannan. *Chem. Commun.*, **46**, 1902 (2010)
200. L.Hu, R.Ma, T.C.Ozawa, T.Sasaki. *Angew. Chem., Int. Ed.*, **48**, 3846 (2009)
201. L.Ma, M.Yuan, C.Liu, L.Xie, F.Su, S.Ma, G.Sun, H.Li. *Dalton Trans.*, **46**, 12724 (2017)
202. Y.Sun, N.Chu, Q.Gu, G.Pan, G.Sun, S.Ma, X.Yang. *Eur. J. Inorg. Chem.*, 5506 (2013)
203. Y.Sun, G.Pan, Q.Gu, X.Li, G.Sun, S.Ma, X.Yang. *Mater. Res. Bull.*, **48**, 4460 (2013)
204. W.Li, Q.Gu, F.Su, Y.Sun, G.Sun, S.Ma, X.Yang. *Inorg. Chem.*, **52**, 14010 (2013)
205. Q.Gu, F.Su, S.Ma, G.Sun, X.Yang. *Chem. Commun.*, **51**, 2514 (2015)
206. Q.Gu, G.Pan, T.Ma, G.Huang, G.Sun, S.Ma, X.Yang. *Mater. Res. Bull.*, **53**, 234 (2014)
207. R.Ju, Q.Gu. *Appl. Organomet. Chem.*, **32**, e3926 (2018)
208. Q.Gu, Y Sun, N.Chu, S.Ma, Z.Jia, X.Yang. *Eur. J. Inorg. Chem.*, 4407 (2012)
209. Q.Gu, N.Chu, G.Pan, G.Sun, S.Ma, X.Yang. *Eur. J. Inorg. Chem.*, 559 (2014)
210. Q.Gu, W.Chen, F.Duan, R.Ju. *Dalton Trans.*, **45**, 12137 (2016)
211. Q.Gu, M.Yuan, S.Ma, G.Sun. *J. Lumin.*, **192**, 1211 (2017)
212. Q.Gu, X.Liu, Y.Hu, L.Zhang, Y.Li. *J. Photochem. Photobiol. A: Chem.*, **335**, 268 (2017)
213. Y.Zhao, J.-G.G.Li, M.Guo, X.Yang. *J. Mater. Chem. C*, **1**, 3584 (2013)
214. X.Wang, P.Feng, Y.Zhao, J.-G.Li, X.Yang. *Chemi. Select*, **1**, 17 (2016)
215. Y.Zhong, G.Chen, X.Liu, D.Zhang, N.Zhang, J.Li, S.Liang, R.Ma, G.Qiu. *Nanoscale*, **9**, 8185 (2017)
216. A.D.Yapryntsev, A.E.Baranchikov, A.V.Zabolotskaya, L.P.Borilo, V.K.Ivanov. *Russ. J. Inorg. Chem.*, **59**, 1383 (2014)
217. A.E.Baranchikov, A.D.Yapryntsev, A.E.Goldt, V.K.Ivanov. *Curr. Microw. Chem.*, **2**, 1 (2015)
218. Y.Shi, C.Zhu, L.Wang, C.Zhao, W.Li, K. K.Fung, T.Ma, A.Hagfeldt, N.Wang. *Chem. Mater.*, **25**, 1000 (2013)
219. A.W.Xu, M.Antonietti, H.Cölfen, Y. P. Fang. *Adv. Funct. Mater.*, **16**, 903 (2006)
220. J.Yang, L.Yao, J.Sun, B.Sun. *J. Inorg. Organomet. Polym.*, **23**, 1240 (2013)
221. Q.Wang, B.Geng, S.Wang, J.Liu, Z.Cheng, D.Si. *CrystEngComm*, **11**, 1317 (2009)
222. V.K.Ivanov, P.P.Fedorov, A.Y.Baranchikov, V.V.Osiko. *Russ. Chem. Rev.*, **83**, 1204 (2014)
223. A.D.Yapryntsev, A.Y.Bykov, A.E.Baranchikov, K.Y.Zhizhin, V.K.Ivanov, N.T.Kuznetsov. *Inorg. Chem.*, **56**, 3421 (2017)
224. M.Watanabe, S.Fujihara. *J. Solid State Chem.*, **210**, 130 (2014)
225. G.V.Manohara, D.A.Kunz, P.V.Kamath, W.Milius, J.Breu. *Langmuir*, **26**, 15586 (2010)
226. A.D.Yapryntsev, A.E.Baranchikov, V.K.Ivanov. *J. J. Inorg. Chem.*, **1**, 1 (2016)
227. P.Madhusudan, M.V.Kumar, T.Ishigaki, K.Toda, K.Uematsu, M.Sato. *Environ. Sci. Pollut. Res.*, **20**, 6638 (2013)
228. B.Bann, S.A.Miller. *Chem. Rev.*, **58**, 131 (1958)
229. E.Wirnhier, M.B.Mesch, J.Senker, W.Schnick. *Chem. – Eur. J.*, **19**, 2041 (2013)
230. B.V.Lotsch, W.Schnick. *Chem. – Eur. J.*, **13**, 4956 (2007)
231. O.Okay, W.Oppermann. *Macromolecules*, **40**, 3378 (2007)
232. Negrete, J.-M.Letoffe, J.-L.Putaux, L.David, E.Bourgeat-Lami. *Langmuir*, **20**, 1564 (2004)
233. A.R.Mermut, G.Lagaly. *Clays Clay Miner.*, **49**, 393 (2001)
234. M.Meyn, K.Beneke, G.Lagaly. *Inorg. Chem.*, **29**, 5201 (1990)
235. K.A.Carrado, J.E.Forman, R.E.Botto, R.E.Winans. *Chem. Mater.*, **5**, 472 (1993)
236. S.P.Newman, W.Jones. *J. Solid State Chem.*, **148**, 26 (1999)
237. N.Chu, Y.Sun, Y.Zhao, X.Li, G.Sun, S.Ma, X.Yang. *Dalton Trans.*, **41**, 7409 (2012)
238. L.Liu, M.Yu, J.Zhang, B.Wang, W.Liu, Y.Tang. *J. Mater. Chem. C*, **3**, 2326 (2015)
239. L.-L.Liu, Q.Wang, D.Xia, T.-T.Shen, M.-H.Yu, W.-S.Liu, Y.Tang. *Chin. Chem. Lett.*, **24**, 93 (2013)
240. F.L.Theiss, G.A.Ayoko, R.L.Frost. *J. Colloid Interface Sci.*, **402**, 114 (2013)
241. Yu.A.Kokotov. *Ionity i Ionnyi Obmen*. (Ion Exchangers and Ion Exchange). (Leningrad: Khimiya, 1980)
242. Z.Wang, J.-G.Li, Q.Zhu, X.Li, X.Sun. *Dalton Trans.*, **45**, 5290 (2016)
243. H.Kim, B.-I.Lee, H.Jeong, S.-H.Byeon. *J. Mater. Chem. C*, **3**, 7437 (2015)
244. F.Su, R.Guo, Z.Yu, J.Li, Z.Liang, K.Shi, S.Ma, G.Sun, H.Li. *Dalton Trans.*, **47**, 5380 (2018)
245. X.Wang, W.Chen, Y.-F.Song. *Eur. J. Inorg. Chem.*, 2779 (2014)
246. B.-I.Lee, S.-H.Byeon. *Chem Commun*, **47**, 4093 (2011)
247. D.Stefanakis, D.F.Ghanotakis. *J. Nanopart. Res.*, **18**, 177 (2016)
248. L.Zhang, D.Jiang, J.Xia, N.Zhang, Q.Li. *RSC Adv.*, **4**, 17856 (2014)
249. H.Jeong, B.-I.Lee, S.-H.Byeon. *Dalton Trans.*, **41**, 14055 (2012)
250. T.Shen, Y.Zhang, W.Liu, Y.Tang. *J. Mater. Chem. C*, **3**, 1807 (2015)
251. Q.Zhu, S.Li, J.Jin, Z.Xu, X.Li, X.Sun, J.-G.Li. *Chem. – Asian J.*, **13**, 3664 (2018)
252. R.Mas-Balleste, C.Gomez-Navarro, J.Gomez-Herrero, F.Zamora. *Nanoscale*, **3**, 20 (2011)
253. L.A.Aslanov, S.F.Dunaev. *Russ. Chem. Rev.*, **87**, 882 (2018)
254. L.Hu, R.Ma, T.C.Ozawa, T.Sasaki. *Chem. – Asian J.*, **5**, 248 (2010)
255. L.Gorb, A.Asensio, I.Tuñóøn, M.F.Ruiz-López. *Chem. – Eur. J.*, **11**, 6743 (2005)
256. J.Legendziewicz, T.Głowiak, G. Oczko, D. C. Ngoan. *J. Less Common Met.*, **125**, 45 (1986)

257. Q.Zhu, Z.Xu, J.-G.Li, X.Li, Y.Qi, X.Sun. *Nanoscale Res. Lett*., **10**, 132 (2015)
258. A.D.Yapryntsev, K.B.Ustinovich, A.A.Rodina, V.A.Lebedev, O.I.Pokrovskiy, K.E.Yorov, A.V.Gavrikov, A.E.Baranchikov, V.K.Ivanov. *J. Supercrit. Fluids*, **150**, 40 (2019)
259. B.Shao, Y.Feng, S.Zhao, S.Yuan, J.Huo, W.Lü, H.You. *Inorg. Chem*., **56**, 6114 (2017)
260. Y.S.Yoon, S.H.Byeon, I.S.Lee. *Adv. Mater*., **22**, 3272 (2010)
261. K.-W.Jeon, L.Zhang, S.Choi, I.S.Lee. *Small*, **14**, 1802174 (2018)
262. J.Liang, R.Ma, F.Geng, Y.Ebina, T.Sasaki, J.Liang, R.Ma, F.Geng, T.Sasaki. *Chem. Mater*., **22**, 6001 (2010)
263. A.D.Yapryntsev, L.S.Skogareva, A.E.Gol'dt, A.E.Baranchikov, V.K.Ivanov. *Russ. J. Inorg. Chem*., **60**, 1027 (2015)
264. K.-H.Lee, B.-I.Lee, J.-H.You, S.-H.Byeon. *Chem. Commun*., **46**, 1461 (2010)
265. B.-I.Lee, S.-H.Byeon. *Bull. Korean Chem. Soc*., **36**, 804 (2015)
266. S.-S.Lee, B.-I.Lee, S.Kim, S.-H.Byeon, J.-K.Kang. *Inorg. Chem*., **51**, 10222 (2012)
267. X.Wang, J.-G.Li, M.S.Molokeev, X.Wang, W.Liu, Q.Zhu, H.Tanaka, K.Suzuta, B.N.Kim, Y.Sakka. *RSC Adv*., **7**, 13331 (2017)
268. X.Wang, J.-G.Li, Q.Zhu, X.Sun. *J. Mater. Res*., **31**, 2268 (2016)
269. A.C.T.Cursino, V.Rives, G.G.C.Arizaga, R.Trujillano, F.Wypych. *Mater. Res. Bull*., **70**, 336 (2015)
270. S.Narushima, R.Shimonishi, M.Hagivara, S.Fujihara. *J. Ceram. Soc. Jap*., **126**, 286 (2018)
271. Y.Yoon, B.-I.Lee, K.S.Lee, H.Heo, J.H.Lee, S.-H.Byeon, I.S.Lee. *Chem. Commun*., **46**, 3654 (2010)
272. J.-C.G.Bünzli, S.V.Eliseeva. In *Comprehensive Inorganic Chemistry II*. (Amsterdam: Elsevier, 2013). P. 339
273. V.V.Utochnikova, N.P.Kuzmina. *Russ. J. Coord. Chem*., **42**, 679 (2016)
274. K.Binnemans. *Coord. Chem. Rev*., **295**, 1 (2015)
275. H.Jeong, B.-I.Lee, S.-H.Byeon. *ACS Appl. Mater. Interfaces*, **8**, 10946 (2016)
276. J.A.Capobianco, P.P.Proulx, M.Bettinelli, F.Negrisolo. *Phys. Rev. B*, **42**, 5936 (1990)
277. M.A.Drezdzon. *Inorg. Chem*., **27**, 4628 (1988)
278. E.D.Dimotakis, T.J.Pinnavaia. *Inorg. Chem*., **29**, 2393 (1990)
279. T.Kwon, T.J.Pinnavaia. *Chem. Mater*., **1**, 381 (1989)
280. K.Sakuma, S.Fujihara. *J. Ceram. Proc. Res*., **14**, s26 (2013)
281. F.Su, C.Liu, Y.Yang, S.Ma, G.Sun, X.Yang. *Mater. Res. Bull*., **88**, 301 (2017)
282. V.Khudoleeva, L.Tcelykh, A.Kovalenko, A.Kalyakina, A.Goloveshkin, L.Lepnev, V.Utochnikova. *J. Lumin*., **201**, 500 (2018)
283. C.Davesnne, A.Ziani, C.Labbé, P.Marie, C.Frilay, X.Portier. *Thin Solid Films*, **553**, 33 (2014)
284. P.R.Matthes, C.J.Höller, M.Mai, J.Heck, S.J.Sedlmaier, S.Schmiechen, C.Feldmann, W.Schnick, K.Müller-Buschbaum. *J. Mater. Chem*., **22**, 10179 (2012)
285. P.Feng, X.Wang, Y.Zhao, D.-C.Fang, X.Yang. *RSC Adv*., **8**, 3592 (2018)
286. P.P.Zak, V.A.Lapina, T.A.Pavich, A.V.Trofimov, N.N.Trofimova, Y.B.Tsaplev. *Russ. Chem. Rev*., **86**, 831 (2017)
287. Q.Gu, F.Su, L.Ma, S.Ma, G.Sun, X.Yang. *J. Mater. Chem. C*, **3**, 4742 (2015)
288. E.Coronado, C.Martí-Gastaldo, E.Navarro-Moratalla, A.Ribera, S.J.Blundell, P.J.Baker. *Nat. Chem*., **2**, 1031 (2010)
289. J.Wang, J.Zhou, Z.Li, Y.Song, Q.Liu, Z.Jiang, M.Zhang. *Chem. – Eur. J*., **16**, 14404 (2010)
290. G.Abellán, G.M.Espallargas, G.Lorusso, M.Evangelisti, E.Coronado. *Chem. Commun*., **51**, 14207 (2015)
291. J.T.Coutinho, C.C.L.Pereira, J.Marçalo, J.J.Baldoví, M.Almeida, B.Monteiro, L.C.J.Pereira. *Dalton Trans*., **47**, 16211 (2018)
292. B.Monteiro, J.T.Coutinho, C.C.L.Pereira, L.C.J.Pereira, J.Marçalo, M.Almeida, J.J.Baldoví, E.Coronado, A.Gaita-Ariño. *Inorg. Chem*., **54**, 1949 (2015)
293. B.Monteiro, C.C.L.Pereira, J.T.Coutinho, L.C.J.Pereira, J.Marçalo, M.Almeida. *Eur. J. Inorg. Chem*., 5059 (2013)
294. B.-I.Lee, H.Jeong, S.-H.Byeon. *Chem. Commun*., **49**, 11397 (2013)
295. C.C.L.Pereira, J.C.Lima, A.J.Moro, B.Monteiro. *Appl. Clay Sci*., **146**, 216 (2017)